




University of
Stavanger

FACULTY OF SCIENCE AND TECHNOLOGY

MASTER'S THESIS

Study programme/specialization: Petroleum Engineering/ Drilling Technology	Spring/Autumn semester, 2018 Open
Author: Christian Riise	 (Signature of author)
Programme coordinator: Supervisor(s): Mesfin Belayneh.	
Title of master's thesis: Effect of MWCNT on Duovis biopolymer based laboratory drilling: Experimental and Simulation studies	
Credits: 30	
Keywords: Drilling fluid MWCNT nanoparticle Duovis Rheological properties Tribology Viscoelasticity	Number of pages:87..... + Supplemental material/other: 12..... Stavanger,15-06-/2018..... Date/year

Acknowledgements

First of all, I would like to thank my supervisor and friend Mesfin Belayneh for his endless support, motivation and knowledge during this project. I owe my deepest gratitude to you, Mesfin. I have really enjoyed our time together and wish you all the best for the future.

I also would like to thank my girlfriend Ingrid, my brother Henrik and my father for moral support and the guidance when working with my thesis. I would like to thank my friends and the rest of my family for their patience.

And last but not least I would especially like to thank my mother for her guidance and support, and for always providing me with delicious food throughout the years at the university.

Abstract

In recent years, nanotechnology have shown an improving performance on the properties of drilling fluid, enhanced oil recovery and in cement. The technology is proven in several other industries. However, the research and development in the oil and gas industry is at its early stage.

In this thesis work, several bases fluids have been formulated and the effect of MWCNT on the bases fluids have been evaluated. The main investigation factors considered were effect of pH, temperature and mixing condition. The bases fluid has been formulated by mixing water, bentonite, Duouvis polymer, lignosulfonate and KCl. Nanoparticle based drilling fluid have been formulated by adding 0.02wt%, 0.04wt%, 0.1wt% and 0.3wt% MWCNT in the bases fluid. The performance of the drilling fluid have been evaluated through simulation study.

Main results from the experiments and simulations are summarized as follows:

- The effects of MWCNT on the bases fluid have shown impact on the rheological properties, but the effect was non-linearly as concentration increases
- Addition of 0.3wt% MWCNT decreased the friction coefficient by 43.6%
- Higher pH increased the viscometer responses of the drilling fluid than the lower pH. However, the rheological parameters are the same
- As compared with the mechanical mixing, the ultrasonicated fluid increased the YS and LSYS, but decreased the PV and the friction coefficient by 2.9 %
- In general, the considered MWCNT concentrations have increased the filtrate loss of the base fluid.
- As compared with the base fluid, the viscometer readings of MWCNT treated drilling fluids decreased less with increasing temperature
- As the concentration of MWCNT increases, the storage and loss moduli are increasing
- The reduction of coefficient friction due 0.3wt% MWCNT allowed longer drilling length
- Except for 0.3wt% MWCNT system, the lower concentrations of MWCNT reduced the PV as temperature increases.

Table of content

ACKNOWLEDGEMENTS	1
ABSTRACT	2
1 INTRODUCTION	5
1.1 BACKGROUND	5
1.2 PROBLEM FORMULATION	6
1.3 OBJECTIVE	7
1.4 METHODOLOGY	7
2 LITERATURE STUDY	8
2.1 APPLICATION OF NANOPARTICLES IN DRILLING FLUIDS	8
2.2 DESCRIPTION OF CHEMICALS USED IN THIS STUDY	10
2.2.1 <i>Bentonite</i>	10
2.2.2 <i>Salt (KCl)</i>	13
2.2.3 <i>Duovis</i>	13
2.2.4 <i>Lignosulfonate</i>	14
2.2.5 <i>NaOH</i>	14
2.2.6 <i>MWCNT</i>	15
3 THEORY	16
3.1 RHEOLOGY	16
3.2 RHEOLOGICAL MODELS	18
3.2.1 <i>Newtonian fluid</i>	18
3.2.2 <i>Non-Newtonian fluids</i>	19
3.3 TORQUE AND DRAG	22
3.4 VISCOELASTICITY	24
3.5 HYDRAULICS	27
4 EXPERIMENTAL WORK	30
4.1 DESCRIPTION OF EQUIPMENT	30
4.2 DRILLING FLUID FORMULATION	34
4.3 EFFECT OF MWCNT CONCENTRATION	35
4.3.1 <i>Viscometer data</i>	36
4.3.2 <i>Tribometer</i>	38
4.4 EFFECT OF PH	40
4.4.1 <i>Rheology</i>	40
4.4.2 <i>Friction</i>	43
4.5 EFFECT OF TEMPERATURE	44
4.5.1 <i>With Low pH</i>	44
4.5.2 <i>With High pH</i>	47
4.6 EFFECT OF MIXING	49
4.6.1 <i>Rheology</i>	51
4.6.2 <i>Friction</i>	52
4.7 ANALYSIS OF MUD CAKE STRUCTURE	53
4.8 ANALYSIS OF THE CHEMISTRY OF FILTER LOSS	54
4.9 VISCOELASTICITY OF DRILLING FLUIDS	56
5 PERFORMANCE SIMULATION	59
5.1 RHEOLOGY MODELLING	59
5.1.1 <i>Reference system</i>	60
5.1.2 <i>Reference system + 0.1 MWCNT</i>	61
5.1.3 <i>Reference + 0.2 MWCNT</i>	62
5.1.4 <i>Reference + 0,5 MWCNT</i>	63
5.1.5 <i>Reference + 1,5 MWCNT</i>	64

5.1.6 Comparison of Rheology models.....	65
5.1.7 Effect of MWCNT on Rheology parameters	66
5.2 HYDRAULICS.....	68
5.2.1 Simulation arrangement.....	68
5.2.2 Simulation result.....	69
5.3 TORQUE AND DRAG.....	71
5.3.1 Simulation Setup	72
5.3.2 Simulation Result.....	74
5.4 HOLE CLEANING	76
5.4.1 Simulation setup.....	76
5.4.2 Simulation results.....	77
6 SUMMARY AND DISCUSSION.....	80
5.1 EFFECT OF MWCNT CONCENTRATION ON RHEOLOGICAL PROPERTIES.....	80
5.2 EFFECT OF MWCNT ON COEFFICIENT OF FRICTION	81
5.3 EFFECT OF TEMPERATURE AND PH ON MWCNT SYSTEMS.....	81
5.4 EFFECT OF MIXING ON RHEOLOGY AND FRICTION.....	81
5.5 EFFECT ON VISCOELASTICITY	82
5.6 EFFECT ON HYDRAULICS	82
5.7 EFFECT ON TORQUE AND DRAG.....	83
5.8 EFFECT ON HOLE CLEANING.....	83
7 CONCLUSION.....	84
REFERENCES	86
APPENDIX	88
APPENDIX A	88
APPENDIX B: VISCOELASTICITY OF DRILLING FLUIDS.....	98
LIST OF ABBREVIATIONS	100

1 Introduction

This thesis presents multi-walled carbon nanotube (MWCNT) based drilling fluid formulation and characterization. The effect of nanoparticle concentration, temperature, pH and fluid dispersion effect through mixing are evaluated. The main objective was to examine how nanoparticles can enhance the properties of a conventional drilling fluid, such as rheology, filtrate loss, tribology, viscoelasticity and filter cake. The performance of the drilling fluid system were simulated with respect to hydraulics, hole-cleaning and torque and drag.

1.1 Background

For petroleum production, the primary phase is connecting reservoir with surface. During drilling, the drilling fluid is injected through circulation system. Figure 1.1 illustrates the circulation system.

In the past, the oil industry has a trend to drill more difficult wells to overcome the potential energy crisis [1]. To drill this wells it is necessary to reduce the cost through well and mud design. The drilling mud plays an important role in the drilling process since the rate of penetration could be increased with an optimized drilling fluid, where an optimized drilling fluid helps to get the maximum usage from the pump. To cope with this, it is crucial to reduce the energy loss due to friction. The drilling fluid also transport the cuttings out of the well, cools the bit and maintain the correct well pressure. Water based mud (WBM) and oil based mud (OBM) are the two most common drilling fluids used in the drilling industry, and where OBM only can be used if a zero discharge strategy is decided.

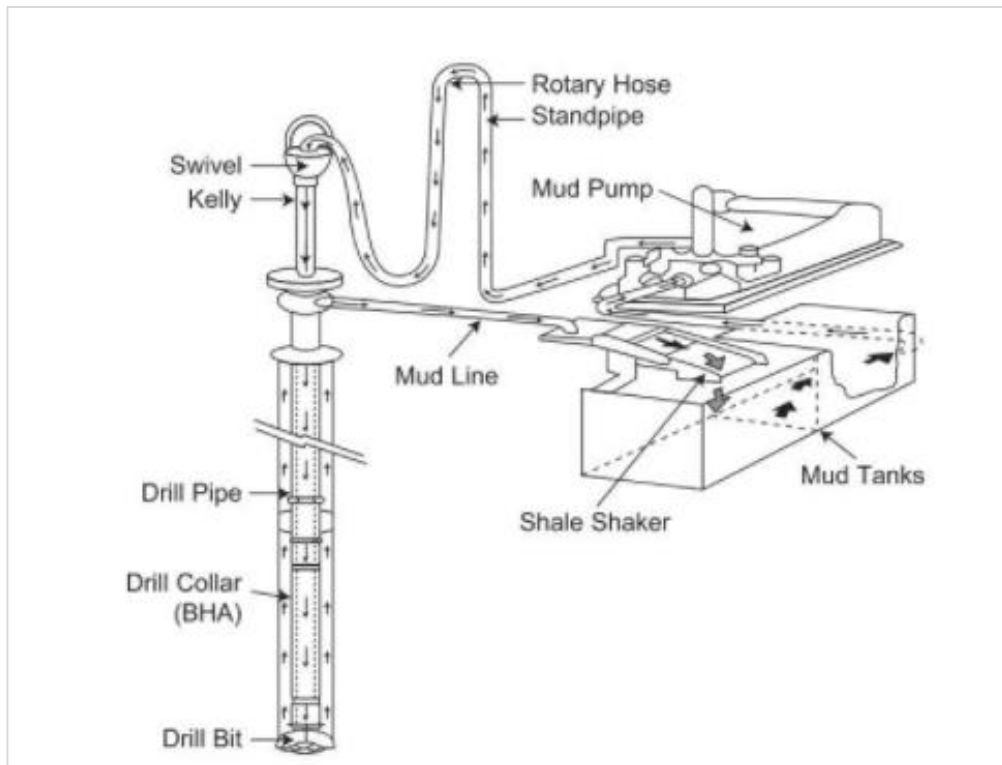


Figure 1.1: Mud circulating system [2]

Nanoparticles (1-100 nm) possess three important properties that can increase the efficiency of the drilling process [3]:

- Possible to enter formation pores where larger particles cannot enter
- Due to the higher surface area to volume ratio, the particles can be engineered to obtain special properties (magnetically, interfacial, electrical and chemical) used to perform special functions.
- When these properties are combined together, nanoparticles could be used to serve several purposes in the oil field.

The application of nanoparticles can be beneficial for enhanced oil recovery, drilling and completion, produced fluid treatment.

1.2 Problem formulation

To improve the lubricity and shale swelling properties of water based mud the addition of nanoparticles may be beneficial and this thesis will address:

- Effect of nanoparticles concentration (MWCNT) in convention drilling fluids
- Effect of pH
- Effect of temperature
- Effect of mixing

1.3 Objective

The primary objective of this thesis is to formulate a drilling fluid modified with MWCNT nanoparticles, characterize how the different properties are changed through experimental work and to perform simulation studies.

1.4 Methodology

The research methodology is divided into three parts (Figure 1.2). The literature study deals with the theory used to describe the behavior of the drilling fluid, application of nanoparticles in drilling fluid and the additives used. In the experimental part the focus was on formulating a nanoparticle based laboratory drilling fluid and characterizing its rheology, tribology, filtrate loss and viscoelastic properties. While the last part was a simulation study of the relevant fluids.

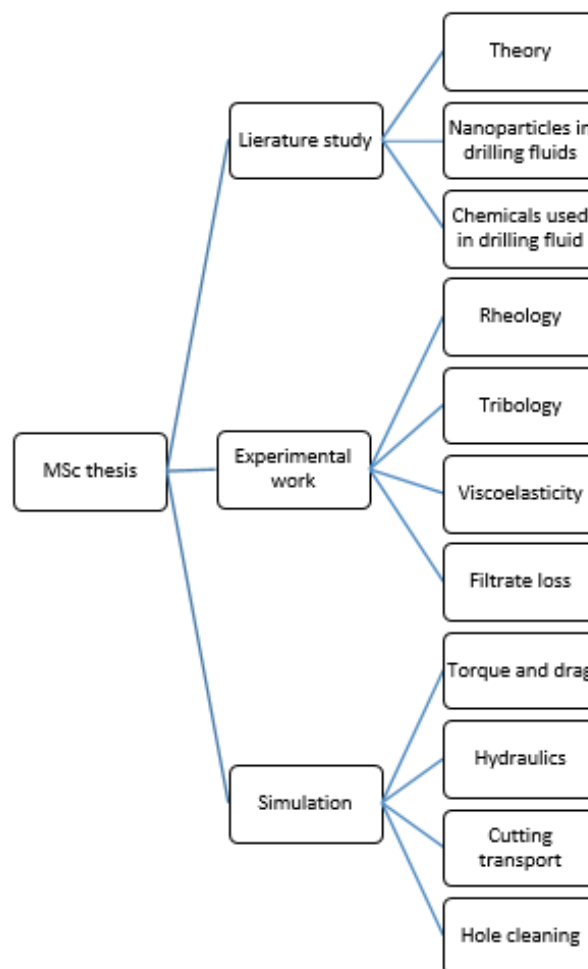


Figure 1.2: Investigation methodology

2 literature study

This chapter present the reviewed application of MWCNT nanoparticles in drilling fluid and the description of chemical additives used in this thesis work.

2.1 Application of Nanoparticles in drilling fluids

Ismail et al. (2014) [4] published a paper where they have tested the effect of multi-walled carbon nanotube (MWCNT) on the rheological properties in water based drilling mud. In this study, they investigated different concentration of nanoparticles and for different temperatures. This paper revealed that the filtrate loss of the drilling fluid is reduced with 65 % and mud cake thickness with 30 % when 1 g of MWCNT is added into 50 ml of surfactant solution. To obtain a good dispersion, the mixture was ultra-sonicated for 4 hours. Plastic viscosity, yield point and gel strength increased when MWCNT were added to the water based drilling fluids. . Since nanoparticles got a large surface area to volume ratio, the nanoparticles builds structural barriers to the pore spaces that reduces the filtrate loss at HPHT conditions.

Baghbanzadeh et al. (2013) [5] investigated the effect of nanoparticles on rheology properties on distilled water. The viscosity of the nanofluids increased with MWCNT concentration where the presence of MWCNT is the reason for increasing viscosity because of the interaction between the liquid molecules and particles. Some nanotubes are very entangled which leads to forming of a skein when dispersed into the fluid, which results into a nanofluid with highly viscous behavior at rest. When the shear stress increases, the nanotubes are organized along the flow directions that contributes to lower viscosity. The advantage of MWCNT is that their tubular structure reduced the ability of their movement in the mixture and between the layers of the fluid.

Rafi et al. (2017) [6] presented a review of recent advances of nanoparticle modification of drilling fluids. The review showed that the addition of nanoparticles usually lead to improvement for rheological properties, lower filtrate loss, thinner and more compact filter cake, which leads to lower permeability and porosity, higher thermal conductivity, consistent rheology and thermal stability at HPHT-conditions. The addition of nanoparticles in water-based mud has resulted in reduced friction coefficient, almost

making Water based muds friction coefficient as low as friction coefficient for oil-based muds. The nanoparticles also leads to better wellbore stability when drilling through shale formations, where the nanoparticles in the drilling fluid plug and seal small pores and fractures.

Aftab et al. (2017) [7] wrote a review of different drilling fluids and their effect in wells and highlighted the need for new wells to overcome a potential fossil fuel crisis. Then it is necessary to drill HPHT wells and where a solution may be drilling fluids with nanoparticles as an additive. The conclusion was that nanoparticles could be a possible solution to solve problems while drilling under extreme conditions, where drilling fluids with nanoparticles decrease the risk for differential pipe sticking, wellbore instability, shale swelling, high filtrate volume and high friction coefficient.

2.2 Description of chemicals used in this study

2.2.1 Bentonite

To provide the correct viscosity, bentonite is used in this thesis. Bentonite is a form of clay formed by weathering of volcanic tuffs. In bentonite, a high concentration of smectite group minerals is found, in addition to smectite there are up to 50% illite or kaolinite and 10-30% non-clay minerals. Smictite minerals were earlier referred to as montmorillonite, and montmorillonite is still the predominant term in the oil industry. The properties of bentonite is the ability to swell, capacity for ion exchange and thixotropy, these properties is linked to the presence of montmorillonite [8][9][10].

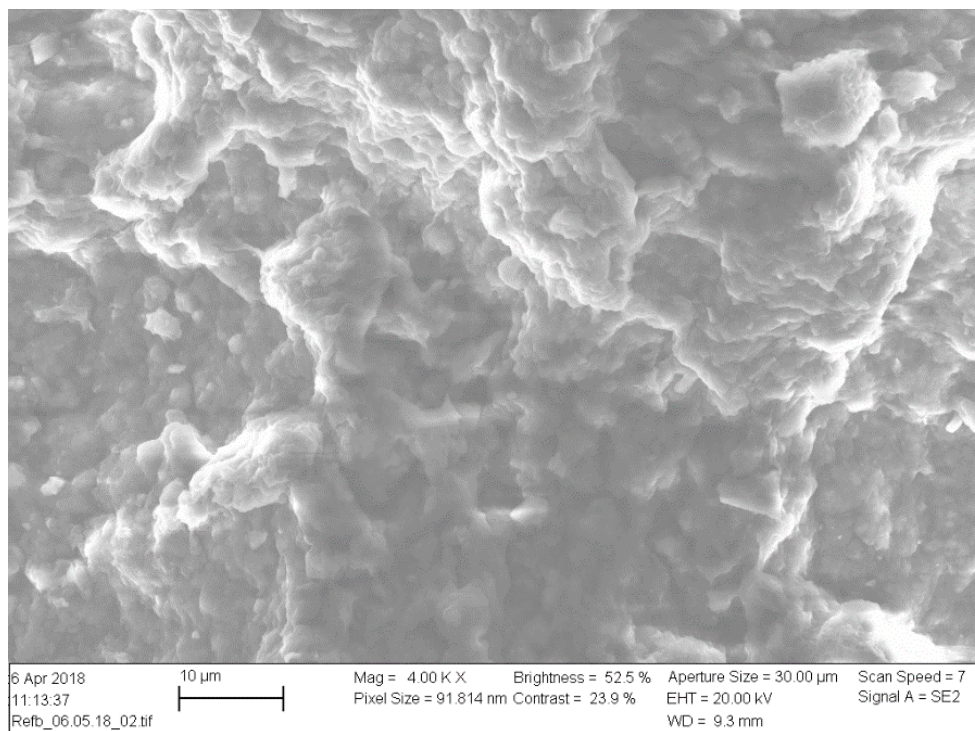


Figure 2.1: SEM picture of Bentonite from a filter cake (Christian Erevik Riise, 2018)

Octahedral sheet and tetrahedral sheets are two fundamental building blocks in bentonite. The octahedral sheet consist of two planes densely packed with either oxygen or hydroxyl molecules, where the oxygen or hydroxyl molecules surrounds alumina molecules and form an octahedral structure. Iron and magnesium molecules may replace

the aluminum molecule. If the alumina molecule is replaced, a brucite structure is formed.

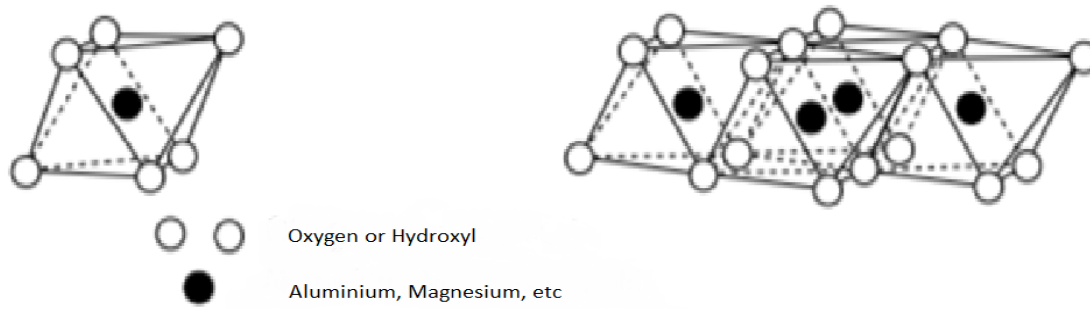


Figure 2.2: Structure of octahedral structure and octahedral sheet, modified after Riise [9]

The tetrahedral sheet consist of a tetrahedral structure with oxygen or hydroxyl atoms in the corner of the structure, while a silica is placed in the center of the structure. Several silica tetrahedral can form into larger aggregates where the structure is hexagonal.

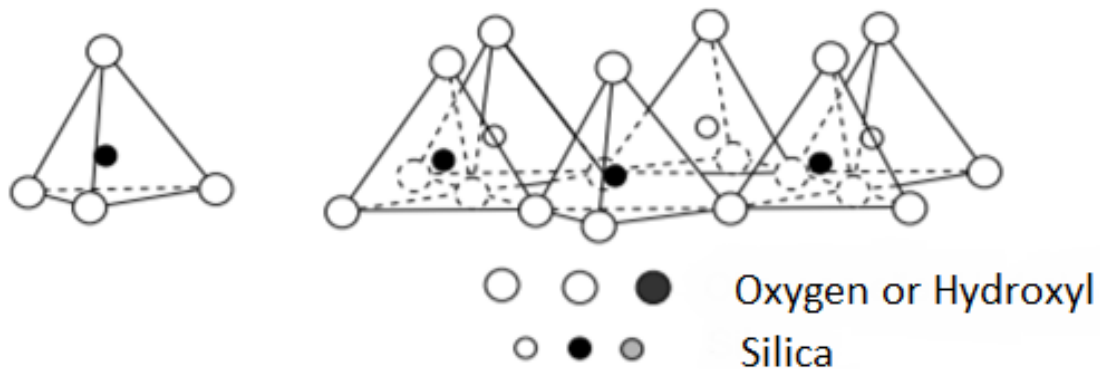


Figure 2.3: Structure of silica tetrahedral and layer structure of tetrahedral structural , modified after Riise [9]

These two fundamental building blocks will now bound together and form a crystal structure where they share the oxygen or hydroxide atom. Montmorillonite mineral is

formed by an octahedral layer with one tetrahedral layer at bottom and top of the octahedral layer [8][9](Figure 2.4).

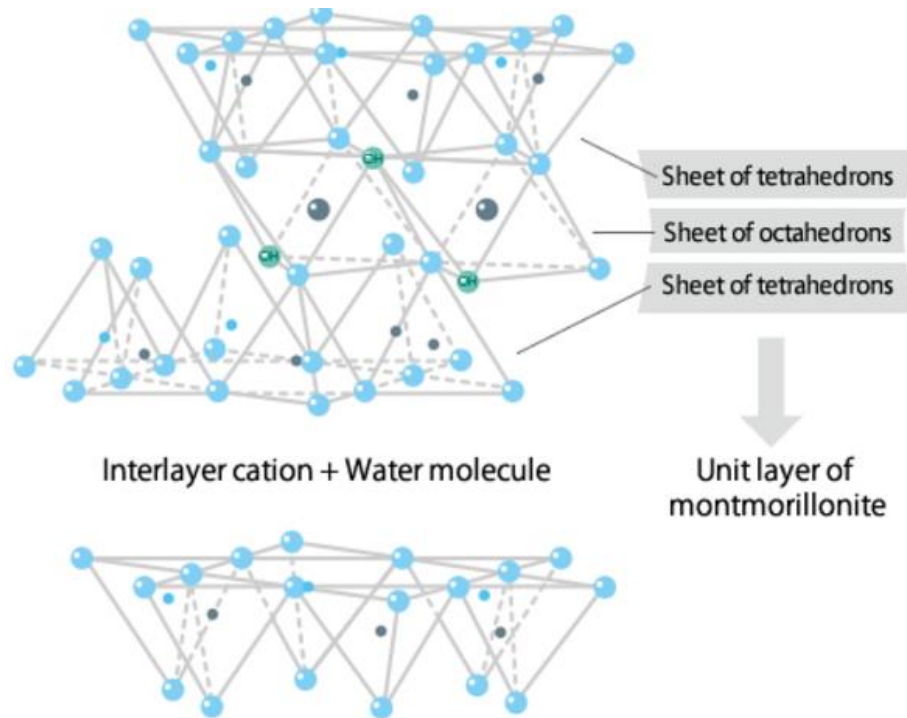


Figure 2.4: Montmorillonite structure [11]

Particle associations

Flocculated System: If a solution got net attractive forces between the particles, the system is flocculated. If a solution is flocculated, the particles will form into clusters, where the particles attach end-to-end or surface-to-surface. The particles will form into clusters when the end of the clay crystals is positively charged and the particles will form a three-dimensional loose network. Viscosity, filtrate loss and yield point will increase if a water based drilling mud is flocculated [8][9].

Deflocculated system: If a solution only undergo repulsive forces between individual particles, the system is deflocculated. A condition for deflocculated system is that the particles got the same electric charge, this may happen in alkaline fluids where the particles are negatively charged. To obtain a complete deflocculated system it is necessary to add a deflocculating chemical (Lignosulfonate used in this thesis) where the deflocculating chemicals will neutralize the positive charged particles. In a deflocculated system, the filtrate loss and yield point will be low due to repulsive forces between the clay particles [8][9].

Aggregated System: If a system is aggregated, the particles are attached together in aggregates. In the system, crystals are packed into aggregates, and the system is free from individual crystals. The sheets may be separated when montmorillonite is in contact with water due to hydration and mechanical impact [8][9].

Dispersed System: If all suspended particles in a solution is split into individual crystals the system is dispersed. The particles, depending on pH, can be both positively and negatively charged at the edges while the particle surface may be negatively charge. This system may flocculate or deflocculates [8][9].

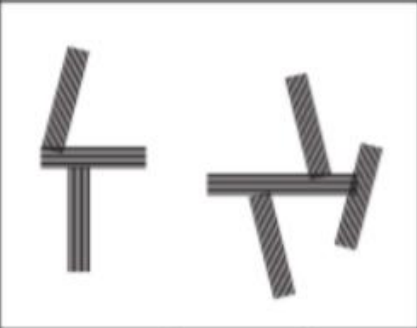



	Flocculated	Deflocculated
Aggregated		
Dispersed		

Figure 2.5: Arrangement of clay particles in drilling fluid [9]

2.2.2 Salt (KCl)

Potassium chloride reduce problems regarding shale swelling, where the inhibiting ion is potassium. Salt also effects polymers added into the drilling fluid where salt inhibit the untangle, elongation effect that arise when a polymer is added [9][12][13].

2.2.3 Duovis

During drilling fluid preparation, Duovis biopolymer was added along with bentonite in order to provide the drilling fluid thixotropic properties. In the oil industry, Duovis is used

in WBM since it helps to achieve viscosity and particles suspension without adding large quantities of bentonite. This makes Duovis ideal for horizontal wells with low annular velocities [13].

2.2.4 Lignosulfonate

Lignosulfonate has a wide application in water-based deflocculated drilling systems, the polymer has the ability to reduce flocculation and then reduce the yield point in the system. This results in reduced filtration loss. Lignosulfonate neutralize the attractive forces between the particles in the mud without affecting the viscosity due to hydration of the clay minerals. When lignosulfonate is adsorbed at the edges of clay particles, the balance of the forces acting on these clay particles changes from an attractive force to a repulsive force and the system is deflocculating. This chemical can be used in drilling fluids with alkaline pH and higher salt levels and are very effective in mud with higher calcium levels. Caustic soda may needed, when using lignosulfonate, since this additives have a pH of 3 [13].

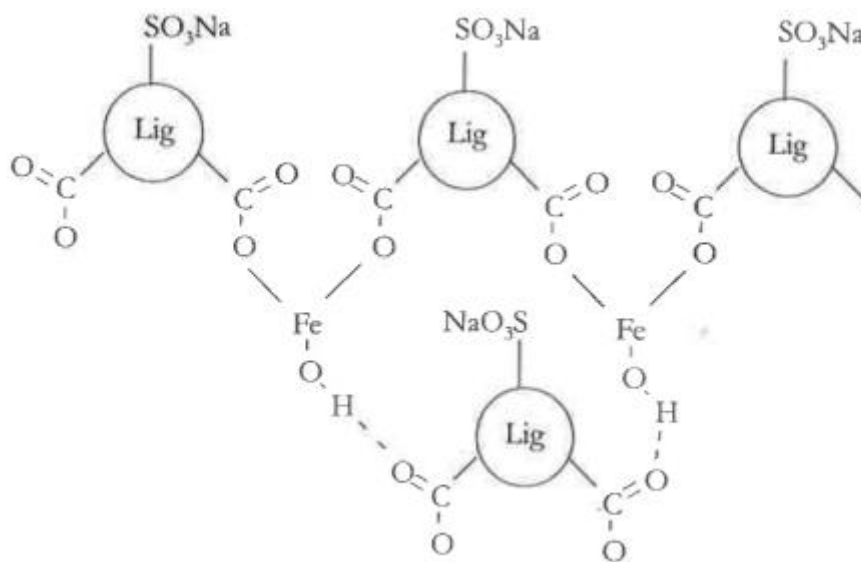


Figure 2.6: Structure of Lignosulfonate [9]

2.2.5 NaOH

NaOH was added to the drilling fluid to increase the pH. There are several reasons to maintain high pH values in a drilling fluid, where two important factors are less corrosion problems and that lignosulfonate works better [8].

2.2.6 MWCNT

Multi walled Carbon Nanotube are composed of concentrically nested multiple graphene sheets where the interlayer are quite similar to those of graphite where the structure either is a single graphene layer rolled up or several single-wall carbon nanotubes nested into each other. As the interlayer are quite similar to those of graphite, the addition of MWCNT in a polymer matrix may increase the effect of the different properties for the polymers, where small amounts improves thermal, electrical and mechanical properties. Since MWCNT is hydrophobic, it is more difficult to dissolve these particles in water, and sonication with use of surfactants is a good solution, where the energy from the sonication overcome van der Waals attractions between nearby tubes which results in disentanglement and greater dispersion [14][15]. MWCNT is produced at temperatures between 700-950 °C with a catalyst-based chemical vapor deposition. Ma-Hock et al. reported that inhalation exposure of MWCNT not lead to toxicity [16].

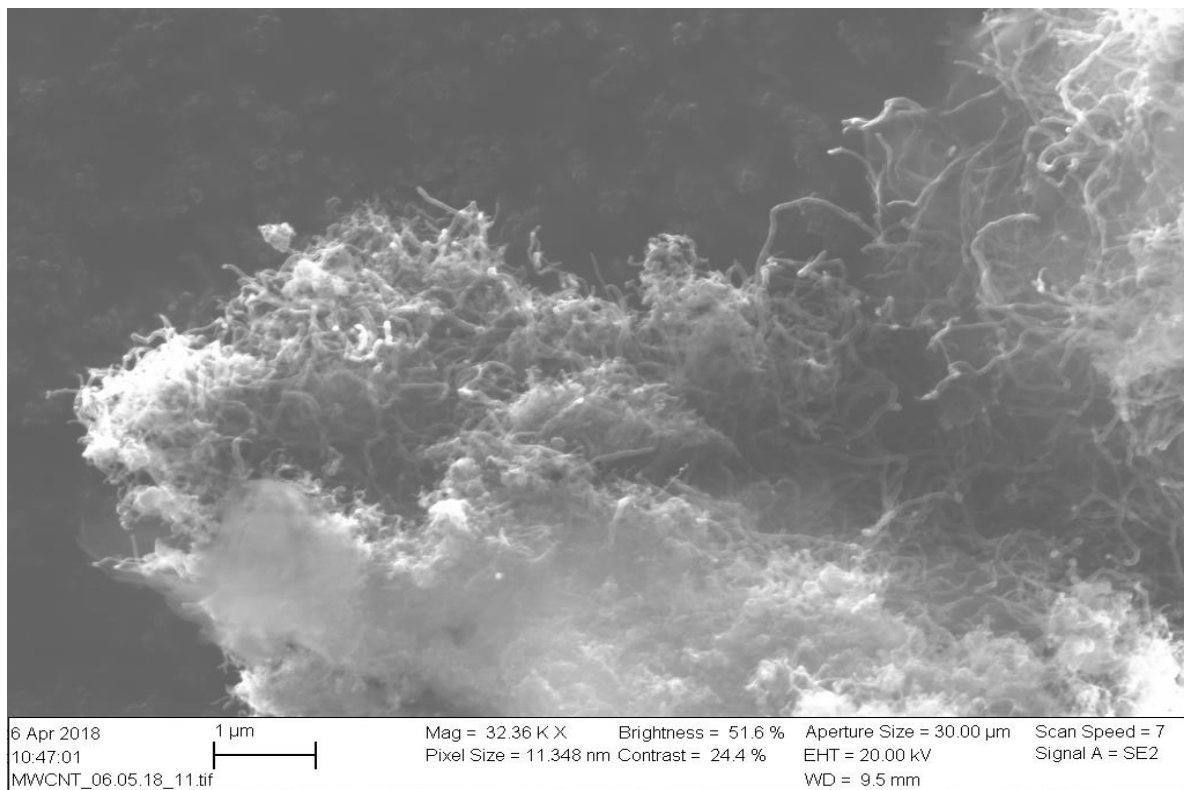


Figure 2.7: Scanning electron microscopy (SEM) image of entangled MWCNT particles. (Christian Riise, 2018)

3 Theory

In this chapter, the relevant theory for the experimental works and simulation is reviewed.

3.1 Rheology

The term rheology deals with the study of the deformation and flow of matter. To solve problems regarding hole cleaning and hole erosion, suspension of cuttings, drilling fluid treatment and hydraulics calculations it is necessary to apply rheological properties for evaluating drilling fluid behavior. There are two different types of rheology models, which are Newtonian and Non-Newtonian. A Newtonian fluid have a linear relationship between shear stress and viscosity while in a Non-Newtonian fluid the stress is proportional to the rate of strain [17][18].

Viscosity

The viscosity of the mud is a measure of fluid resistance to flow under an applied shear stress. The fluid resistance occurs due to friction forces between the different substances and attractive forces between electrical charged particles or ions in the mud [9]. The viscosity of a fluid is determined by the following properties: temperature, pressure, shear stress, time and other physical/chemical processes. The shear-stress is related to the shear rate through the equation [17][18]:

$$\tau = \mu\gamma \quad (1)$$

Where:

$\tau = \textit{shear stress}$

$\mu = \textit{viscosity}$

$\gamma = \textit{Shear rate}$

For Newtonian liquids, μ is sometimes denominated the coefficient of viscosity. However, for most liquids μ is not a coefficient, but a function of the shear rate (γ). The flow properties of a drilling mud are commonly characterized by the following measurements:

- Plastic viscosity
- Yield point
- Gel strength
- Apperant viscosity

Plastic viscosity (PV)

The plastic viscosity characterize the mechanical friction that occurs in the drilling fluid. Mechanical friction occurs between the particles in the drilling fluid, between the particles and the liquid phase and between the different liquid elements. The plastic viscosity depends on the viscosity of the fluid and the concentration, size and shape of the particles in the drilling fluid [9]:

$$PV = \theta_{600} - \theta_{300}, \quad [cP] \quad (2)$$

θ_{600} = Fann viscometer reading at 600 RPM shear rate.

θ_{300} = Fann viscometer reading at 300 RPM shear rate.

Yield point (YP)

The Yield point characterize the fluid resistance in the drilling fluid from attractive forces between particles due to electrical forces. Yield point is dependent on shear rate and reduces with an increase in shear rate [9]:

$$YP = \theta_{300} - PV \quad \left[\frac{lbs}{100} ft^2 \right] \quad (3)$$

Gel strength

Gel strength express the fluids thixotropic properties, i.e. shear rate is dependent on shear time [9].

Apparent viscosity and Marsh funnel

A measurement of the fluids total viscosity. Influenced by plastic viscosity, yield point and gel strength [9].

3.2 Rheological models

Most of the drilling fluids exhibit non-Newtonian behavior. There are several rheology model available in literature. Non-Newtonian fluids are the fluids that do not conform to a direct proportionality between shear stress and shear rate, and there is still not a universal equation that has been proved to successfully describe the rheogram of all fluids[17][19]. However, the yielded power law model as shown in red describe better than the others (Figure 3.1). This will be evaluated later.

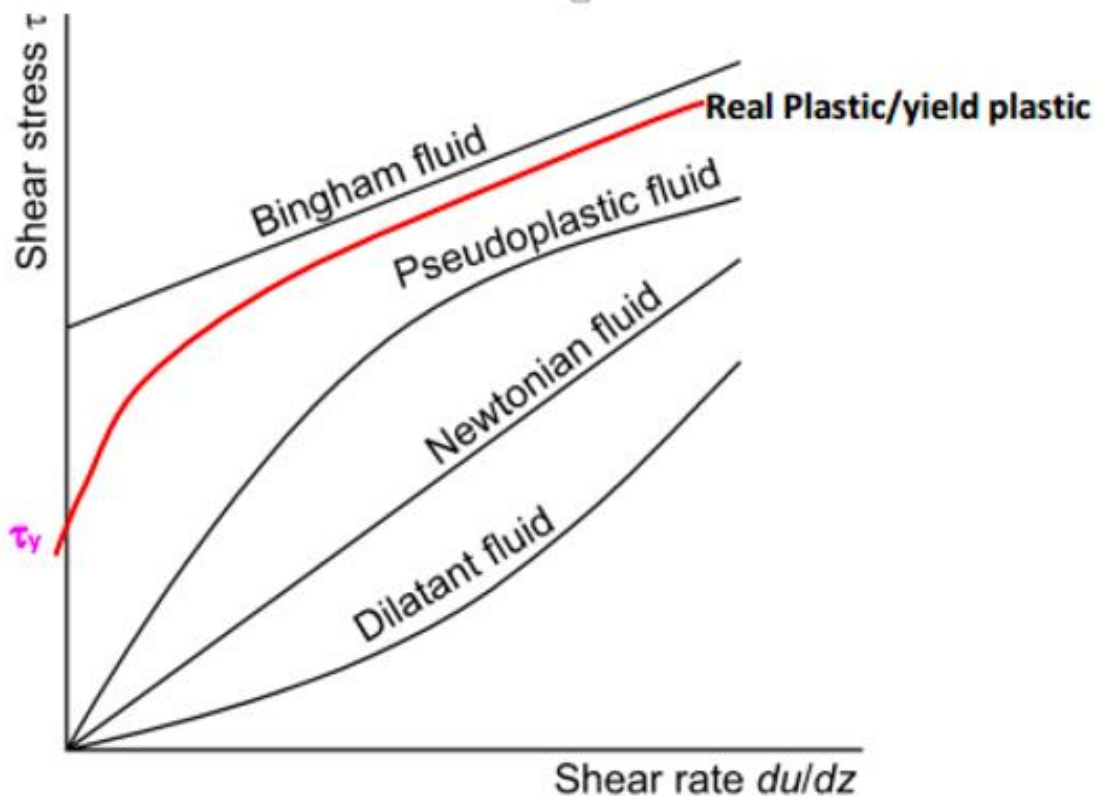


Figure 3.1: Shear stress vs shear rate for different types of fluids[19]

3.2.1 Newtonian fluid

A Newtonian fluid obey Newton's law of viscosity. In a Newtonian fluid the shear stress is proportional to shear rate. The equation used to describe a Newtonian fluid is given by [19]:

$$\tau = \mu\gamma \quad (1)$$

τ = shear stress

μ = viscosity of fluid

γ = shear rate, rate of strain or velocity gradient.

To characterize the fluid behavior we use a viscometer, to transform the laboratory data units from the viscometer to field engineering units we use the following conversion factors:

$$\gamma = 1.703 * RPM \tag{4}$$

$$\tau = 1.067 * Reading \tag{5}$$

Table 3.1: Viscometer readings for Reference fluid.

RPM	Reading
600	24
300	18
200	16
100	13
6	7
3	6

Table 3.2: Field unit transformed data

γ , shear rate sec^{-1}	Shear stress, τ lbf/100sqft
1022	26
511	19
341	17
170	14
10	7.5
5	6.4

Viscosity can be found by the following equation[17]:

$$\mu = 47880 * slope/100 \tag{6}$$

3.2.2 Non-Newtonian fluids

Fluids that does not obey the Newtonian law of viscosity are characterized as non-Newtonian. Most of the drilling fluids are non-Newtonian and will behave as a Bingham

plastic fluid. Complex mixtures like pastes, slurries, polymer solutions, gels are generally non-Newtonian. Non-Newtonian fluids can be independent of time under shear or dependent upon duration of shear [8][19].

Bingham plastic model

Fluids that have both a yield point and a suspension of solid particles are best described by the Bingham plastic model. Visualization of the Bingham plastic model is straightforward, and as such is widely used. The downside of the model is that it does not accurately represent the behavior of the drilling fluid at very low or high shear rates. The equation for Bingham plastic model is given by [17]:

$$\tau = \mu_p \gamma + \tau_y \quad (7)$$

Where:

τ = Shear stress

μ_p = Plastic viscosity

γ = Shear rate

τ_y = Yield point

The parameters can be read from graph or calculated like:

$$\mu_p = R_{600} - R_{300} \quad (8)$$

$$\tau_y = R_{300} - \mu_p \quad (9)$$

Where:

R_{600} = Shear rate at 600 RPM

R_{300} = Shear rate at 300 RPM

Power Law Model

The Power Law model give a better representation of the drilling fluids than the Bingham model. While the Bingham plastic model assumes a linear relationship between shear stress and shear rate, the Power Law model is based on a logarithmic relationship. The Power law model makes it possible to use all values of shear rates. The Power Law model is given by the following equation [17][9]:

$$\tau = K\gamma^n \quad (10)$$

K = consistence index.

n = flow behavior index.

Estimations of Power-Law parameters can be made by the following equations:

$$n = 3.32 \log\left(\frac{R_{600}}{R_{300}}\right) \quad (11)$$

$$K = \frac{R_{300}}{511^n} = \frac{R_{600}}{1022^n} \quad (12)$$

Herschel-Bulkley Model

Unlike Bingham Plastic and Power Law model which is described by two parameters, the Herschel-Bulkley Model defines a fluid by three-parameter and can be described by the following equations[17]:

$$\tau = \tau_0 + K\gamma^n \quad (13)$$

τ = Shear stress

τ_0 = Yield stress

K = Consistency index

γ = Shear rate

n = Flow index.

Where:

$$\tau_0 = \frac{\tau^{*2} - \tau_{min}\tau_{max}}{2\tau^* - \tau_{min} - \tau_{max}} \quad (14)$$

Where the parameter τ^* is determined from the corresponding geometric mean of the shear rate, γ^* , and is determined by:

$$\gamma^* = \sqrt{\gamma_{min} - \gamma_{max}} \quad (15)$$

Unified model

The Unified model is a simplified version of the Herschel-Bulkley model. The difference between the Herschel-Bulkley model and Unified model is based on the determination of the yield strength (τ_{yl}). The Unified model is described by [17]:

$$\tau = \tau_y + K\gamma^n \quad (16)$$

Where:

$$\tau_y = 1.066*(2Q_3-Q_6) \quad (17)$$

Robertson and Stiff Model

The Robertson and Stiff Model is superior to Bingham and Power-Laws models, but due to its complexity in evaluating the three different parameters it has found little use in the drilling industry. The Robertson and Stiff Model has superior fit of rheological stress/rate of strain data. The basic equation is [17]:

$$\tau = A(\gamma + C)^B \quad (18)$$

Where A,B and C are model parameters. A and B are similar to the parameters K and n of the Power-Law model. The C parameter is a correction factor to the shear rate and the term ($\gamma+C$) represent the effective shear rate. The parameter C is given by[17]:

$$C = \frac{\gamma_{max}\gamma_{min}-\gamma^{*2}}{2\gamma^*-\gamma_{max}-\gamma_{min}} \quad (19)$$

Where γ^* is the shear rate value which is determined by interpolation from the shear stress, τ^* , [17]

$$\tau^* = \sqrt{\tau_{min} * \tau_{max}} \quad (20)$$

3.3 Torque and drag

In deviated wellbores it is important to overcome torque and drag to successfully complete the well, as issues related to torque and drag in highly deviated wellbores are more challenging to overcome. Torque and drag forces emerge from frictional forces which occur between tubulars and the wellbore, and work against the direction of motion.

Excessive torque and drag can overcome the top drive capacity and result in failure to land the casing or completion string. [20] To minimize torque and drag in highly deviated wells, and to improve drill string techniques it is very important to predict the frictional loads on the drill pipe. This is done by performing drill string mechanism simulation studies using software such as Wellplan [20].

Drag

Compared to a freely rotating drill string, drag is the additional load resulting from frictional forces generated by the drill strings contact with the wellbore. When pulling out of the well the drag load is positive, while negative when running into the hole. As the Johansick model is implemented in the WellPlan™ software, this model is reviewed in the following. Figure 3.2 shows a drill string divided into modelling segments [19][20].

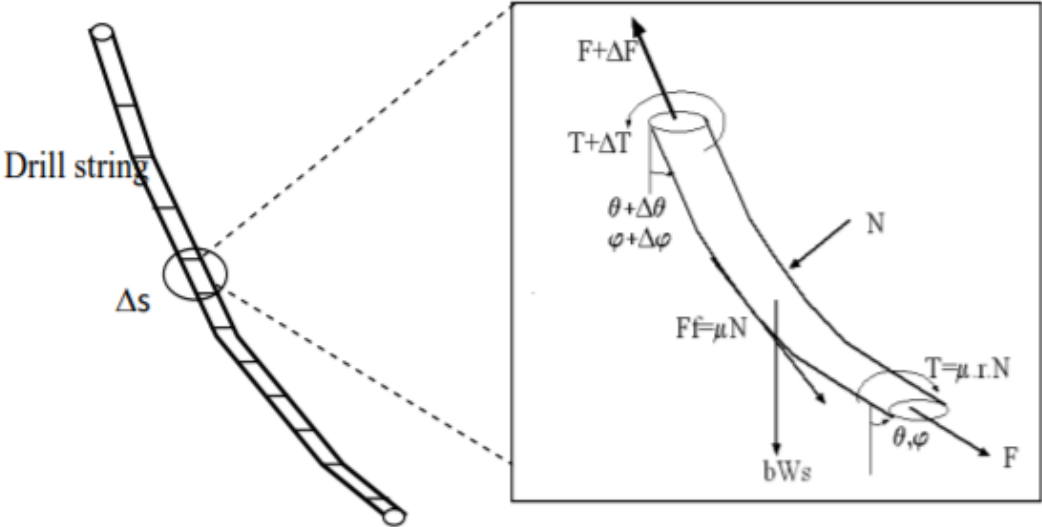


Figure 3.2: Drill string divided into modelling segments and the load on each segment [19]

The individual segments are loaded at the top and the bottom with either compressive or tensile loads, as seen in Figure 3.2. To obtain Johansick first order differential force, it is necessary to balance between the net force and the vector sum of the axial component of the weight, W and the friction force. The first order differential force is a function of well inclination and azimuth [19]:

$$\frac{dF}{ds} = \pm\mu \left(\sqrt{\left(\beta w_s \sin\theta + F \frac{d\theta}{ds}\right)^2 + \left(F \sin\theta \frac{d\varphi}{ds}\right)^2} \right) + \beta w_s \cos\theta \quad (21)$$

- $\varphi = azimuth$
- $\theta = inclination$
- "+" = *running out of the hole*
- "-" = *running into the hole*

Torque: To overcome the frictional forces exerted on the drill pipe during rotation, it is necessary to apply sufficient torque to the drill string. In a deviated well, torque loss is a major limiting factor to how long it is possible to drill since the torque loss may be significant. In the simulation it is important to stay within the operation window, otherwise drill pipe failure may occur when the make-up torque of a connection is exceeded [19][20]. The torque loss is expressed as [19]:

$$T_{i+1} = T_i + \sum_{i=1}^n \mu_t r_i N_i (S_{i+1} - S_i) \quad (22)$$

Where:

- T_i = Torque at bit.
- μ_t = tangential coefficient of friction given as [19]:

$$\mu_t = \mu \frac{\Omega r}{\sqrt{(\Omega r)^2 + v_a^2}} \quad (23)$$

$$- \Omega = \frac{2\pi x n}{60} \quad (24)$$

- v_a is axial velocity and - n is number of rotation.

3.4 Viscoelasticity

Drilling fluids exhibit both viscous and elastic responses under deformation. Fluids having such properties are named as viscoelastic fluids. To evaluate important parameters such as gel structure, gel strength, and solid suspension, characterization of viscoelastic properties of drilling fluid are important. Viscoelasticity strongly depends on temperature and gelling time. Viscoelastic fluids can show both linear and nonlinear viscoelastic

behavior. In the nonlinear viscoelastic range the viscous property is dominant, while elastic property is dominant in the linear range. Drilling fluids are usually in the nonlinear range, but under infinitesimal deformation, the gel structure shows viscoelastic response to the deformation. Since a purely viscous model may not be sufficient to model these phenomena, it is necessary to use a viscoelastic model to characterize the response of drilling fluids in this range of strain. If the temperature increases the linear viscoelastic, storage modulus, loss modulus and complex viscosity range decreases. This plays an important role for gel structure, gel strength, barite sag, hydraulic modelling and solid suspension. To determine the linear viscoelastic range and detect the structural stability, gel strength and dynamic yield point it is possible to use oscillatory testing, were amplitude sweep test is used. To quantify the viscoelastic properties, the elastic (storage) modulus (G') and viscous (loss) modulus (G'') has to be measured [21][22].

Viscoelastic theory

To find the applied shear strain (γ) and the measured shear stress (τ), the following formulas could be used [23]:

$$\gamma(t) = \gamma_o \sin(\omega t) \quad (25)$$

$$\tau(t) = \tau_o \sin(\omega t + \delta) \quad (26)$$

$$\tau(t) = \tau_o [\sin(\omega t) \cos\delta + \cos(\omega t) \sin\delta] \quad (27)$$

$$\tau(t) = \gamma_o \left[\left(\frac{\tau_o}{\gamma_o} \cos\delta \right) \sin(\omega t) + \left(\frac{\tau_o}{\gamma_o} \sin\delta \right) \cos(\omega t) \right] \quad (28)$$

$$\tau(t) = \gamma_o [G' \sin(\omega t) + G'' \cos(\omega t)] \quad (29)$$

From the following equations, loss and storage modulus can be found [23]:

$$G' = \left(\frac{\tau_o}{\gamma_o} \cos\delta \right) \quad (30)$$

$$G'' = \left(\frac{\tau_o}{\gamma_o} \sin\delta \right) \quad (31)$$

The damping factor is found by:

$$\tan\delta = \left(\frac{G''}{G'}\right) \quad (32)$$

$$\delta = \tan^{-1}\left(\frac{G''}{G'}\right) \quad (33)$$

Where:

δ = phase angle.

Oscillatory amplitude sweep test

One form of oscillatory test is the amplitude sweep test which are performed at variable amplitudes, while keeping the frequency at constant value. To determine the linear viscoelastic range, where the range of strain G' and G'' are constant, it is necessary to determine the response of the fluid, where deformation changes from linear viscoelastic response to nonlinear response. The sample will be deformed viscoelastic under small strain, when the strain is increased to a critical strain the structure of the sample will be irreversibly deformed [21].

In the linear viscoelastic (LVE) range, where the amplitude values are low, the Storage Modulus (G') and the Loss Modulus (G'') are constant. By analyzing the LVE range, it is possible to describe the viscoelastic character of a sample. If $G' > G''$, the elastic behavior dominates the viscous behavior. If the elastic behavior dominates the viscous behavior the fluid has characteristics as a solid or a gel. If $G' < G''$ the viscous behavior dominates the elastic one and displays the character of a liquid. If $G' = G''$, the fluid behaves like equal portion of elastic and viscous behavior. At this point one can determine the flow point of the fluid, where the fluid starts to flow [21].

3.5 Hydraulics

Hydraulics is one of the most critical parameters that affects the performance of the drilling fluid, where an optimized system will make the maximum usage of the pumps power. To achieve an optimized system, it is necessary to minimize the energy loss from friction in the circulating system. The pump pressure in the circulating system equals to the sum of these forces [2]:

$$p_p = \Delta p_s + \Delta p_{dp} + \Delta p_{dc} + \Delta p_{mt} + \Delta p_b + \Delta p_{dca} + \Delta p_{dpa} \quad (34)$$

Where:

- p_p = pump pressure
- Δp_s = pressure loss in surface equipment
- Δp_{dp} = pressure loss inside drill pipe
- Δp_{dc} = pressure loss inside the drill collars
- Δp_{mt} = pressure loss inside the mud motor
- Δp_b = pressure drop at the bit
- Δp_{dca} = pressure loss in the drill collar annulus
- Δp_{dpa} = pressure loss in the drill pipe annulus

To maintain the correct equivalent circulating-mud density (ECD) during drilling is important, this to avoid potential kicks and losses, ECD takes friction into account and is given by [24]:

$$ECD = \rho_{st} + \frac{\Delta P_{annulus}}{g.TVD} \quad (35)$$

- ρ_{st} = *Static mud density*
- ΔP = *Pressure loss in annulus*
- TVD = *True veritcal depth*

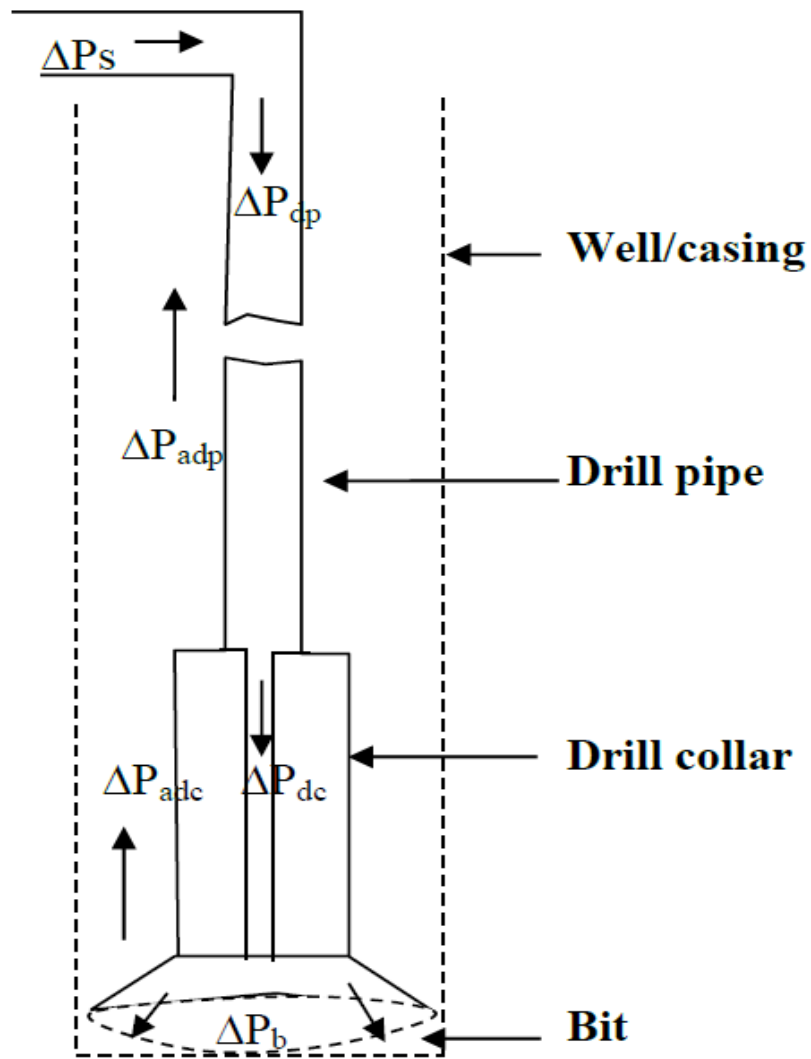


Figure 3.3: Circulation system and friction pressure losses [17]

For the analysis of the hydraulic performance of the formulated drilling fluids used in this thesis, the Unified model was used. This model is presented in Table 3.3 [17]. Sadigov have demonstrated that this model gives a good prediction with experimental data [25].

Table 3.3: The equations used in the Unified Model [17]

Unfiled Model	
Pipe Flow	Annular Flow
$\mu_p = R_{600} - R_{300} \cdot [cP] \quad \tau_y = R_{300} - \mu_p \cdot \left[\frac{lbf}{100ft^2} \right] \quad \tau_0 = 1.066 * (2 * R_3 - R_6)$	
$n_p = 3.32 * \log \left(\frac{2 * \mu_p + \tau_y}{\mu_p + \tau_y} \right)$ $k_p = 1.066 \left(\frac{\mu_p + \tau_y}{511^{n_p}} \right)$	$n_a = 3.32 \log \left(\frac{2 * \mu_p + \tau_y - \tau_y}{\mu_p + \tau_y - \tau_y} \right)$ $k_a = 1.066 \left(\frac{\mu_p + \tau_y - \tau_0}{511^{n_a}} \right)$ $k = [lbf * \frac{sec^n}{100ft^2}]$
$G = \left(\frac{(3 - \alpha)n + 1}{(4 - \alpha)n} \right) * \left(1 + \frac{\alpha}{2} \right)$ $\alpha = 1$ for pipe $\alpha = 1$ for annulus	
$v_p = \frac{24.51 * q}{D_p^2}$	$v_a = \frac{24.51 * q}{D_2^2 - D_1^2}$ $v = \left[\frac{ft}{min} \right]$
$\gamma_w = \frac{1.6 * G * v}{D_R} = [sec^{-1}]$	
$\tau_w = \left[\left(\frac{4 - \alpha}{3 - \alpha} \right)^n \tau_0 + (k * \gamma_w^n) \right] = \left[\frac{lbf}{100ft^2} \right]$	
$f_{laminar} = \frac{16}{N_{RE}}$ $f_{transient} = \frac{16 * N_{RE}}{(3470 - 1370 * n_p)^2}$ Turbulent: $f_{turbulent} = \frac{a}{N_{RE}^b}$ $a = \frac{\log(n) + 3.93}{50} \quad b = \frac{1.75 - \log(n)}{7}$	$f_{laminar} = \frac{24}{N_{RE}}$ $f_{transient} = \frac{16 * N_{RE}}{(3470 - 1370 * n_a)^2}$ Turbulent: $f_{turbulent} = \frac{a}{N_{RE}^b}$ $a = \frac{\log(n) + 3.93}{50} \quad b = \frac{1.75 - \log(n)}{7}$
$f_{partial} = (f_{transient}^{-8} + f_{turbulent}^{-8})^{-1/8}$	
$f_p = (f_{partial}^{12} + f_{laminar}^{12})^{1/12}$	$f_a = (f_{partial}^{12} + f_{laminar}^{12})^{1/12}$
$\left(\frac{dp}{dL} \right) = 1.076 * \frac{f_p v_p^2 * p}{10^5 D_p} = \left[\frac{psi}{ft} \right]$ $\Delta_p = \left(\frac{dp}{dL} \right) * \Delta L = [psi]$	$\left(\frac{dp}{dL} \right) = 1.076 * \frac{f_a v_a^2 * p}{10^5 (D_2 - D_1)} = \left[\frac{psi}{ft} \right]$ $\Delta_p = \left(\frac{dp}{dL} \right) * \Delta L = [psi]$
$\Delta p_{nozzles} = \frac{156 * p * q^2}{(D_{N1}^2 - D_{N2}^2 - D_{N3}^2)^2} = [psi]$	

4 Experimental work

The primary objective of this thesis is to formulate a drilling fluid modified with nanoparticles and to characterize how the different properties are changed through experimental work. In this chapter, the formulated drilling fluid will be presented and characterized.

4.1 Description of equipment

Fann 35 viscometer

To measure the rheology of the drilling fluids, a Fann 35 viscometer was used. The different fluids were mixed for 5 minutes to ensure particle dispersion. The test was performed at 72°F, 130°F and 180°F. The Fann 35 viscometer uses a rotational cylinder to measure the rheology, that can be set to shear rates of 600, 300, 200, 100, 60, 30, 6 and 3 rpm.

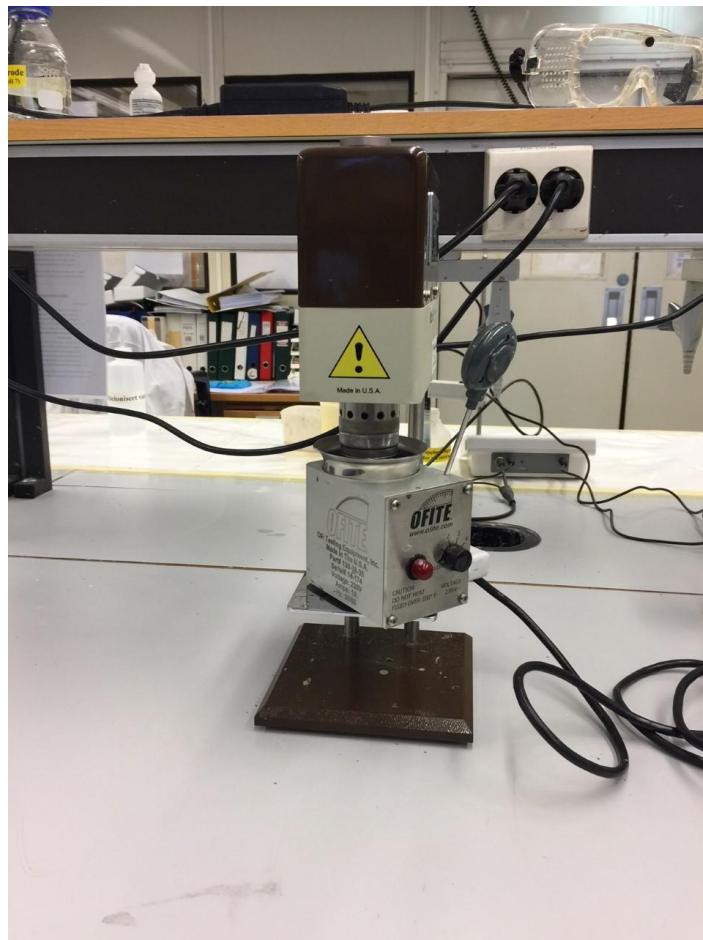


Figure 4.1: Picture of Fann 35 viscometer

Filtrate loss

An API static filter press as shown in Figure 4.2 was used to perform the filtrate loss tests. The different fluids were mixed for 5 minutes before the test to ensure a homogeneous fluid. The test was performed at 22°C and for 7.5 minutes.



Figure 4.2: Picture of filter press

pH

A pH-meter as shown in Figure 4.3 was used to determine the pH-values of the different drilling fluids. The pH-meter was calibrated before each test.

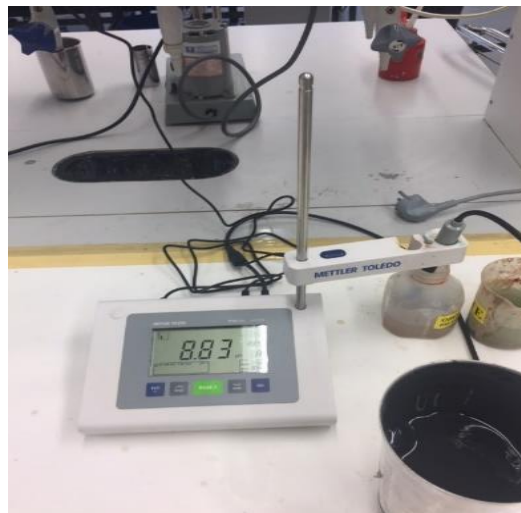


Figure 4.3: Picture of pH-meter

Tribometer

To conduct the friction test, an CSM DIN 50324 tribometer was used (Figure 4.4). The test was carried on at constant temperature (22°C), 5 N normal force at 6 cm/s for 9 minutes. The pin-on ball and disc were cleaned and checked for damage before each test to ensure correct measurement method and consistency.

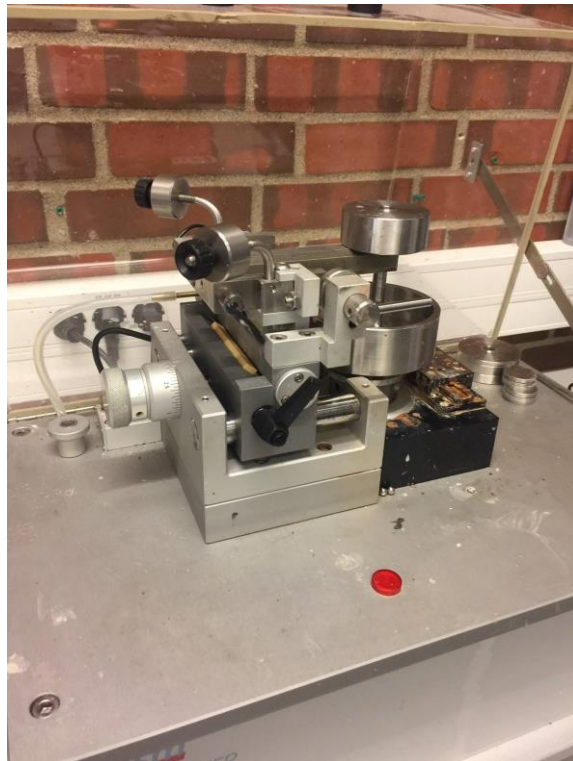


Figure 4.4: Picture of tribometer

Rheometer

The Anton Paar MCR 301 Rheometer (Figure 4.5) was used to conduct Oscillatory Amplitude Sweep test, which is used to determine the flow point, yield point and the linear viscoelastic range. The temperature was kept constant at 22 °C .To get a homogeneous mixture, the fluids were mixed in a Hamilton beach mixer before the rheometer testing, to get exact readings the rheometer test were conducted multiple times. The fluids were stirred magnetically while waiting for a new test. It was used a parallel plate, with a constant frequency at 10 rad/s and strain rate between 0.0005% and 100%



Figure 4.5: Rheometer with cooling apparatus

ICP-OES

Inductively Coupled Plasma-Optical Emission spectrometry were used to measure the concentration of ions in the filtrate fluids (Figure 4.6). This is a measurement well suited for analyzing trace metals in a solution. The different liquids were injected into an argon gas plasma contained by a strong magnetic field. The different elements in the fluid sample gets excited by the plasma and the electrons release energy at a characteristic wavelength as they return to their ground state, then the emitted light is measured by optical spectrometry[26].



Figure 4.6: Picture of Inductively Coupled Plasma-Optical Emission spectrometry

SEM – analysis

A Zeiss Supra 35VP scanning electron microscope was utilized to perform SEM imaging of the mud cake structure. The Zeiss Supra 35VP is fitted with a Gemini objective lens, capable to deliver solid resolution down to 20 V and 12 x to 1 000 000 x magnification [27].



Figure 4.7: Picture of Supra 40VP

4.2 Drilling fluid formulation

To find the optimum drilling fluid formulation, a screening test was conducted to see how the different concentrations of salt, Duovis and lignosulfonate in 500 g tap water and 25 g Bentonite affected the fluid. See Appendix A for the screening results. The drilling fluid listed in Table 4.1 will be selected and used as a reference for the rest of the experimental analysis, as this fluid gave realistic viscosities for a drilling fluid. To evaluate the effect of MWCNT in the Reference fluid, different concentrations was added.

Table 4.1: Additives in Reference fluid

Additives	Reference fluid
Water	500g
Bentonite	25g
Douvis	0.5g
Lignosulfonate	0.2g
KCL	5.0g

Except for the nanoparticles additives, if not stated, all fluids will have the same chemical composition, mixing, aging and testing procedure. The fluids were mixed in the following order since this is important for fluid behavior:

1. Water
2. Salt
3. MWCNT
4. Duovis
5. Lignosulfonate
6. Bentonite

In order to let the bentonite clay swell, the drilling fluid was aged for 24 hours. Afterwards the drilling fluids was further characterized with viscometer, filtrate loss, pH, friction coefficient, viscoelasticity, SEM analysis and filtrate fluid element analysis.

4.3 Effect of nanoparticle concentration (Room temperature data)

Different amounts of MWCNT was added to the reference drilling fluid system to examine how this will affect the system's rheological properties, friction coefficient, viscoelasticity and filtrate loss. See Table 4.2 for fluid formulation

Table 4.2: Formulation of the different drilling fluids.

Drilling fluids with different amounts of MWCNT					
	Ref	Ref + 0.1 g MWCNT	Ref + 0.2 g MWCNT	Ref + 0.5 g MWCNT	Ref + 1.5 g MWCNT
Water	500 g	500 g	500 g	500 g	500 g
Bentonite	25 g	25 g	25 g	25 g	25 g
KCl	5 g	5 g	5 g	5 g	5 g
Douvis	0.5 g	0.5 g	0.5 g	0.5 g	0.5 g
Lignite	0.2 g	0.2 g	0.2 g	0.2 g	0.2 g
MWCNT	0.0 g	0.1 g	0.2 g	0.5 g	1.5 g

4.3.1 Viscometer data

Figure 4.8 shows the viscometer data, of the drilling fluids containing MWCNT together with the reference fluid.

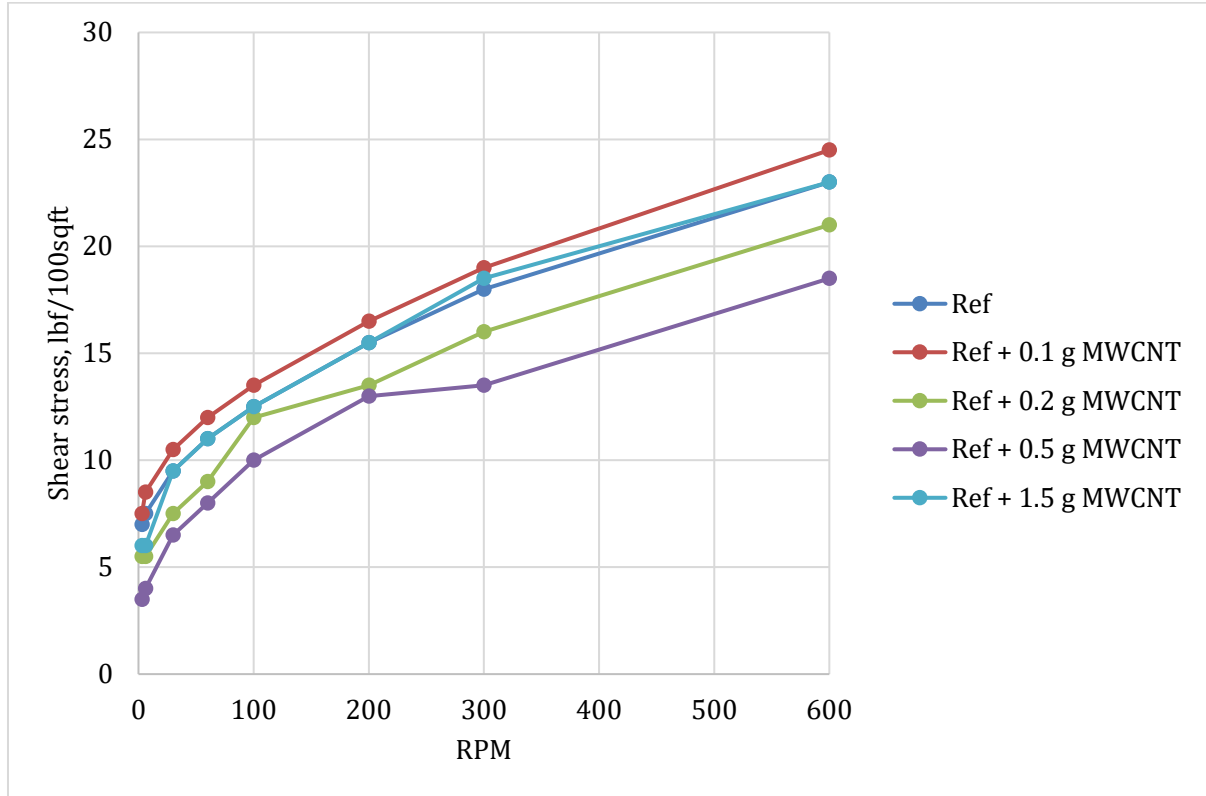


Figure 4.8: Viscometer data for MWCNT fluids.

When using MWCNT as an additive, data from the viscometer showed some changes to the fluids containing MWCNT compared to the reference fluid. The shear stress decreased for the two drilling fluids containing 0.2 g and 0.5 g MWCNT and increased for the drilling fluid containing 0.1 g MWCNT, while the fluids containing 1.5 g MWCNT were quite similar to the reference fluid. In Figure 4.9 and 4.10 the Bingham and Power-Law parameters from the viscometer readings are presented.

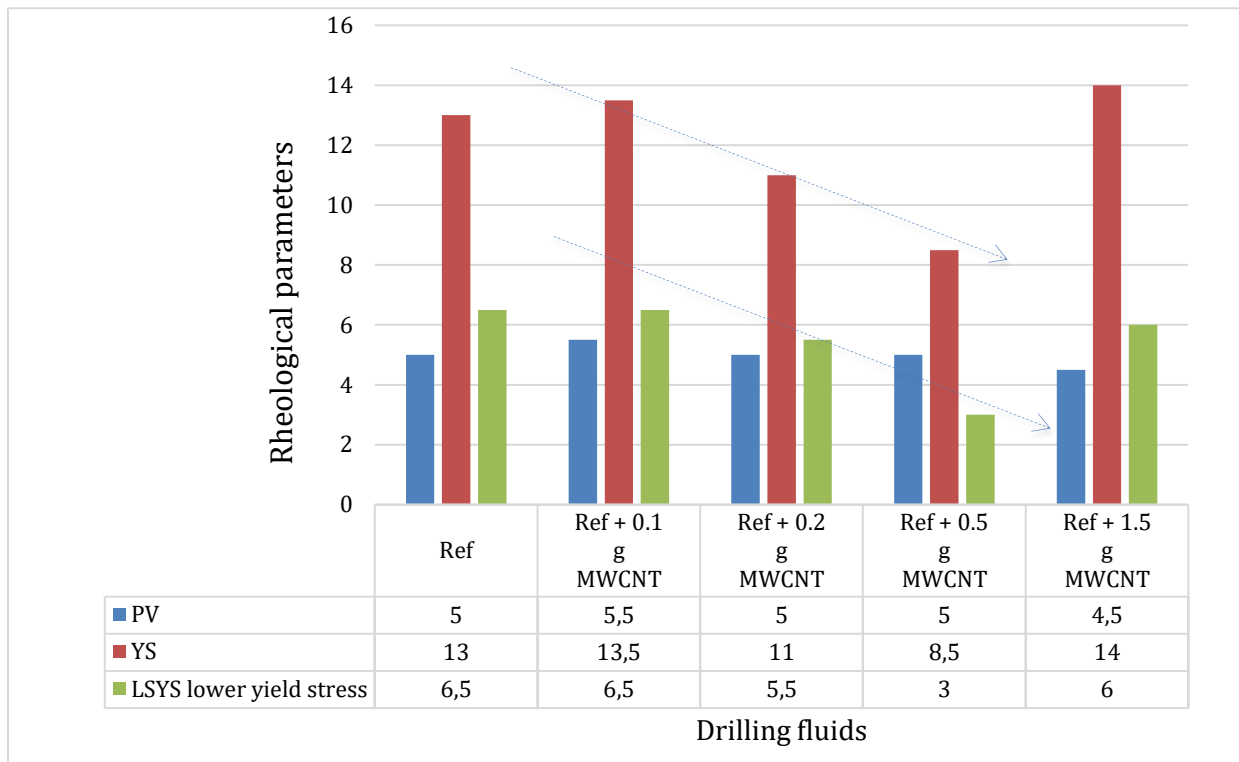


Figure 4.9: Bingham parameters for MWCNT fluids.

From the Bingham parameters, it can be observed that:

- PV increased with 9.1% for Ref + 0.1 g MWCNT, decreased with 11.1% for Ref + 1.5 g MWCNT and remained unchanged for the rest of the fluids.
- YS increased with 3.1% for Ref + 0.1 g MWCNT and with 7.14% for Ref + 1.5 g MWCNT, while a reduction in YS were observed for Ref + 0.2 g MWCNT with 18.2% and 52.9% for Ref + 0.5 g MWCNT.
- LSYS (Lower shear yield stress) remained unchanged for Ref + 0.1 g MWCNT, slightly decreased for Ref + 0.2 g MWCNT and Ref + 1.5 g MWCNT and dramatically decreased for Ref + 0.5 g MWCNT.

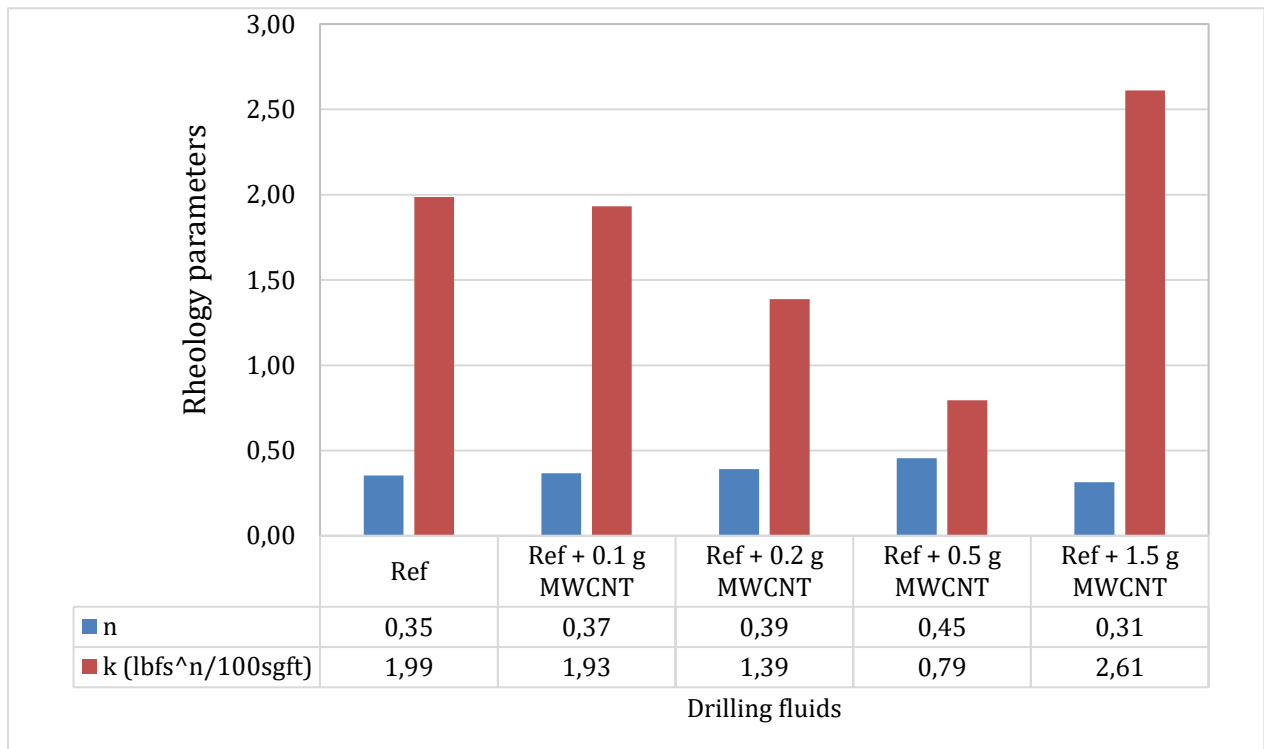


Figure 4.10: Power-Law parameters for MWCNT drilling fluids.

From the Power-Law parameters, it can be observed that:

- The flow index increased for all of the drilling fluids containing MWCNT compared with the reference fluid except Ref + 1.5MWCNT, which experienced a decrease. All the fluids has pseudo plastic behavior according to the flow index values.
- Regarding the consistency index values, the values decreased for all of the fluids except Ref + 1.5MWCNT. The largest decrease was observed for Ref + 0.5MWCNT which decreased with 150%. Ref + 1.5 MWCNT increased with 23.95%.

4.3.2 Tribometer

In this section, results from the frictional test measured with the CSM tribometer will be presented. The results from the tribometer provides information with respect to the lubricating effect of the different drilling fluids. To ensure that the data from the tribometer was reliable, the measurements were repeated several times. In Figure 4.11 the average values for the different drilling fluids are presented. Ref + 1.5 g MWCNT experienced the lowest friction coefficient. The tribometer readings decreased for all of the MWCNT treated fluids.

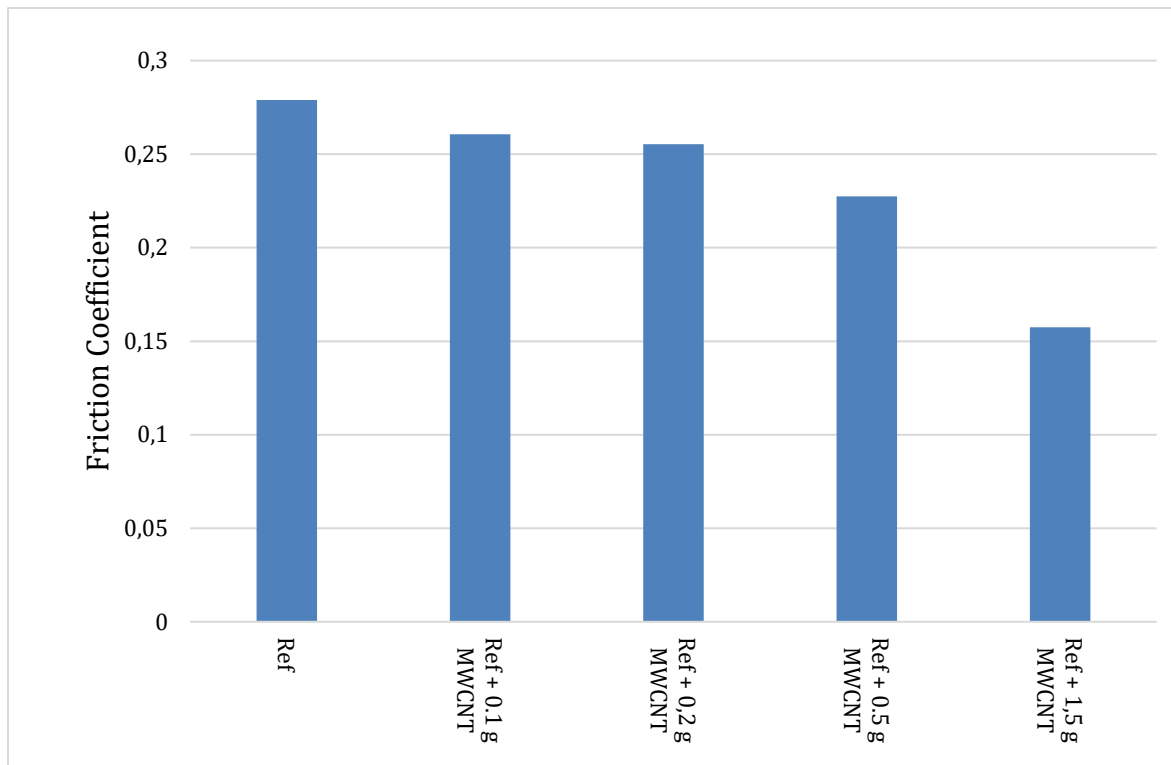


Figure 4.11: Coefficient of friction for the different drilling fluids.

The coefficient of friction changes in terms of percentage are presented in Figure 4.12. From the figure it can be seen that the reduction in friction is close to a linear trend line when the concentration of nanoparticles is increasing. The coefficient of friction decreased with 6.7% for Ref + 0.1 g MWCNT, 8.5% for Ref + 0.2 g MWCNT, 18.5% for Ref + 0.5 g MWCNT and 43.6% for Ref + 1.5 g MWCNT.

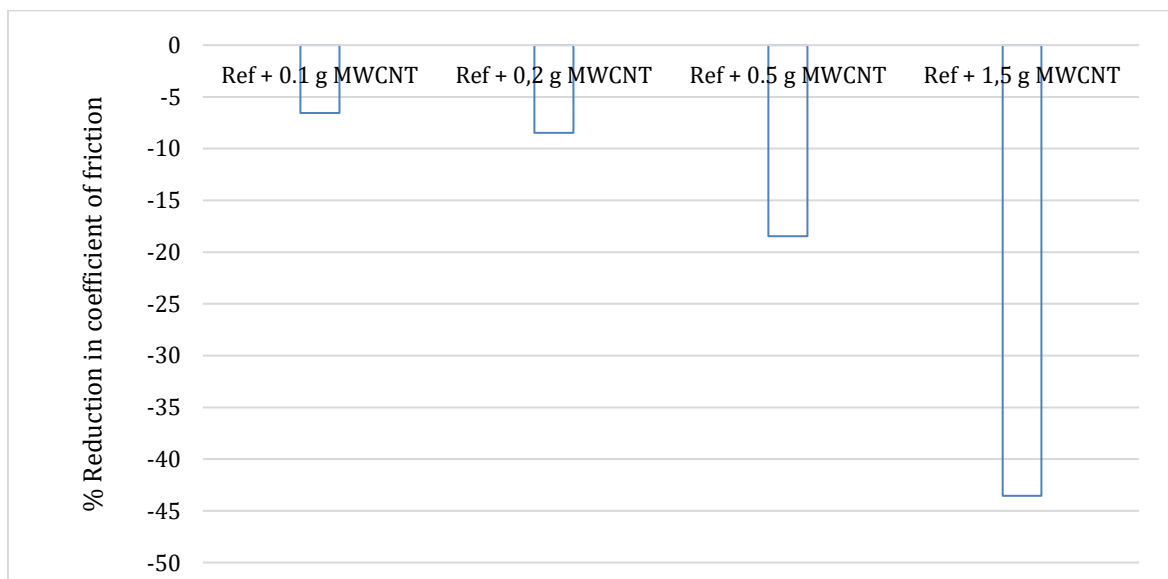


Figure 4.12: Percent change for coefficient of friction.

4.4 Effect of pH

As the optimal pH for a drilling fluid should lie between 9 - 11, it was necessary to add some NaOH to increase the pH of the drilling fluids evaluated earlier. With an optimized pH, additives such as polymers and thinners will work more efficiently, bentonite interaction (swelling) will be better which also affects the yield-stress behavior. pH also counteract corrosion[9][28]. As NaOH could affect rheology and friction it was necessary to evaluate these parameters. The drilling fluids were formulated in the same manner as the drilling fluids in 4.2, however, now the NaOH was added after the bentonite:

1. Water
2. Salt
3. MWCNT
4. Duovis
5. Lignosulfonate
6. Bentonite
7. NaOH.

In Table 4.3 the pH of the fluids are listed with and without pH-modifications.

Table 4.3: pH of drilling fluids with and without NaOH.

	Ref	Ref + 0.1 g MWCNT	Ref + 0.2 g MWCNT	Ref + 0.5 g MWCNT	Ref + 1.5 g MWCNT
Fluid	8.12	8.07	8	8.16	8.18
Fluid + NaOH	9.05	9.43	9.09	9.12	9.91

4.4.1 Rheology

Figure 4.13 shows the viscometer data of the drilling fluids containing MWCNT along with the reference fluid compared to the drilling fluids adjusted with NaOH.

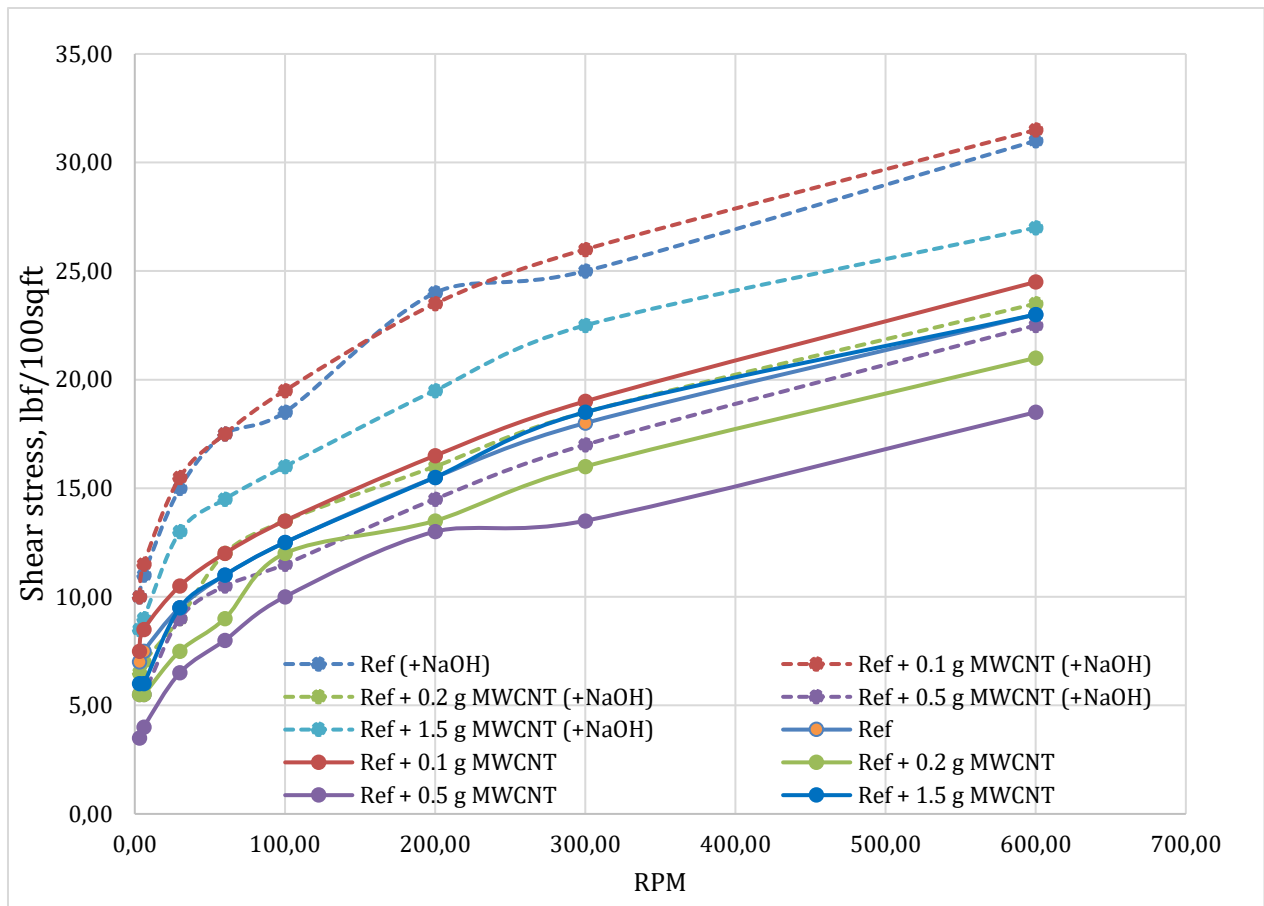


Figure 4.13: Viscometer data for comparison of NaOH effect

When using NaOH to increase pH, data from the viscometer indicated some changes compared to the fluids without NaOH. The shear stress decreased for all of the drilling fluids with NaOH compared to the same fluid without NaOH. When considering the pH modified drilling fluids, the fluid containing 0.1 g MWCNT increased the shear stress while the others decreased compared to the reference fluid. In Figure 4.14 and Figure 4.15 the Bingham and Power-Law parameters from the viscometer readings are presented.

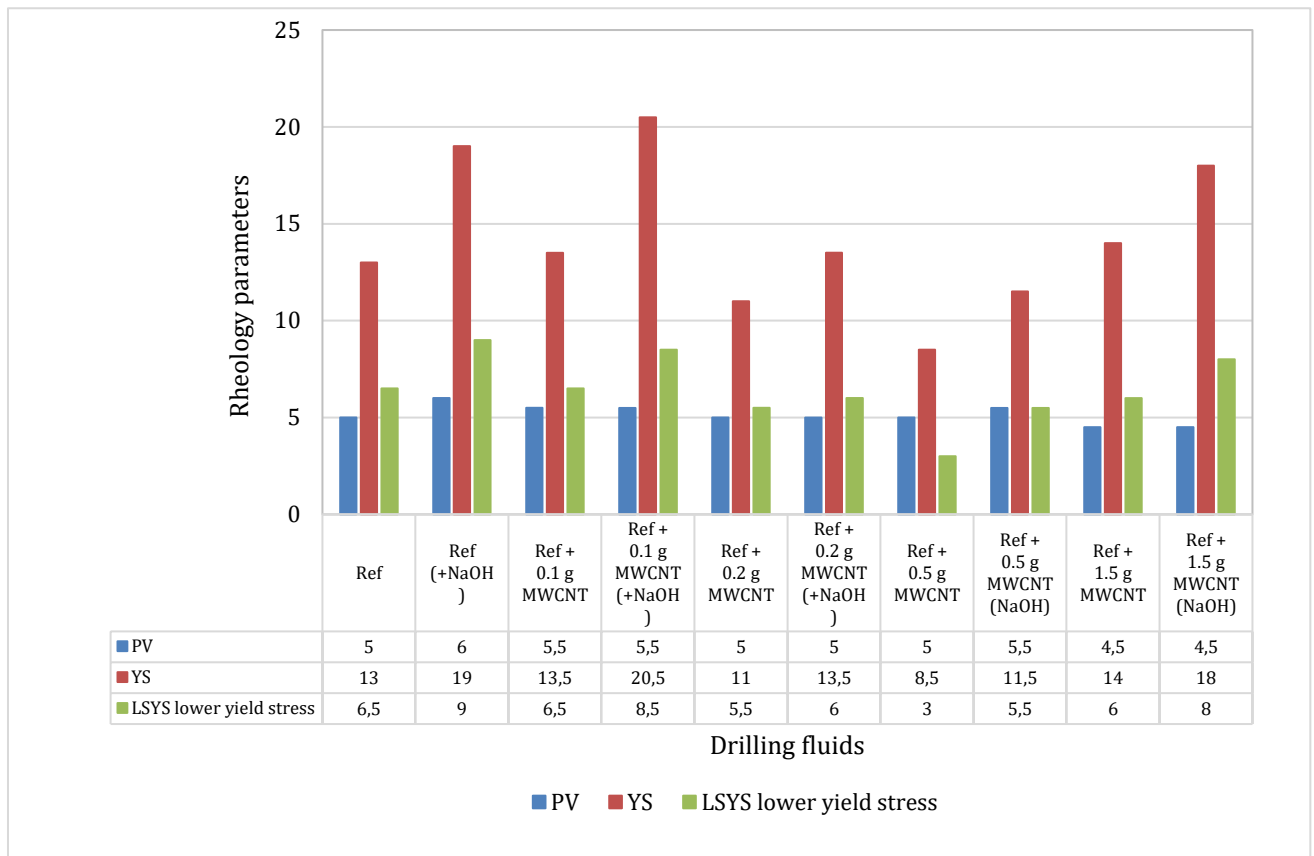


Figure 4.14: Bingham parameters for comparison of NaOH-effect.

From the Bingham parameters, it can be observed that:

- PV increased with 16.7% for Ref (+NaOH) compared to Ref, and remained unchanged for the rest of the fluids when compared to the same fluids without NaOH
- Comparing Ref (+NaOH) with the fluids containing MWCNT and NaOH, it can be observed that PV is reduced for all of the fluids containing MWCNT
- YS increased for all of the pH-modified fluids, where the reference fluid increased the most (31.6%)
- When comparing the pH-modified fluids with each other, the following observation was made: YS increased with 7.3% for Ref + 0.1 g MWCNT, while the rest of the fluids experienced a reduction in YS
- LSYS increased for all of the pH-modified fluids, when comparing them to the same non-modified fluids

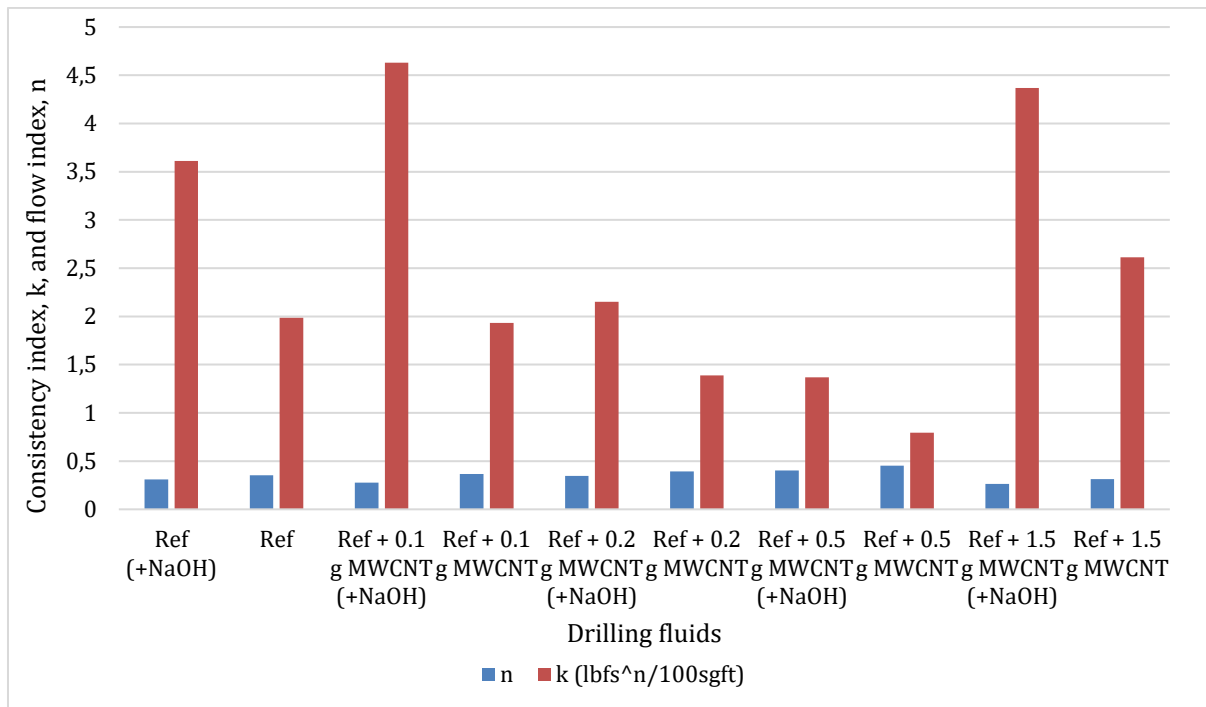


Figure 4.15: Power-Law parameters for comparison of NaOH-effect.

From the Power-Law parameters, it can be observed that:

- The flow index increased for all of the drilling fluids modified with NaOH compared with the same non-formulated fluids. All the fluids has pseudo plastic behavior according to the flow index values
- The consistency index decreased for all of the drilling fluids modified with NaOH compared with the same non-formulated fluids
- When comparing the pH-modified drilling fluids with each other, following observation were made: The flow index increased for Ref + 0.1 g MWCNT and REF + 1.5 g MWCNT, and decreased for the rest of the fluids. Regarding the consistency index values, the values decreased for Ref + 0.1 g MWCNT and Ref +1.5 g MWCNT and increased for the rest

4.4.2 Friction

In this section, the effect of NaOH on friction is evaluated. In Figure 4.16 the coefficient of friction of the different fluids before and after the addition of NaOH is presented. For all

of the fluids except Ref + 1.5 g MWCNT, the coefficient of friction decreases as the pH-modifier are added to the drilling fluid. The coefficient of friction is quite similar for Ref + 1.5 g MWCNT.

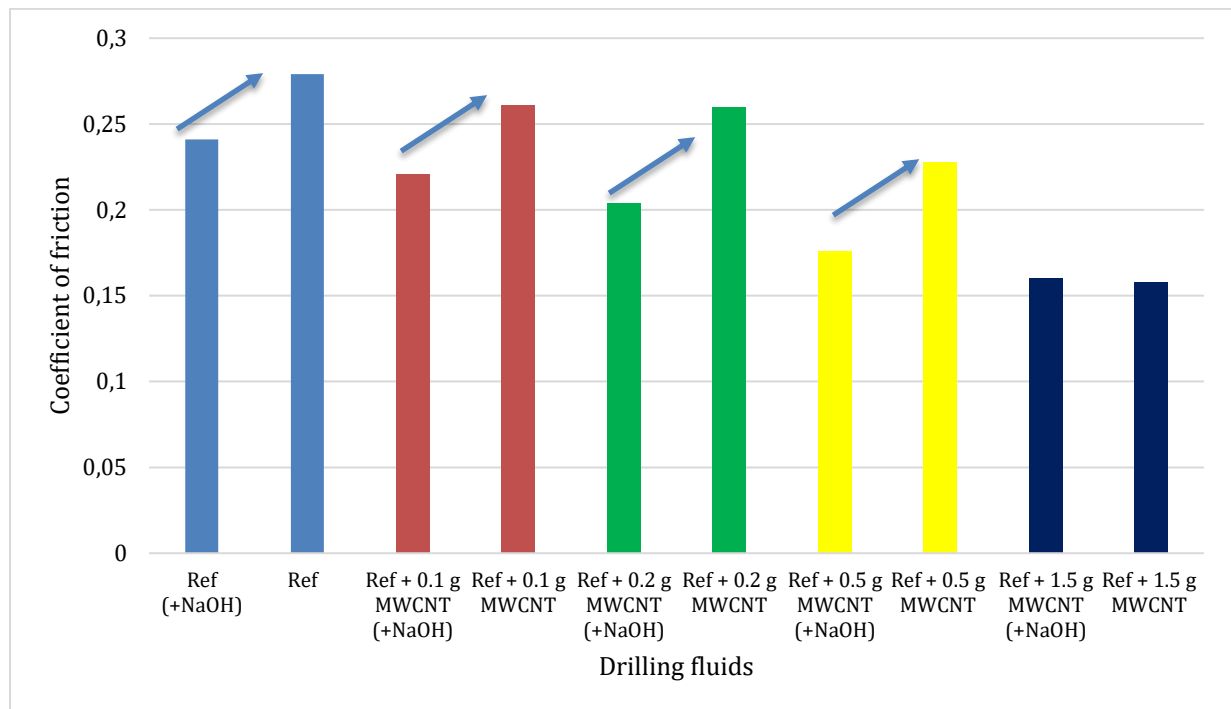


Figure 4.16: comparison of friction coefficient

4.5 Effect of temperature

It is important to understand how temperature effect the drilling fluids, since the temperature is increasing as we drill in to deeper sections. To determine the effect temperature has on nanoparticles in water based muds, the fluid systems reviewed in 4.3 and 4.4 were used. The fluids rheology were measured at three different temperatures: 72°F, 130°F and 180°F.

4.5.1 With Low pH

The temperature effect was first evaluated for the drilling fluids with lower pH. From Figure 4.17 it can be seen that the rheology readings differs little with increasing temperature and all the fluids experience a slight decrease in shear stress with increasing temperature. The results in Figure 4.18 indicates that YS decreased with increasing temperature for Ref, Ref + 0.1 g MWCNT and Ref + 0.2 g MWCNT, while Ref + 0.5 g MWCNT and Ref + 1.5 g MWCNT first increases at 130°F and then decreases to the lowest value at

180°F. PV experience a slightly decrease for the three first fluids, while the two last fluids had some unconformity for the readings at 130°F. The viscometer readings for Ref fluid decreased with 16.3% when the temperature increased from 72°F to 180°F, while Ref + 1.5 g MWCNT decreased with 12.8%.

For the Power law parameters in Figure 4.19, there are no correlation between nanoparticle concentration and parameter behavior. The pH level for all of the drilling fluids drops as the temperature increases.

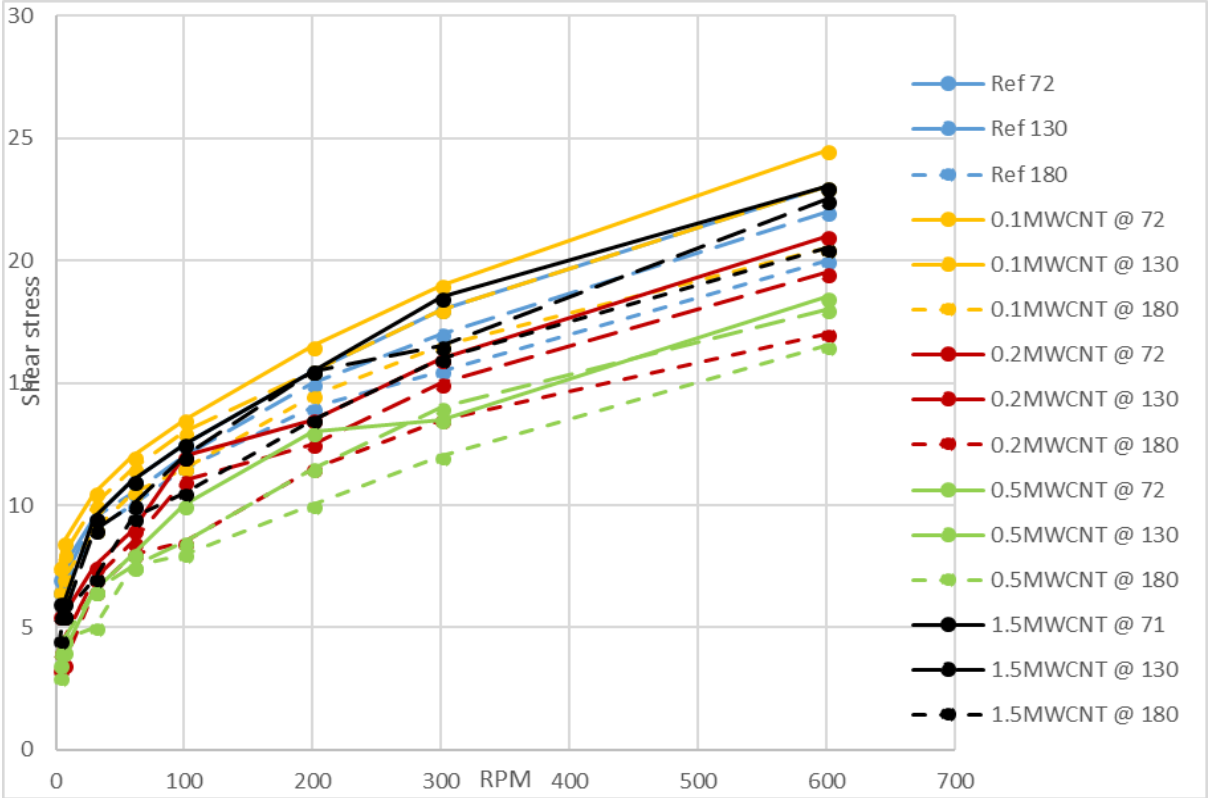


Figure 4.17: Viscometer response for the different drilling fluids with increasing temperature.

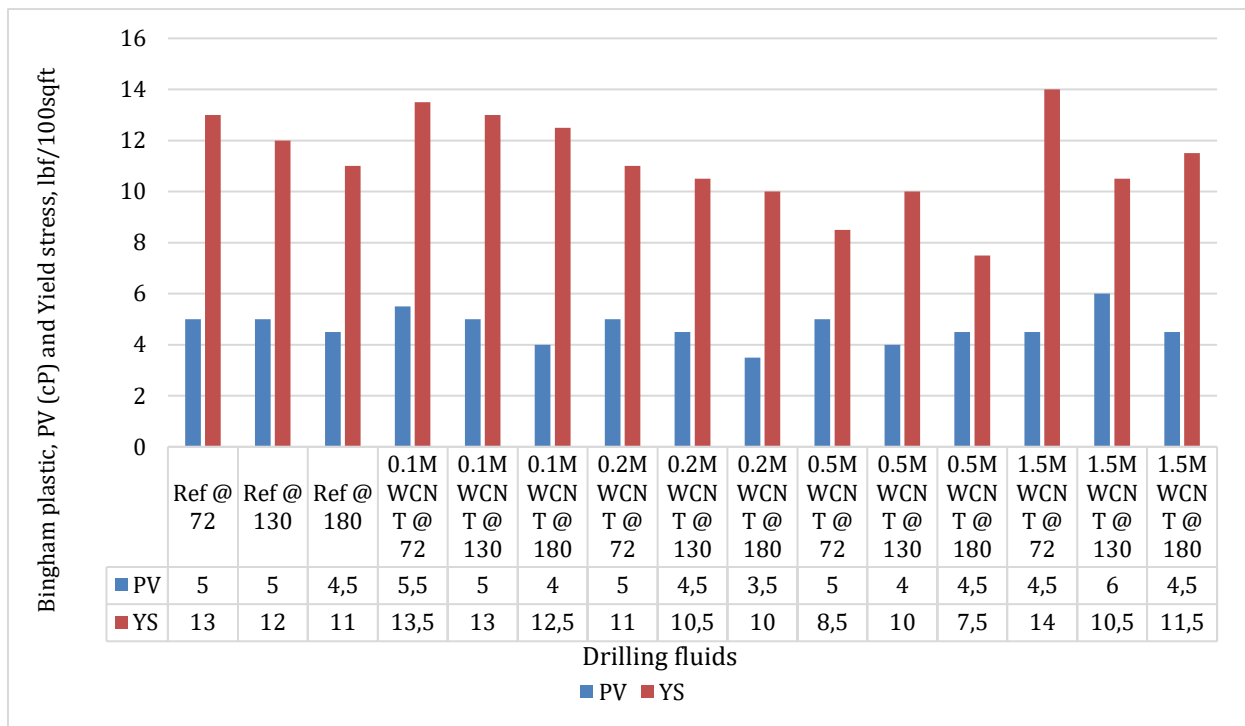


Figure 4.18: Bingham parameters for the different drilling fluids with increasing temperature

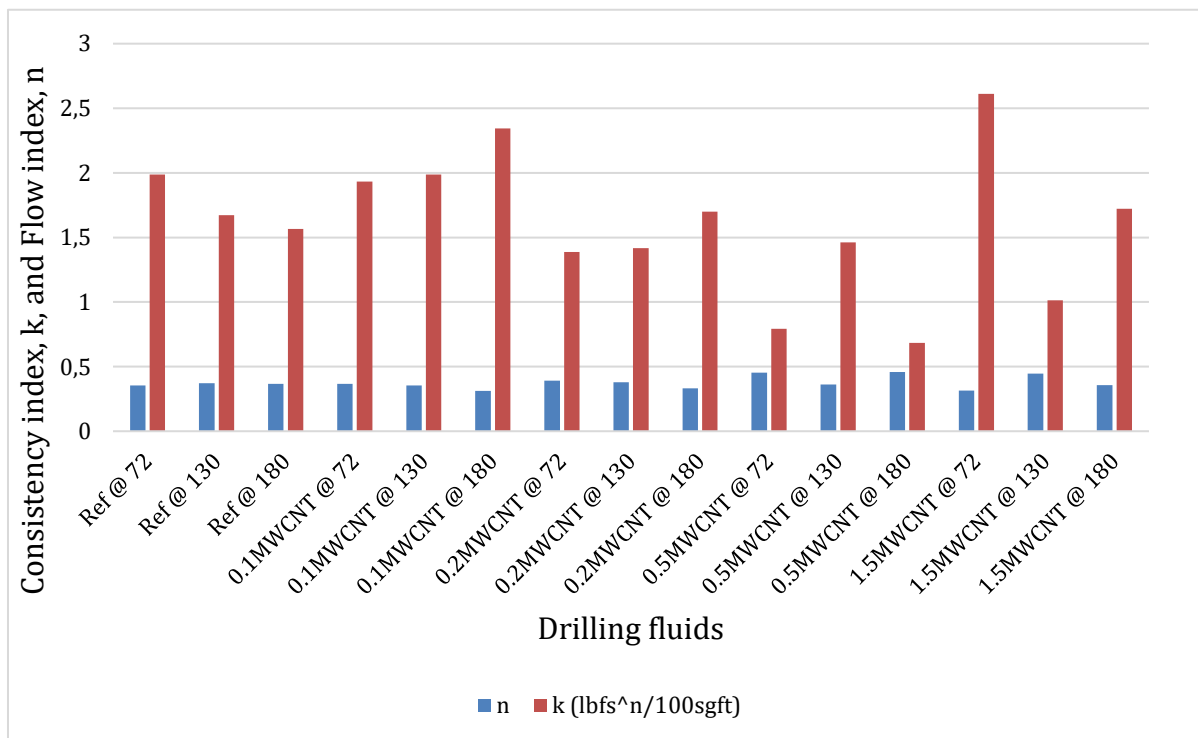


Figure 4.19: Power Law parameters for the different drilling fluids with increasing temperature

4.5.2 With High pH

Considering the fluids with higher pH, Figure 4.20 shows quite similar behavior for rheology with increasing temperature. Figure 4.21 shows how YS decreased for all of the fluids when the temperature increases from 72°F to 180°F. PV exhibit similar results compared to the fluids with low pH, where a minor decrease is observed for Ref, Ref + 0.1 g MWCNT and Ref + 0.2 g MWCNT, while Ref + 0.5 g MWCNT and Ref + 1.5 g MWCNT had some unconformity for the readings at 130°F. The viscometer readings for Ref fluid decreased with 18% when the temperature increased from 72°F to 180°F, while Ref + 1.5 g MWCNT decreased with 12%.

For the Power law parameters in Figure 4.22, there appears to be no correlation between nanoparticle concentration and parameter behavior. Upon comparing the fluids with high and low pH it can be observed that the behavior is similar for fluids with high and low pH, but the fluids with higher pH indicated higher values for plastic viscosity. When comparing the Power law parameters for the different drilling fluids with high and low pH, the consistency index values increased with higher pH, and the flow index decreased slightly with increasing pH. With increasing temperature, the pH decreased for the tested drilling fluids.

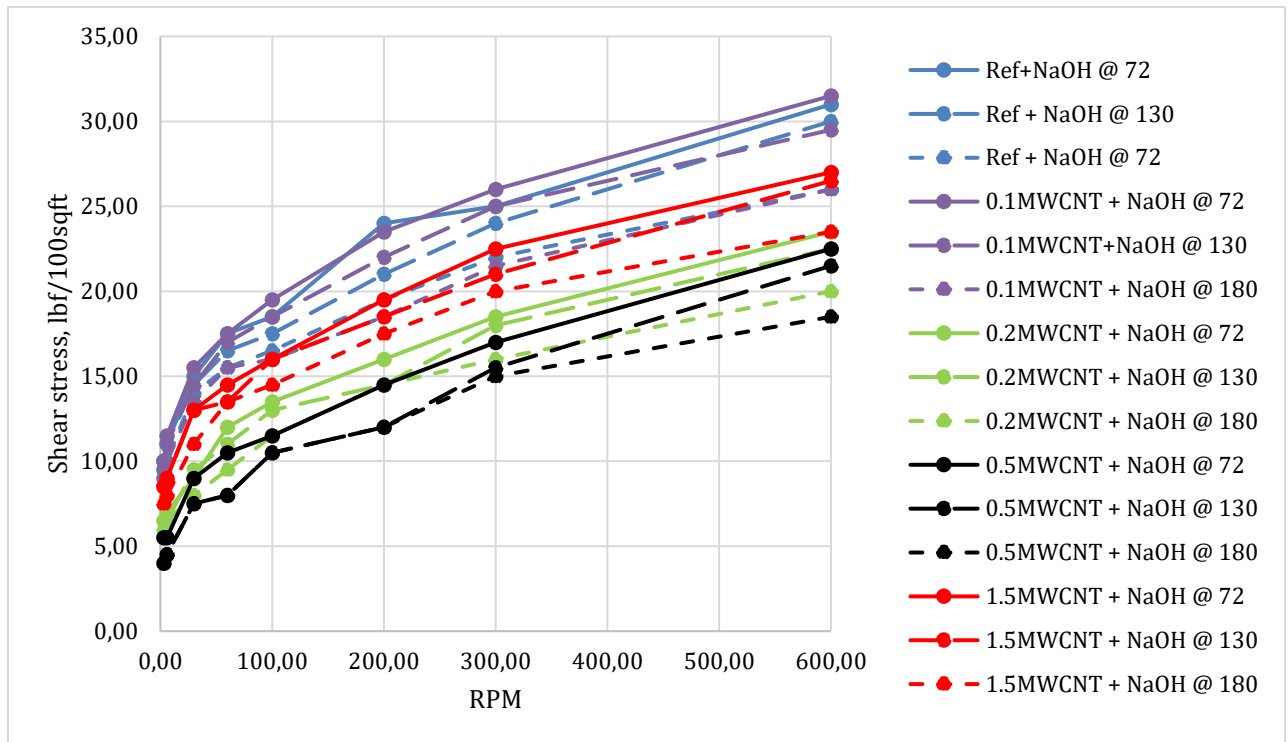


Figure 4.20: Viscometer response for the different drilling fluids with increasing temperature.

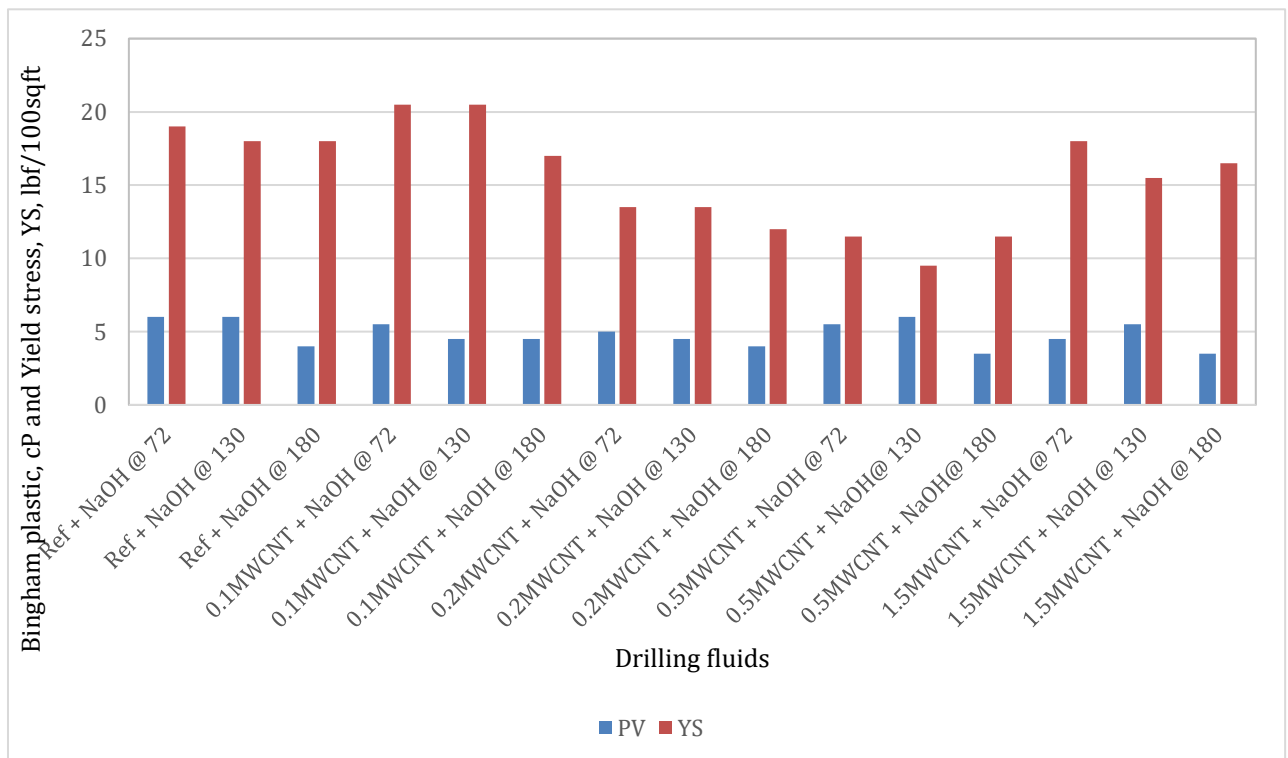


Figure 4.21: Bingham parameters for the different drilling fluids with increasing temperature.

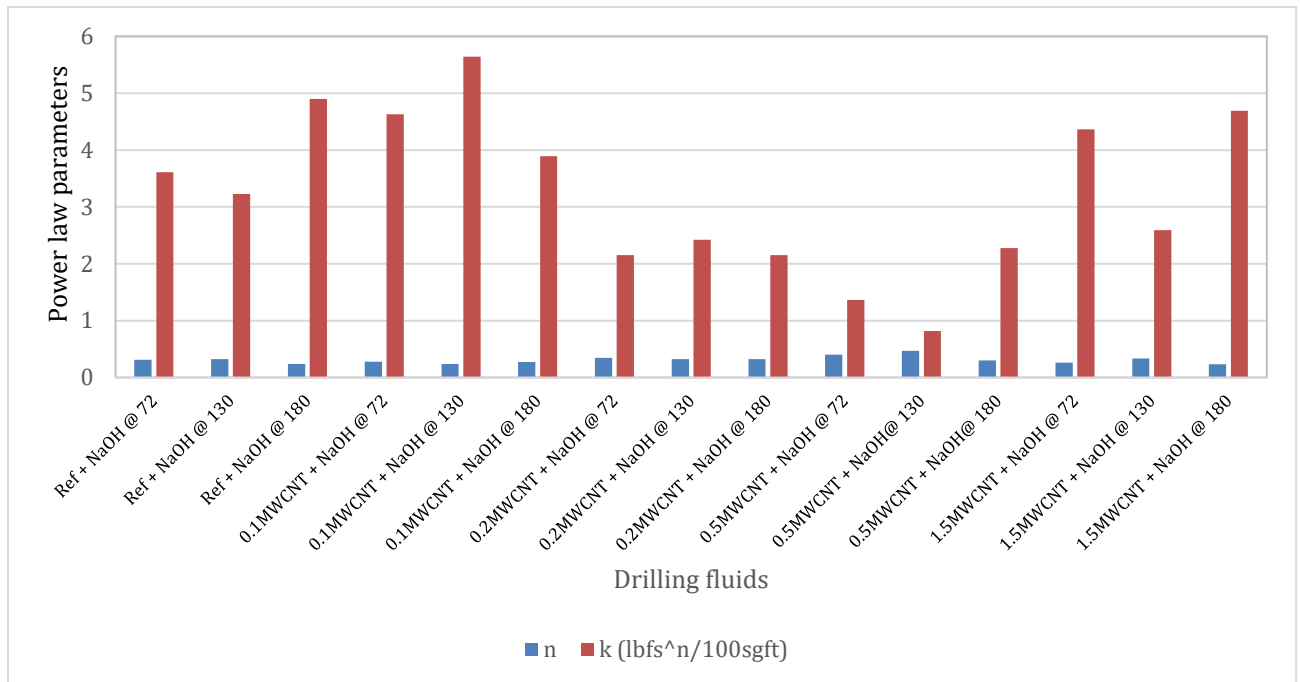


Figure 4.22: Power Law parameters for the different drilling fluids with increasing temperature.

4.6 Effect of mixing

Mixing effect can affect drilling fluid properties, and this will be examined in this section.

To see how mixing affect the properties, two fluids with the same content will be mixed with different methods. The fluids was mixed in the following order:

1. Water
2. KCl
3. MWCNT
4. Lignosulfate
5. Duovis
6. Bentonite
7. NaOH

The first fluid (FluidA) was mixed mechanical, while the second fluid (FluidB) was mixed mechanical and then with sonication. Subsequently both the fluids were placed at rest for 24 hours to evaluate the dispersion of the solution. After 24 hours the polymers and bentonite was added. Then the bentonite swelled for 24 hours. Figure 4.23 displays the fluid A and B specimen after mixing. Figure 4.24 the stability of the solutions after 24hrs.

As shown, Fluid B experience better dispersion of particles, which was due to the energy provided by the ultra sonicator.

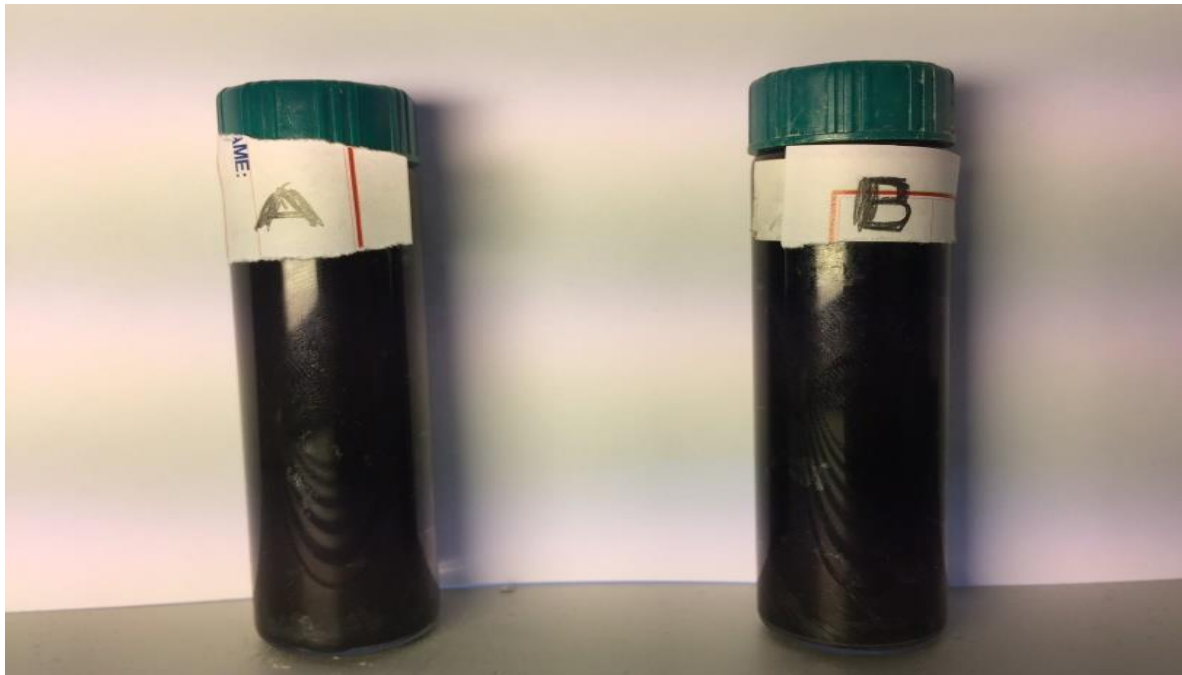


Figure 4.24: Fluid A and B after mixing and addition of MWCNT.

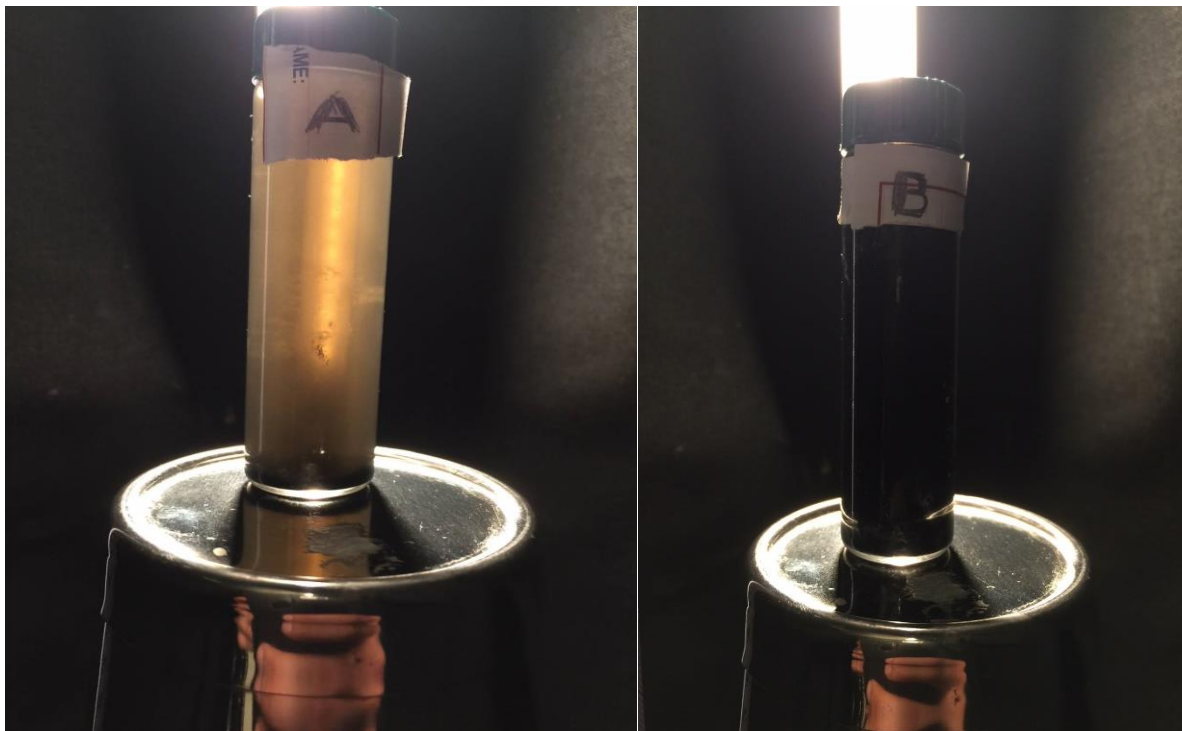


Figure 4.24: Fluid A and B after 24 hours

Figure 4.24 indicates that Fluid B experience better dispersion of particles.

4.6.1 Rheology

Figure 4.25 shows the viscometer data for the drilling fluids with different mixing arrangement.

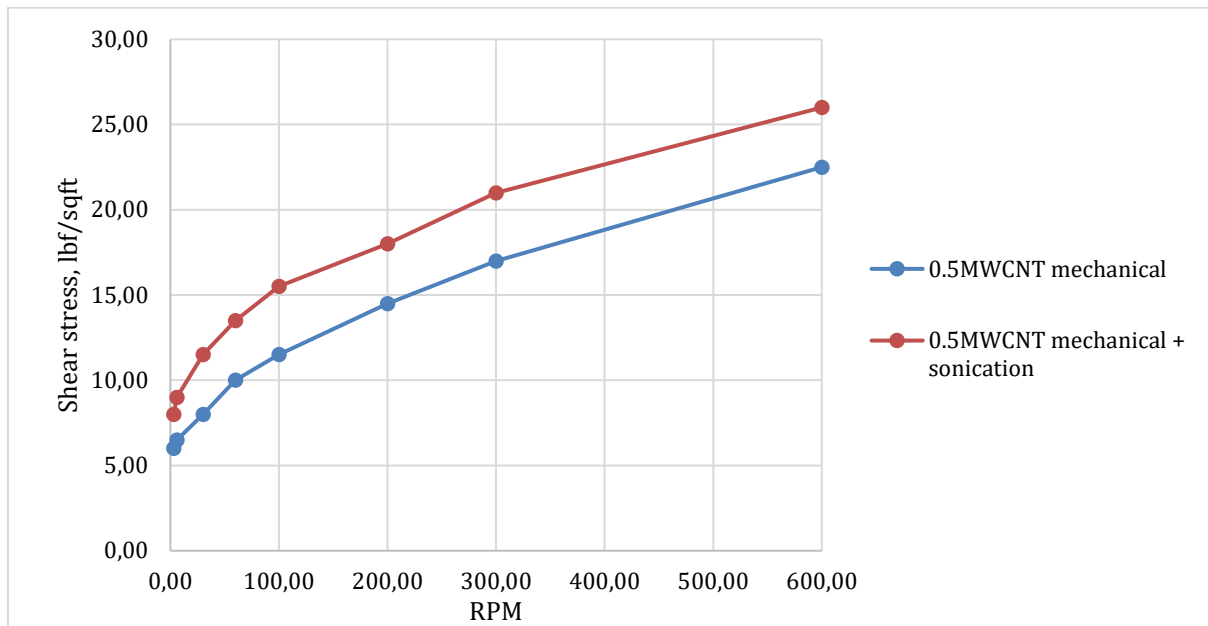


Figure 4.25: Viscometer data to evaluate mixing effect.

When the drilling fluid is mixed using the combination of mechanical mixing and sonication, data from the viscometer showed that the shear stress increased with 15%. In Figure 4.26 and 4.27 the Bingham and Power-Law parameters from the viscometer readings is presented:

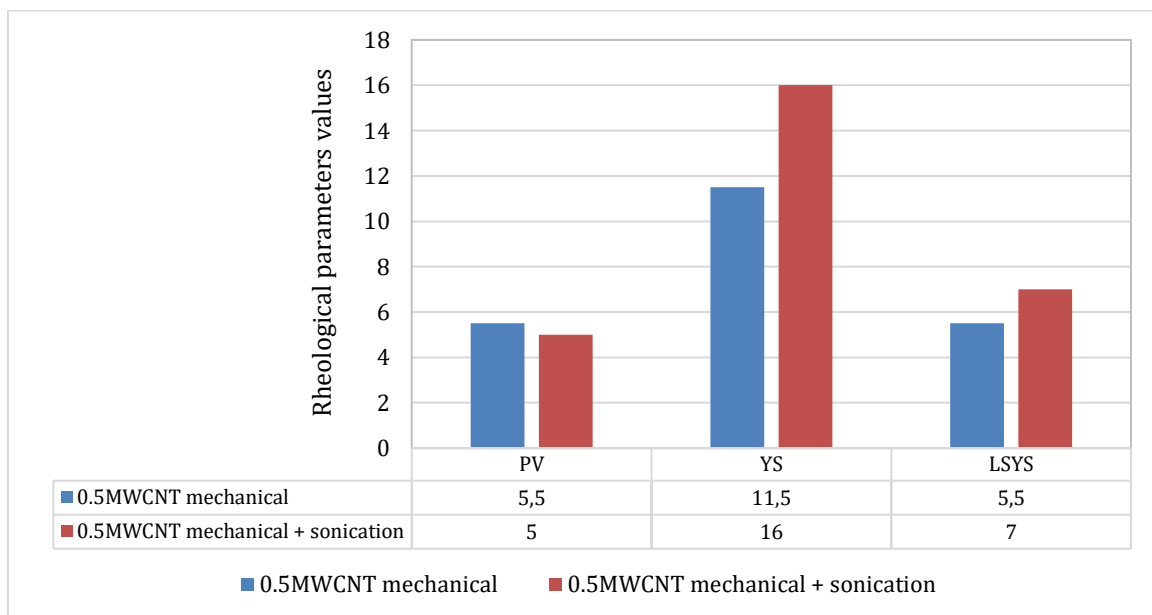


Figure 4.26: Bingham parameters

From the Bingham parameters, it can be observed that:

- PV decreased with 9.1% for Fluid B.
- YS increased with 39.1% for Fluid B.
- LSYS increased with 27.3% for Fluid B.

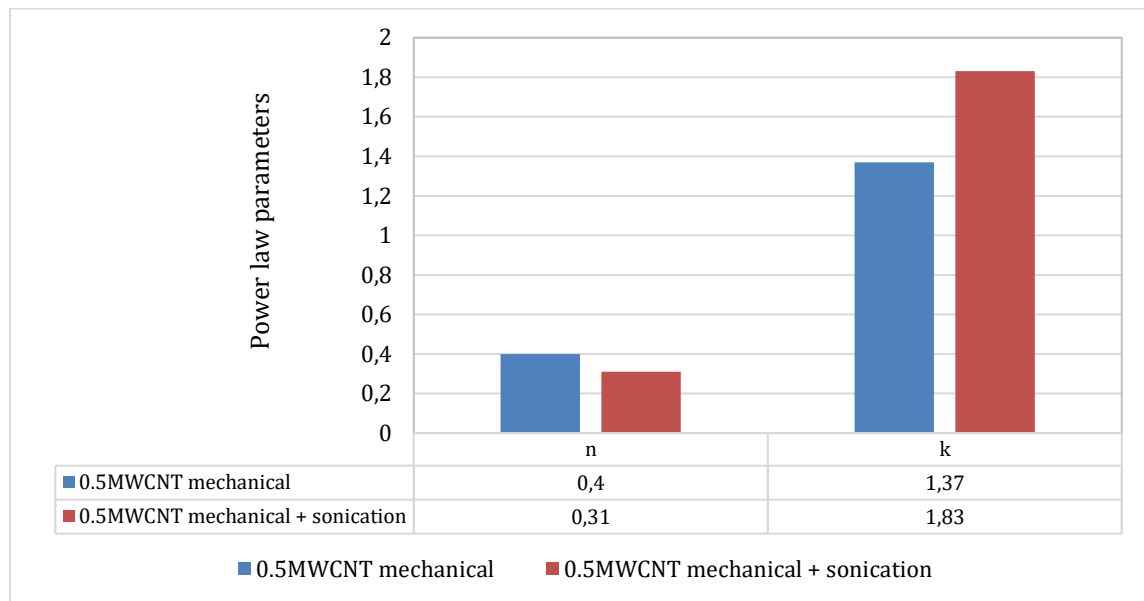


Figure 4.27: Power-Law parameters.

From the Power-Law parameters, it can be observed that:

- The flow index decreased for Fluid B. All the fluids has pseudo plastic behavior according to the flow index values.
- Regarding the consistency index values, the values increased for Fluid B.

4.6.2 Friction

In Figure 4.28 the coefficient of friction for the two fluids with different mixing arrangement is presented. It can be observed that the mixing method has little effect on the coefficient of friction for the two different fluids, and the fluid mixed mechanical and with sonication experiences a small decrease in friction.

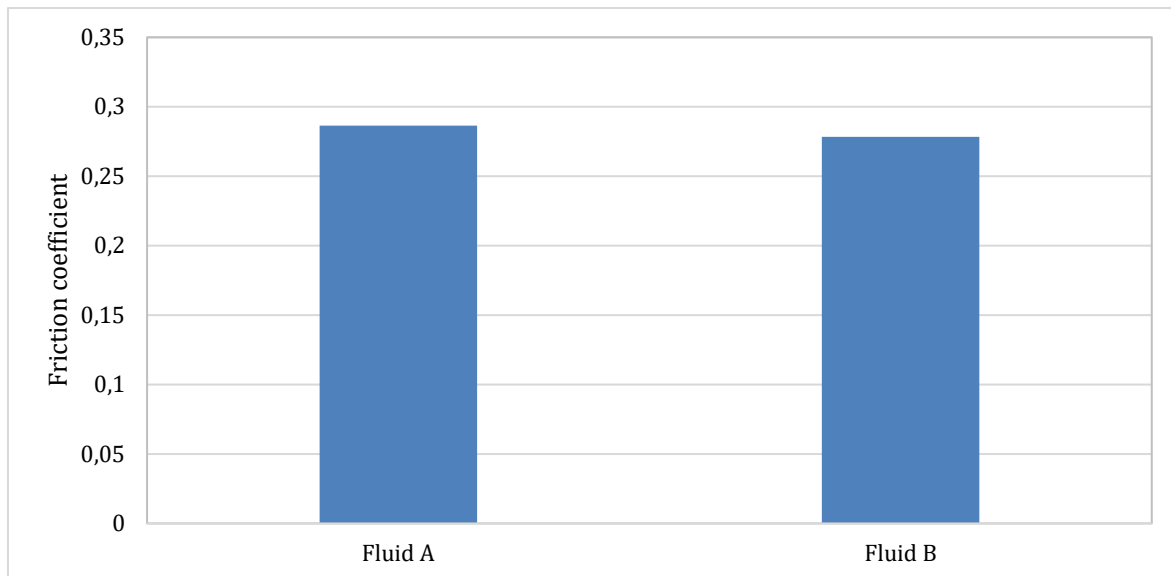


Figure 4.28: Mixing effect on CoF

4.7 Analysis of mud cake structure

To analyze how the mud cake structure changes when adding MWCNT, SEM pictures were taken of reference fluid and Ref + 1.5 g MWCNT (Figure 29) and (Figure 30). When investigating the pictures from Ref + 1.5 g MWCNT, it could be observed that the nanoparticles accumulated in several areas and that other areas did not show any nanoparticles. This may be due to mixing effect.

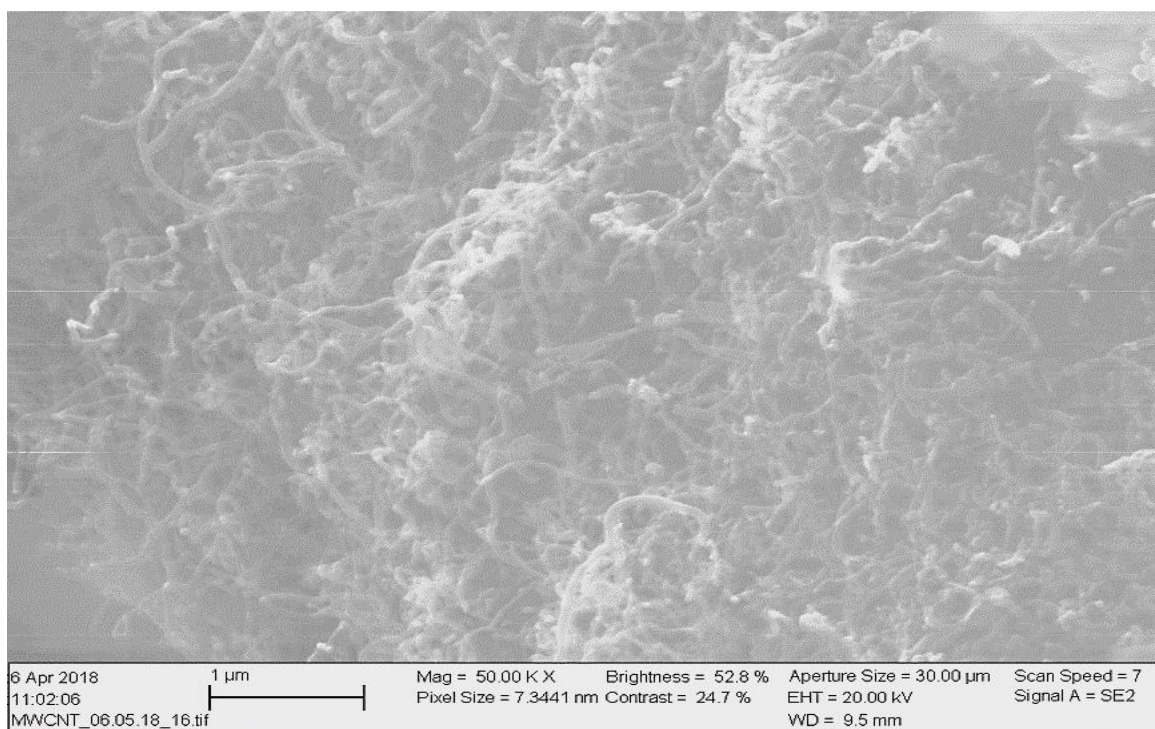


Figure 4.29: SEM picture from mud cake (Ref + 1.5 g MWCNT)

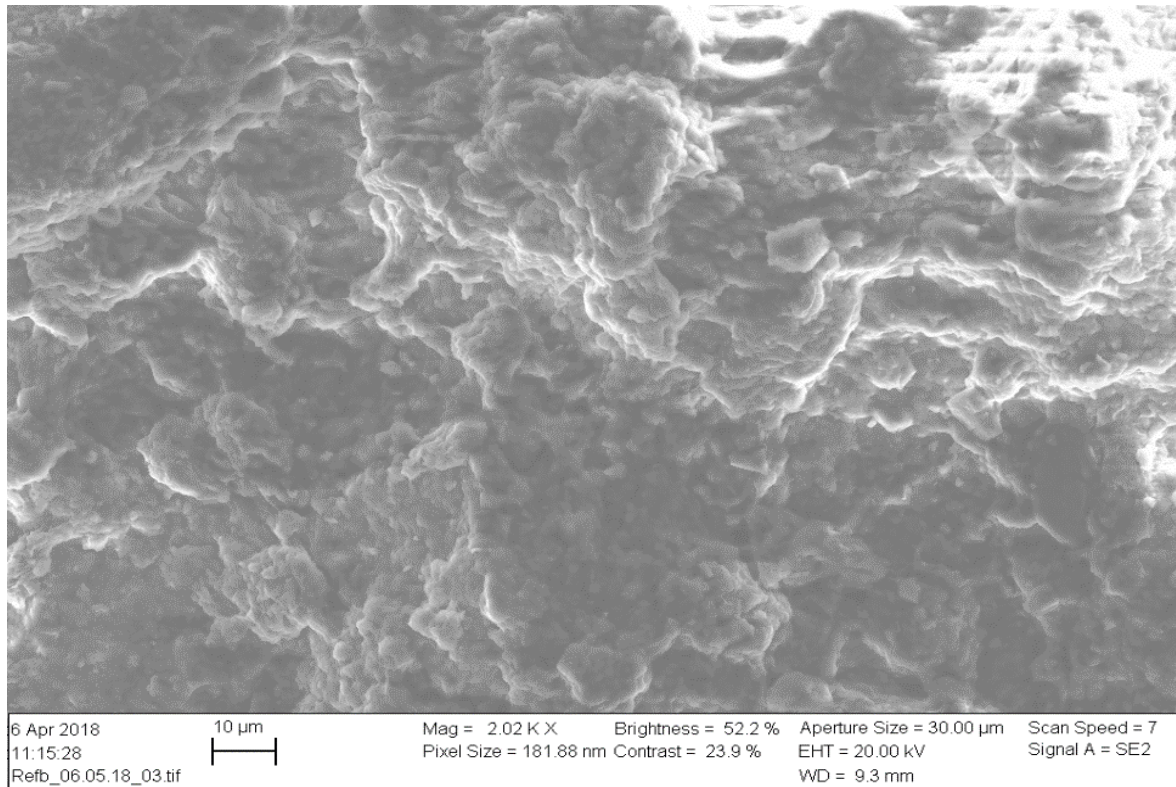


Figure 4.30: SEM picture from mud cake (Ref)

4.8 Analysis of the chemistry of filter loss

As described in section 2.1, MWCNT can decrease the filtrate loss when added to drilling fluids. From Figure 4.31 it can be observed that the filtrate loss increased with up to 1 mm for three of the fluids, while Ref + 0.5 g MWCNT had the same fluid loss as reference fluid, this indicates poor filtrate loss control for the additive. In Figure 4.32 the cation concentration of the filtrate loss is showed, where higher concentrations of potassium may be to poor bounding between salt and bentonite. The concentration of the cations is quite similar for the fluids, however the fluids with nanoparticles show higher concentration of barium and strontium.

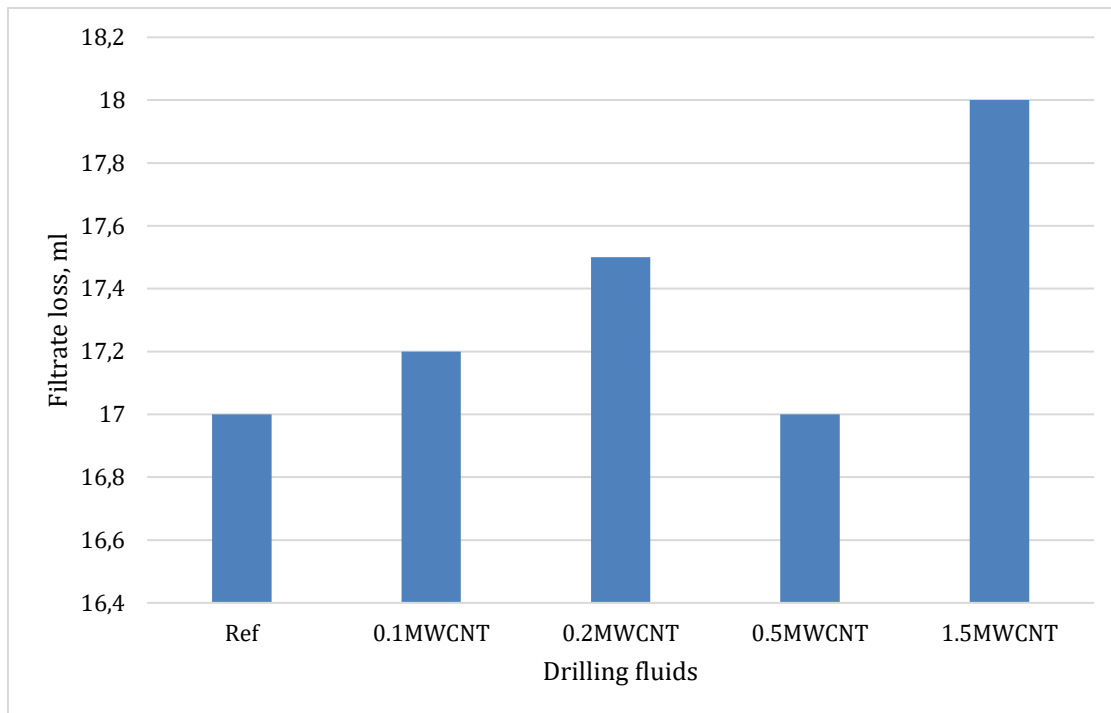


Figure 4.31: Filtrate loss

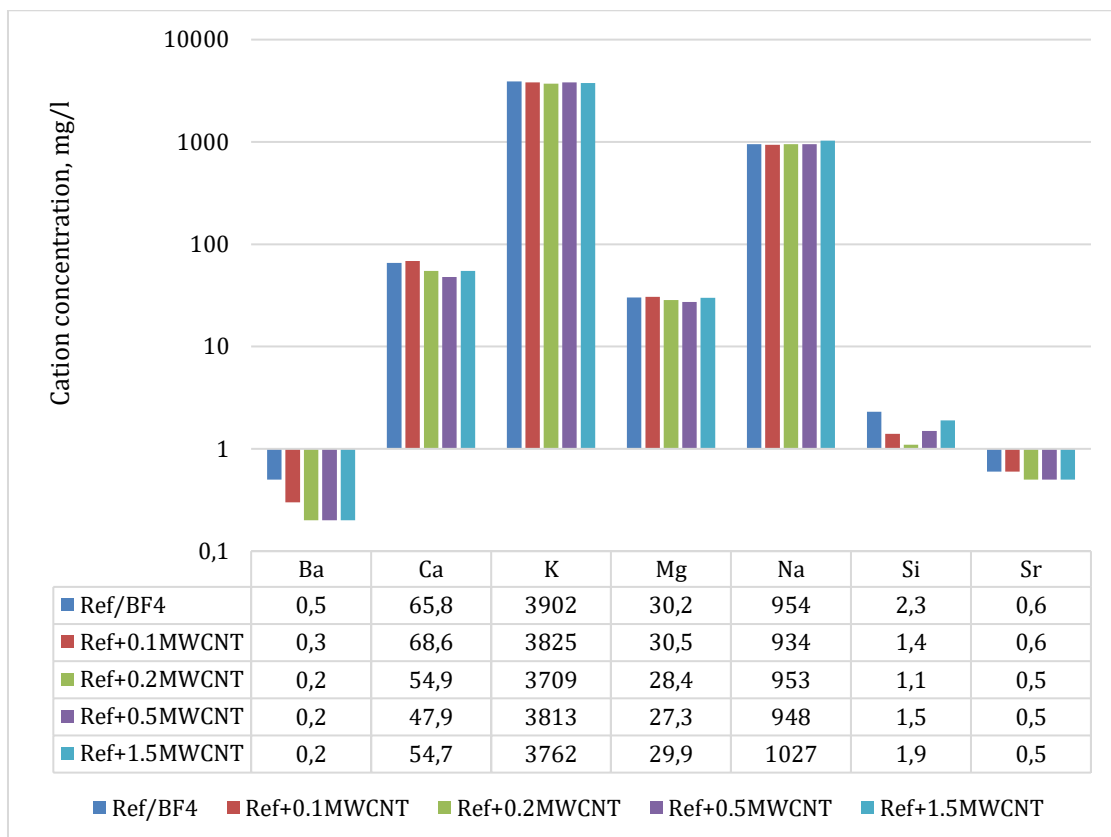


Figure 4.32: ICP-OES analysis

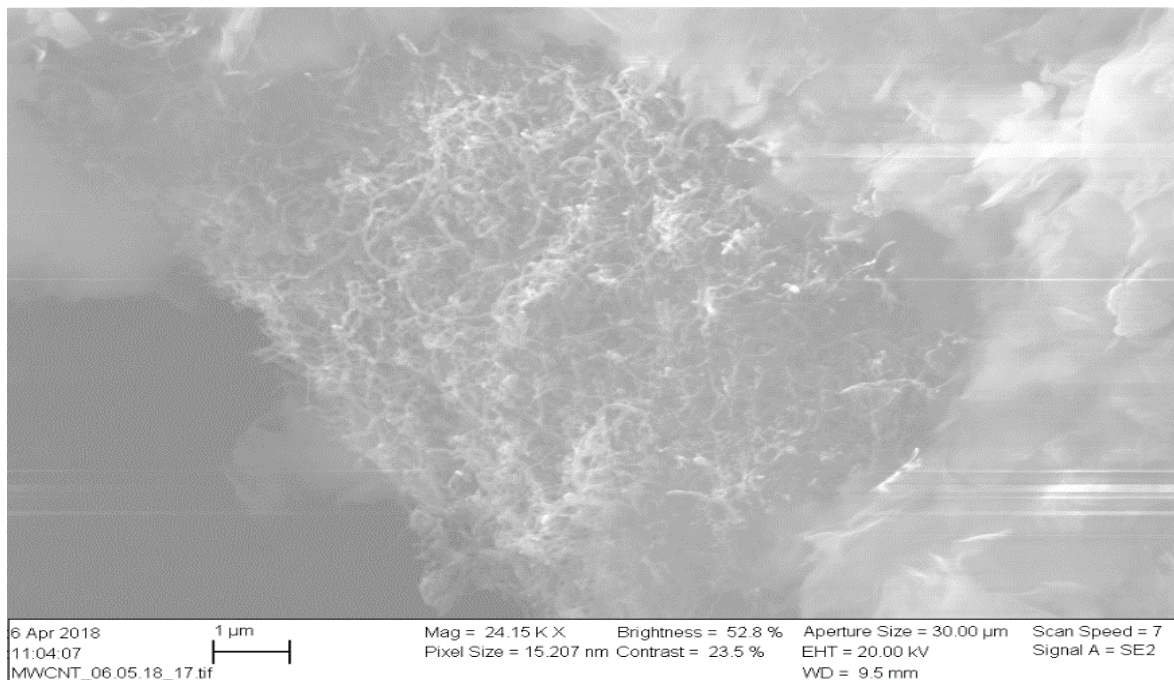


Figure 4.33: SEM picture of MWCNT dispersion in mud cake.

4.9 Viscoelasticity of drilling fluids

In this section the effect of MWCNT on the viscoelasticity of a selected set of drilling fluids will be evaluated. The same fluids evaluated earlier were characterized with the rheometer. See 4.1 for measurement setup and description of the rheometer.

In Figure 4.34 and Figure 4.35 the particular results from the amplitude sweep measurements are presented. In this section only the Ref and Ref + 1.5 g MWCNT are presented, the results for rest of the fluids are presented in Appendix B. Both fluids shows similar behavior for viscoelasticity, from the plot we can observe that the storage modulus is higher than the loss modulus in the LVE area, which shows that the fluids undergo gel like behavior. The fluids experience gel behavior since the elastic portion dominates the viscous part, as described in the theory part. The fluids is quite stable at lower shear rates, however at higher shear rates the LVE range is exceeded and the viscous portion will become the dominating one as the gel structure breaks.

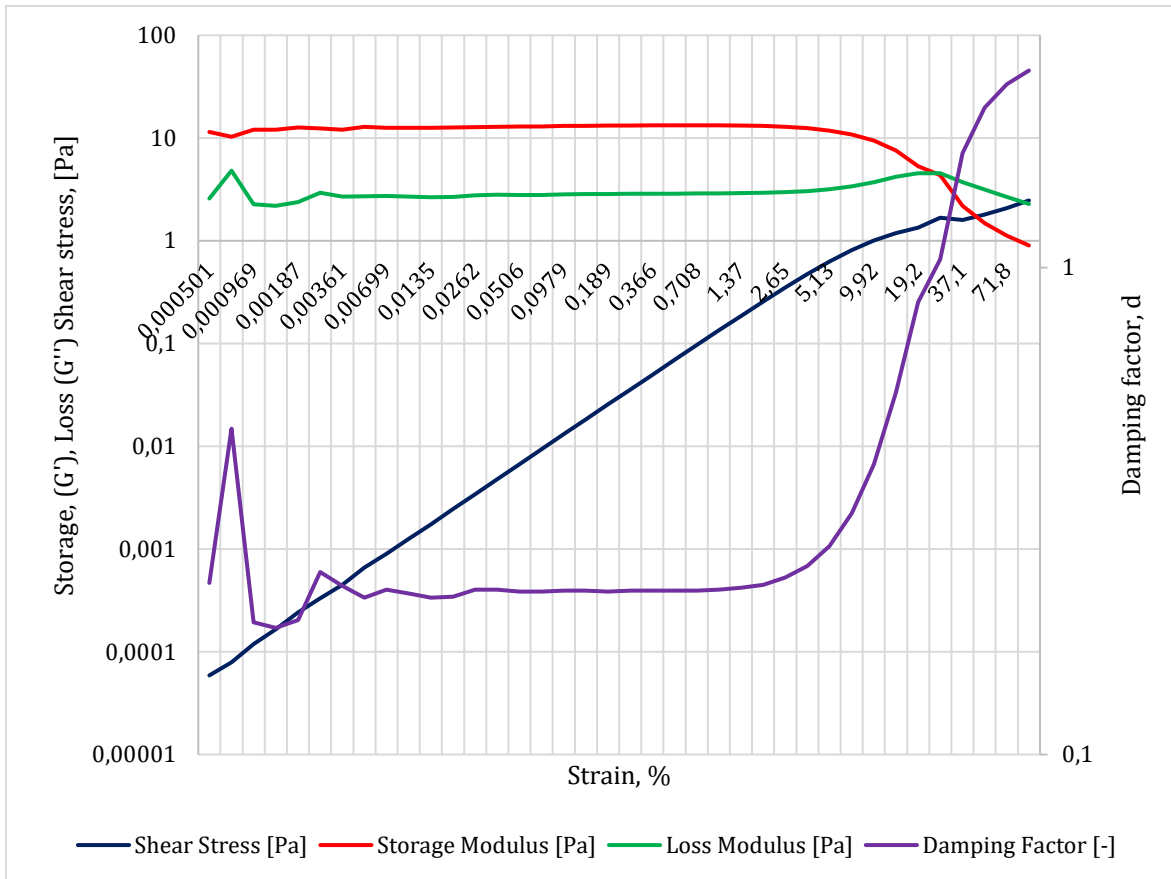


Figure 4.34: Amplitude sweep measurement for Ref fluid.

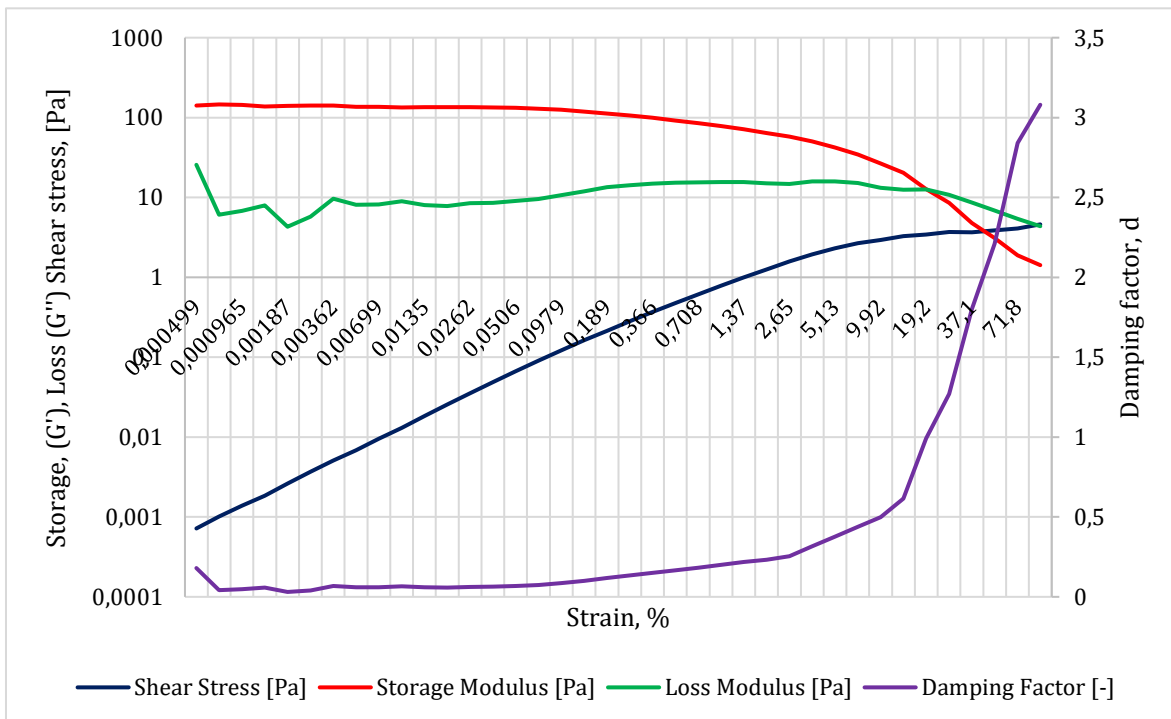


Figure 4.35: Amplitude sweep measurement for Ref + 1.5 g MWCNT fluid.

In Figure 4.36 the flow point for the different selected drilling fluids is presented. The flow point is where the Storage modulus curve and Loss modulus curve crosses in Figure 4.34 and Figure 4.35, and at this point the fluids will start to flow. At this point the damping factor increase rapidly. From the plot, it can be observed that the flow point is increasing with the addition of MWCNT. The fluids shows a linear increase in flow point with increasing MWCNT, except the fluid containing 0.2 g MWCNT which show an even larger increase for Flow Point.

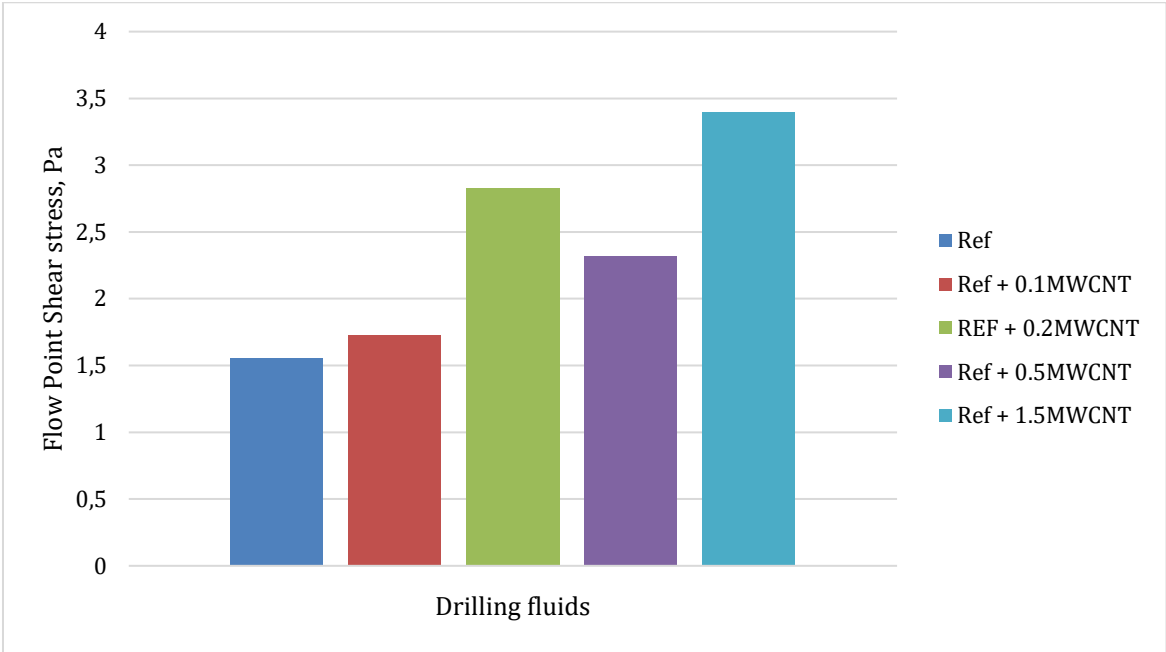


Figure 4.36: Flow point for the different drilling fluids.

5 Performance Simulation

5.1 Rheology modelling

In this section, the results from rheological modelling will be presented. To describe the selected formulated drilling fluids, the relevant parameters were calculated with a calculator created in Microsoft Excel 2013. From this, it was possible to see how the drilling fluids correlated with the relevant rheology models. The relevant parameters were calculated according to the following rheological models:

- Herschel Bulkley
- Unified
- Power Law
- Bingham
- Robertson and Stiff

The Newtonian model is omitted since as it does not describe drilling fluids behavior. From the calculator, the deviation between the model and the viscometer Fann data are computed in percent. In the following sections, the obtained models for the best fluid system with the parameters and the best models will be presented.

5.1.1 Reference system

The trend-lines for the relevant rheology models for Reference fluid are plotted in Figure 5.1. In Table 5.1 the corresponding parameters and equations are presented.

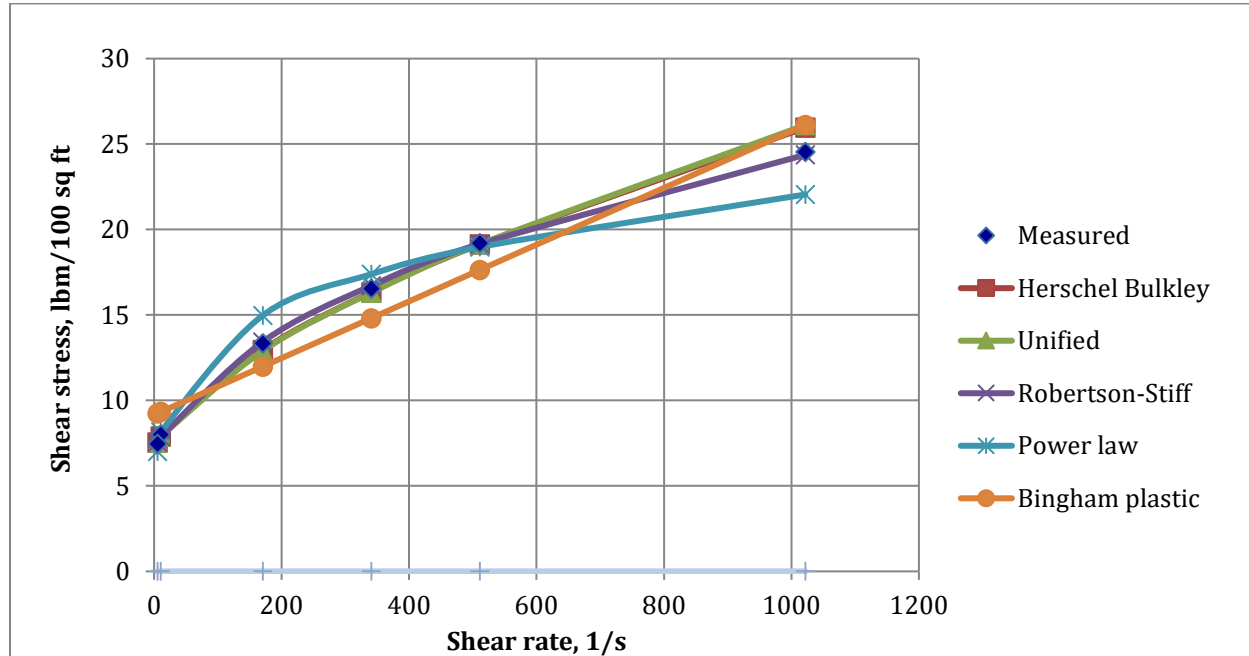


Figure 5.1: Viscometer readings and the different rheology models.

Table 5.1: Overview of the different rheology models for Ref fluid.

Model	Equation	τ_0, τ_y, A	k, C	n, B	μ_p, μ	% Deviation	cP
Herschel Bulkley	$6.899 + 0.2248 \cdot \gamma^{0.64080}$	6.899	0.2248	0.64080		2.11	
Unified	$6.936 + 0.2094 \cdot \gamma^{0.6519}$	6.936	0.2094	0.6519		2.31	
Power Law	$4.929 \cdot \gamma^{0.2162}$		4.929	0.2162		6.10	
Bingham	$0.0166 \cdot \gamma + 9.156$	9.156			0.0166	12.58	7.94
Robertson and Stiff	$1.892 \cdot (38.3762 + \gamma)^{0.3669}$	1.8919	38.3762	0.3669		0.92	

As seen in Figure 5.1/ Table 5.1, Robertson and Stiff model describes the drilling fluid most adequate with only 0.92% deviation, while Bingham shows a deviation of 12.58%. The rest of the models have a deviation between 2.11% and 6.10%. As Robertson and Stiff model displays lowest percent deviation, it is most suitable for modelling the Ref. fluid.

5.1.2 Reference system + 0.1 g MWCNT

The trend-lines for the relevant rheology models for Reference fluid + 0.1 g MWCNT are plotted in Figure 5.2. In Table 5.2 the corresponding parameters and equations are presented.

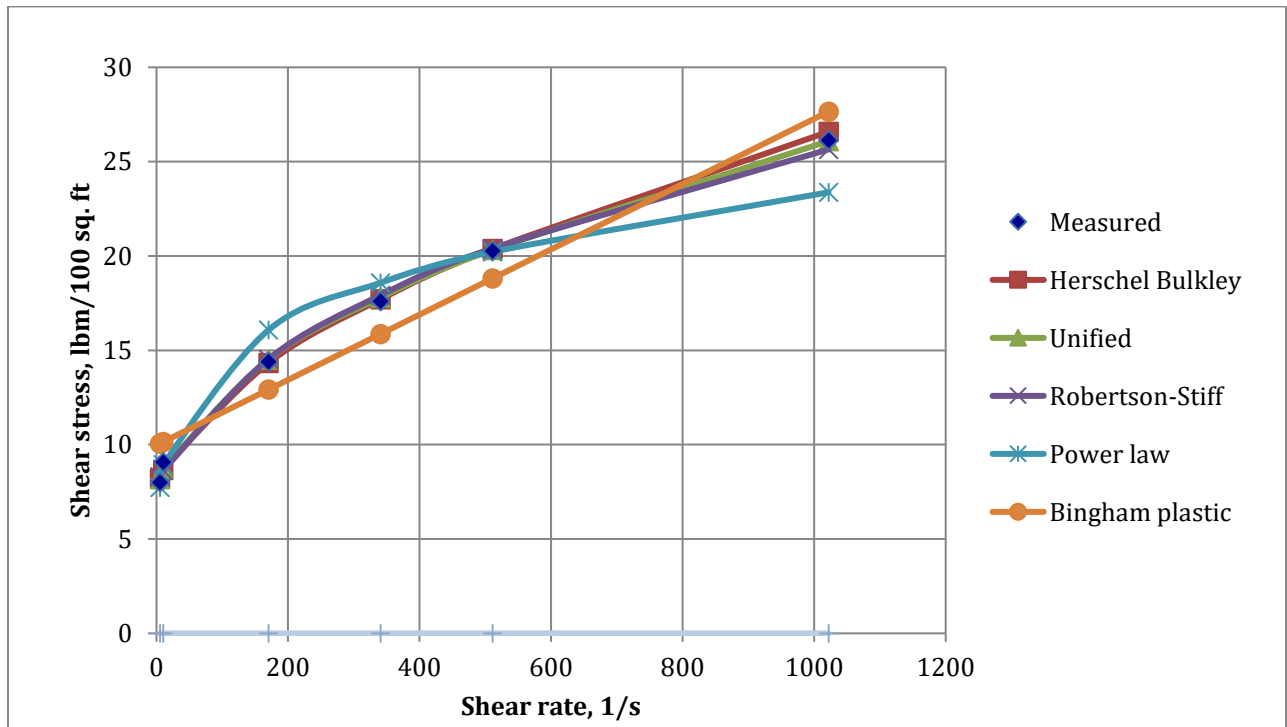


Figure 5.2: Viscometer readings and the different rheology models for Ref + 0.1 g MWCNT

Table 5.2: Overview of the different rheology models for Ref + 0.1 g MWCNT

Model	Equation	$\tau_0, \tau_y,$ A	k, C	n, B	μ_p, μ	Error	cP
Herschel Bulkley	$7.175 \cdot \gamma^{0.4102} + 0.55660$	7.175	0.4102	0.55660		1.67	
Unified	$6.936 + 0.5344 \cdot \gamma^{0.5165}$	6.936	0.5344	0.5165		1.42	
Power Law	$5.4965 \cdot \gamma^{0.2089}$		5.4965	0.2089		5.49	
Bingham	$0.0173 \cdot \gamma + 9.972$	9.972			0.0173	11.80	8.28
Robertson and Stiff	$2.2903 \cdot (35.7219 + \gamma)^{0.3469}$	2.2903	35.7219	0.3469		2.27	

As seen in Figure 5.2/Table 5.2, the Unified model describes the drilling fluid most adequate with only 1.42% deviation, and Herschel Bulkley following close by with only 1.67% deviation. Bingham still shows the largest deviation with 11.80%. The remaining models have a deviation between 2.27% and 5.49%. Since the Unified model displays lowest percent deviation, it is most suitable for modelling the Ref. fluid + 0.1 g MWCNT.

5.1.3 Reference + 0.2 g MWCNT

The trend-lines for the relevant rheology models for Reference fluid + 0.2 g MWCNT are plotted in Figure 5.3. In Table 5.3 the corresponding parameters and equations are presented.

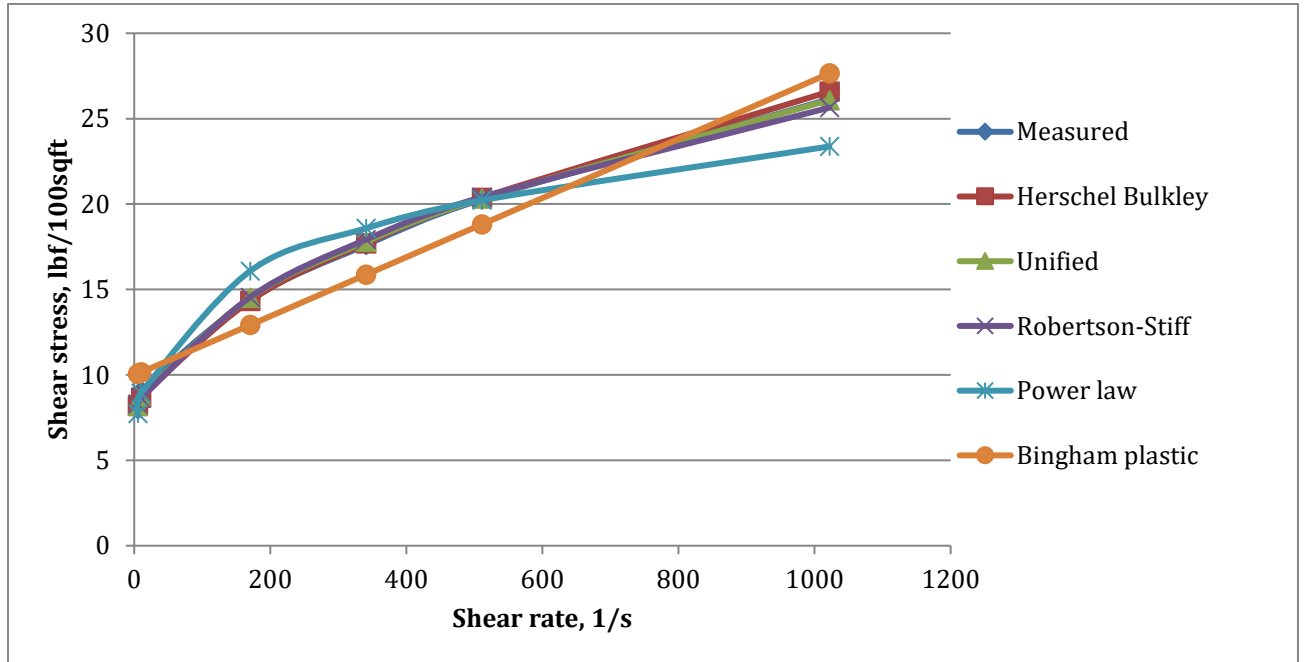


Figure 5.3: Viscometer readings and the different rheology models for Ref + 0.2 g MWCNT

Table 5.3: Overview of the different rheology models for Ref + 0.2 g MWCNT

Model	Equation	τ_0, τ_y, A	k, C	n, B	μ_p, μ	Error	cP
Herschel Bulkley	$4,714 \cdot \gamma^{0,3145} + 0,59280$	4.714	0.3145	0.59280		3.91	
Unified	$15,228 + 0,1056 \cdot \gamma^{0,7641}$	5.228	0.1056	0.7641		6.59	
Power Law	$3,383 \cdot \gamma^{0,2611}$		3.383	0.2611		4.98	
Bingham	$0,0161 \cdot \gamma + 7,485$	7.485			0.0161	18.60	7.7
Robertson and Stiff	$7,8943 \cdot (36,3811 + \gamma)^{0,2373}$	1.8651	16.0442	0.356		2.74	

As observed in Figure 5.3/Table 5.3, the Robertson and Stiff model describes the drilling fluid most adequate with 2.74% deviation. Bingham still shows the largest deviation with 18.60%. The rest of the models deviates between 3.91% and 6.59%. Since the Robertson and Stiff models displays lowest percent deviation, it is most suitable for modelling the Ref. fluid + 0.2 g MWCNT.

5.1.4 Reference + 0.5 g MWCNT

The trend-lines for the relevant rheology models for Reference fluid + 0.5 g MWCNT are plotted in Figure 5.4. In Table 5.4 the corresponding parameters and equations are presented.

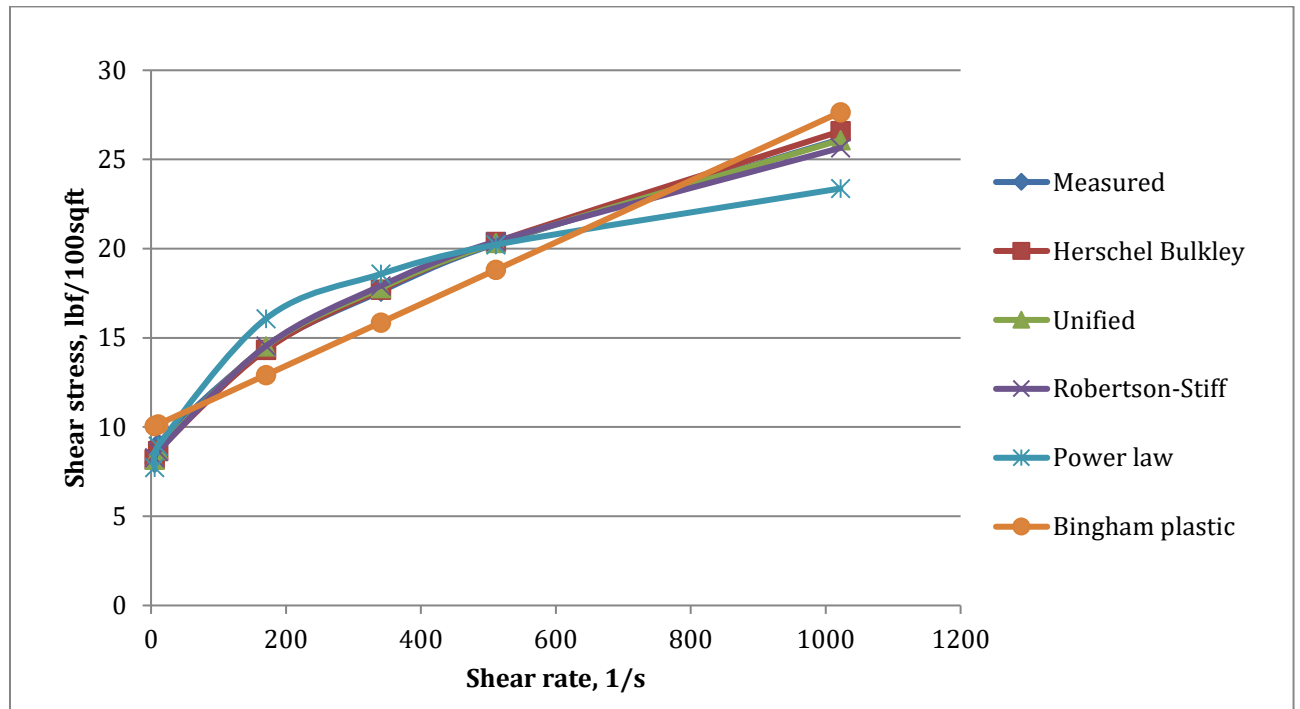


Figure 5.4: Viscometer readings and the different rheology models for Ref + 0.5 g MWCNT

Table 5.4: Overview of the different rheology models for Ref + 0.5 g MWCNT

Model	Equation	τ_0, τ_y, A	k, C	n, B	μ_p, μ	Error	cP
Herschel Bulkley	$2,824 \cdot \gamma^{0,3869} + 0,56250$	2.824	0.3869	0.56250		4.72	
Unified	$3,201 + 0,2142 \cdot \gamma^{0,654}$	3.201	0.2142	0.654		7.19	
Power Law	$2,1213 \cdot \gamma^{0,3195}$		2.1213	0.3195		2.52	
Bingham	$0,0153 \cdot \gamma + 6,019$	6.019			0.0154	27.71	7.37
Robertson and Stiff	$1,2384 \cdot (11,0654 + \gamma)^{0,4054}$	1.2384	11.0654	0.4054		2.79	

As observed in Figure 5.4/Table 5.4, the Power Law model describes the drilling fluid most adequate with 2.52% deviation, and Robertson and Stiff following close by with 2.79 % deviation. Bingham still shows the largest deviation with 27.71%. The rest of the models shows a deviation between 4.72% and 7.19%. As the Power Law model displays lowest percent deviation, it is most suitable for modelling the Ref. fluid + 0.5 g MWCNT.

5.1.5 Reference + 1.5 g MWCNT

The trend-lines for the relevant rheology models for Reference fluid + 1.5 g MWCNT are plotted in Figure 5.5. In Table 5.5 the corresponding parameters and equations are presented.

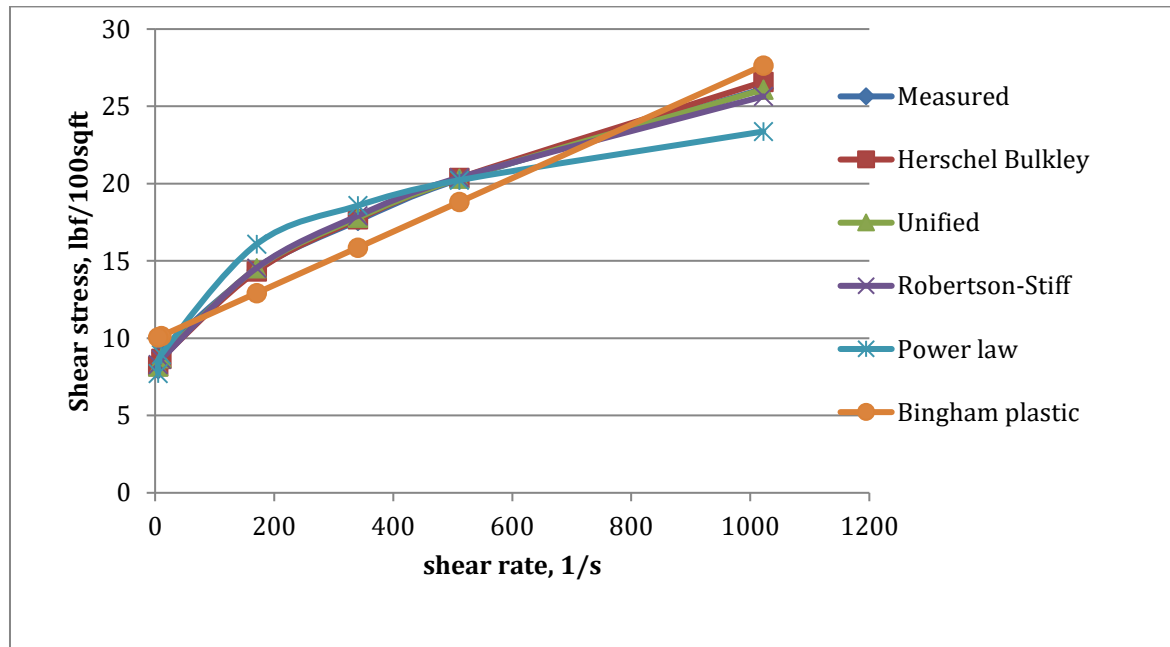


Figure 5.5: Viscometer readings and the different rheology models for Ref + 1.5 g MWCNT

Table 5.5: Overview of the different rheology models for Ref + 1.5 g MWCNT

Model	Equation	τ_0, τ_y, A	k, C	n, B	μ_0, μ	Error	cP
Herschel Bulkley	$5,518 \cdot \gamma^{0,2141} + 0,66860$	5,518	0,2141	0,66860		4,70	
Unified	$5,975 + 0,0569 \cdot \gamma^{0,8793}$	5,975	0,0569	0,8793		8,33	
Power Law	$3,6953 \cdot \gamma^{0,264}$		3,6953	0,264		5,92	
Bingham	$0,018 \cdot \gamma + 8,277$	8,277			0,018	19,23	8,6
Robertson and Stiff	$1,7002 \cdot (22,3152 + \gamma)^{0,3873}$	1,7002	22,3152	0,3873		1,75	

As observed in Figure 5.5/Table 5.5, the Robertson and Stiff model describes the drilling fluid most adequate with 1.75% deviation. Bingham model still shows the largest deviation with 19.23%. The rest of the models shows a deviation between 4.70% and 8.33%. Since the Robertson and Stiff displays lowest percent deviation, it is most suitable for modelling the Ref. fluid + 1.5 g MWCNT.

5.1.6 Comparison of Rheology models

In figure 5.6 the deviation of the rheological models for all the drilling fluids containing MWCNT is presented. From the figure it can be observed that Robertson and Stiff shows the lowest percentage deviation for Ref, Ref + 0.2 g MWCNT and Ref + 1.5 g MWCNT fluids. For Ref + 0.1 g MWCNT Fluid, the Unified model shows the lowest percentage deviation while the Power Law model is the most reliable for the Ref + 0.5 g MWCNT. Regarding the Bingham model, this has the highest percent deviation compared to the Fann measurements for all the fluids.

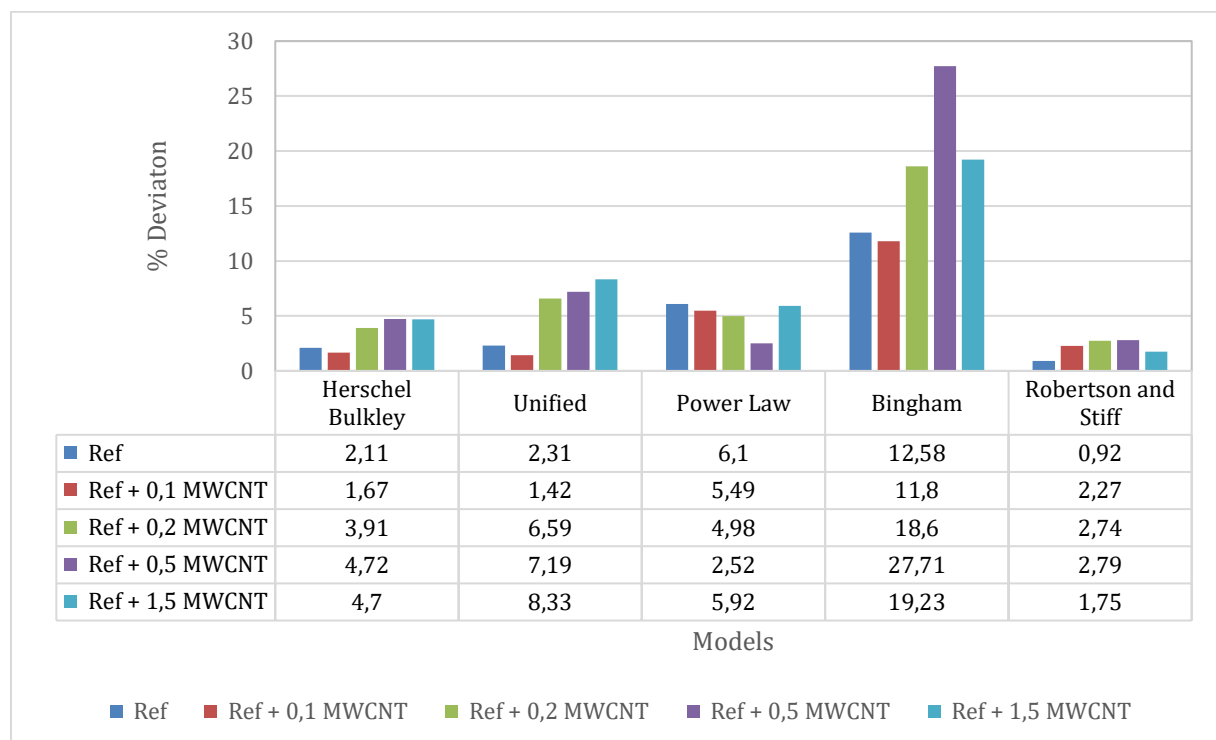


Figure 5.6: Comparison between the different fluids and rheology models

5.1.7 Effect of MWCNT on Rheology parameters

In Table 5.6 the rheological parameters for the different models are presented together with % deviation of the parameters compared to the reference system.

Table 5.6: Rheology parameters for the different models

Model	Parameters	Ref	Ref + 0.1 g MWCNT	Ref + 0.2 g MWCNT	Ref + 0.5 g MWCNT	Ref + 1.5 g MWCNT
Herschel Bulkley	τ_0	6.90	7.18	4.71	2.82	5.52
	% Deviation		4.00	-31.67	-59.07	-20.02
	K	0.23	0.41	0.32	0.39	0.21
	% Deviation		82.47	39.90	72.11	-4.76
	n	0.64	0.56	0.60	0.56	0.67
	% Deviation		-13.23	-7.49	-12.22	4.34
Unified	τ_y	6.94	6.94	5.23	3.20	5.98
	% Deviation		0	-24.63	-53.85	-13.86
	k	0.21	0.53	0.11	0.21	0.06
	% Deviation		155.21	-49.57	2.29	-72.83
	n	0.65	0.52	0.76	0.65	0.88
	% Deviation		-20.77	17.21	0.32	34.88
Power Law	K	4.93	5.50	3.38	2.12	3.70
	% Deviation		11.51	-31.37	-56.96	-25.03
	n	0.22	0.21	0,61	0.32	0.26
	% Deviation		-3.38	20.77	47.78	22.11
Bingham	YS	9.16	9.97	7.49	6.02	8.28
	% Deviation		0,09	-0.18	-0.34	-0.10
	PV	7.95	11.8	7.71	27.71	8.62
	% Deviation		0.49	-0.03	2.49	0.08
Robertson and Stiff	A	1.89	2.29	1.87	1.24	1.70

	% Deviation		0.21	-0.01	-0.35	-0.10
	B	0.34	0.35	0.36	0.41	0.39
	% Deviation		0.03	0.06	0.20	0.15
	C	38.38	35.72	16.04	11.07	22.14
	% Deviation		-0.07	-0.58	-0.71	-0.42

Remarks from table 5.6:

Herschel Bulkley model: When comparing with the Reference fluid, the yield stress (τ_0) increased only for the drilling fluid treated with 0.1 g MWCNT fluid, while the rest of the fluids treated with MWCNT indicates a significantly decrease in yield stress. The decrease in yield stress compared with reference fluid varies between -20% to -59%. For the drilling fluids treated with MWCNT, the reduction of yield stress is highest for the fluids containing 0.2 g MWCNT and 0.5 g MWCNT. For all the systems where greater concentrations of MWCNT are added, more shear stress is required to initiate the flow. For Ref + 1.5 g MWCNT the k-value decreased, while it increased for the rest of the drilling fluids. The n-value increased for the drilling fluid with 1.5 g MWCNT, while decreased for the rest of the drilling fluids. The fluid is shear thinning for all of the drilling fluids except the drilling fluids containing 1.5 g MWCNT.

Unified model: The shear yield stress (τ_y) decreased for all of the drilling fluids treated with MWCNT except for the drilling fluids containing the lowest concentrations of MWCNT. There was no deviation between Ref. and Ref + 0.1 MWCNT. For the rest of the fluids the decrease in shear yield stress varies between -13.86% and -53.85%. The K-value increased for REF + 0.1 g MWCNT and REF + 0.5 g MWCNT, while it decreased for the other two drilling fluid systems. The n-value decreased for the fluids only containing 0.1 MWCNT and increased for the rest of the fluids containing MWCNT.

Power Law model: The k-value decreased for all of the drilling fluids except the drilling fluid with 0.1 g MWCNT. The decrease were in the interval from -25.03% to -56.96%, while the fluid with 0.1 g MWCNT increased by 11.51%. Regarding the n-values, there was an increase for all of the fluids except Ref + 0.1 g MWCNT which experienced a small decrease.

Bingham model: The Yield stress (YS) indicated small % deviation compared to the reference fluid, the % deviation were in the range from -0.34% to +0.09%. The plastic viscosity increased for all of the fluids except the fluid containing 0.2 g MWCNT, which experienced a very small decrease in plastic viscosity.

Robertson and Stiff model: The A-parameter exhibit a small decrease for all of the fluids containing MWCNT except Ref + 0.1 g MWCNT. The % deviation compared with the reference fluids were quite small for all of the fluids containing MWCNT, and were in the range between -0.345% and 0.21%. The B-parameter experienced a small increased for all of the drilling fluids. The C-value decreased with an average value of 0.45% for the drilling fluids containing nanoparticles.

5.2 Hydraulics

In this section the hydraulic performance of the selected drilling fluids with MWCNT will be presented. The hydraulic theory is outlined in 3.4. This research will show how the different concentrations of nanoparticles affect the ECD and total pressure loss in the well compared to the reference fluid without nanoparticles. The ECD is the sum of the static mud weight and the pressure drop in the annulus. The hydraulic models are used to determine these parameters and the unified model was selected for the calculations.

5.2.1 Simulation arrangement

To study how the different amounts of nanoparticles affects the hydraulic performance of the drilling fluids, a vertical well with a depth of 10000 ft was designed in Microsoft Excell 2013 (Figure 5.7). The well was cased with 8.5” casing, and the drill pipe OD was 5” and the ID 4.8”. The drill bit had 3 nozzles and the surface pressure was zero. The flow rate was increased from 50 to 600 gpm, in increments of 50 gpm. During simulation, the density was set to 8.538 ppg for all of the drilling fluids.

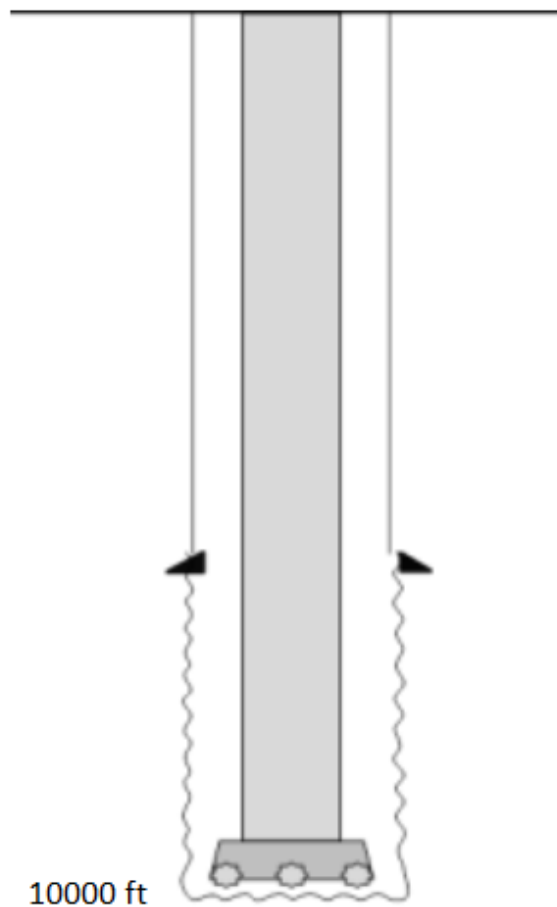


Figure 5.7: Illustration of well for hydraulic simulations.

5.2.2 Simulation result

The hydraulic simulation was carried out for Ref, Ref + 0.1 g MWCNT, Ref + 0.2 g MWCNT, Ref 0.5 g MWCNT and Ref + 1.5 g MWCNT. These fluids were selected due to the reduction in friction. In Figure 5.8 the ECD results from the simulation is presented. All of the nanoparticles fluids except Ref + 0.1 g MWCNT displayed a decrease in ECD compared to the reference fluid, and Ref + 0.5 g MWCNT achieved the lowest ECD. All of the fluids showed an increase in ECD with increasing flow rate, where the increase is due to pressure loss from friction.

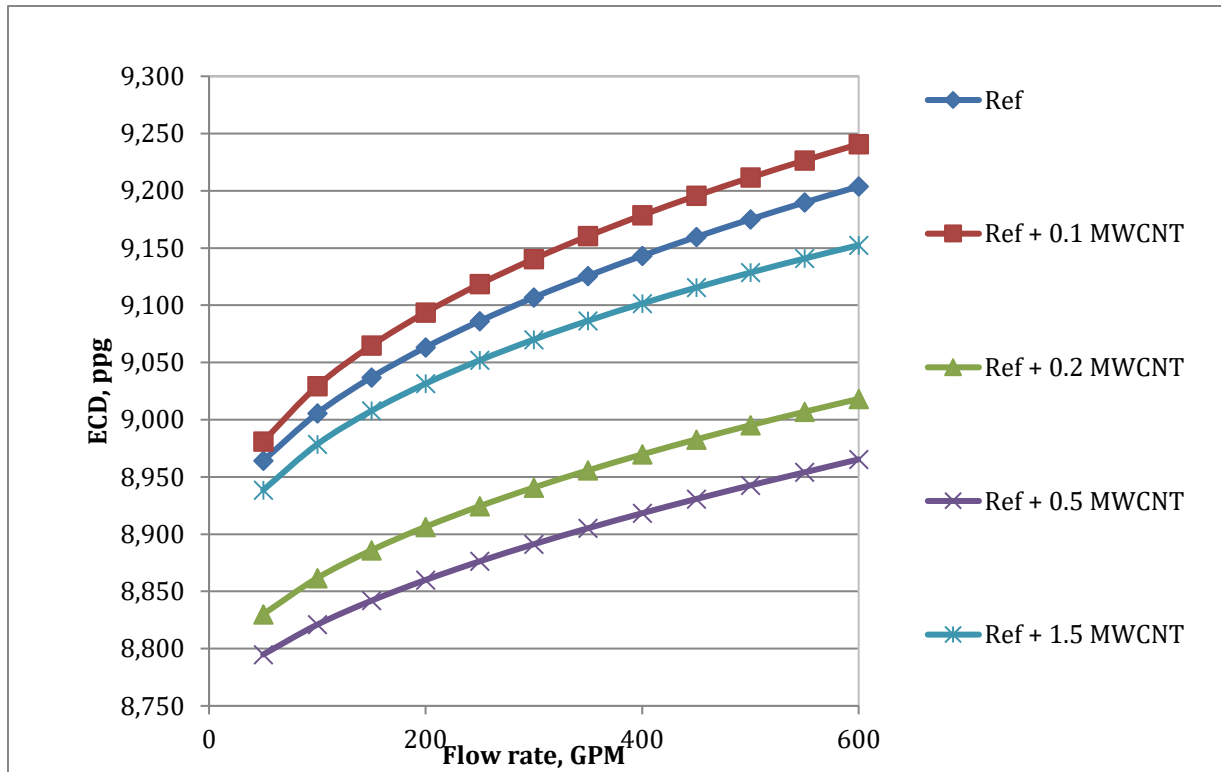


Figure 5.8: Percent deviation in ECD for the different drilling fluids with MWCNT compared to Ref.

In Figure 5.9 the percent deviation in ECD compared with Ref fluid is shown. The deviation increases with increasing flow rate for all of the nanofluids. Ref + 0.5 g MWCNT experienced the largest percent deviation.

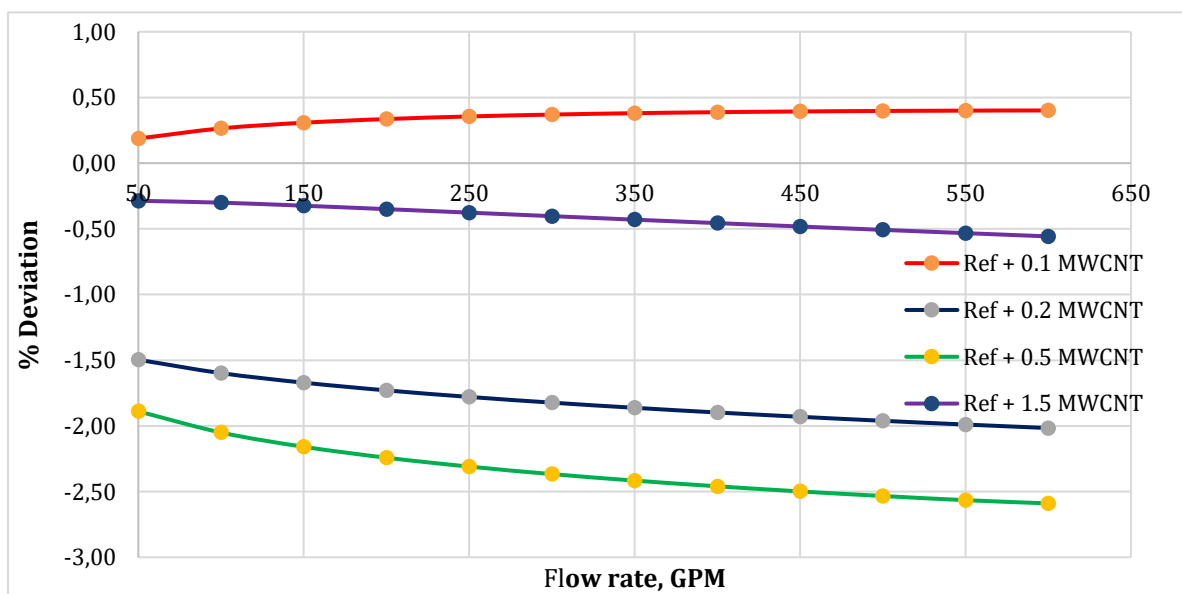


Figure 5.9: ECD deviation for the drilling fluids.

As ECD is a function of friction loss, it is related to total pressure loss and both show similar behavior with increasing flow rate. All of the drilling fluids except Ref + 0.1 g MWCNT experience a decrease in pressure loss compared with the reference. All fluids undergo the largest pressure loss from 400 GPM to 600 GPM. From the hydraulic simulation it can be observed that Ref + 0.2 g MWCNT, Ref + 0.5 g MWCNT and Ref + 1.5 g MWCNT will work better as drilling fluid since the total pressure loss is lower.

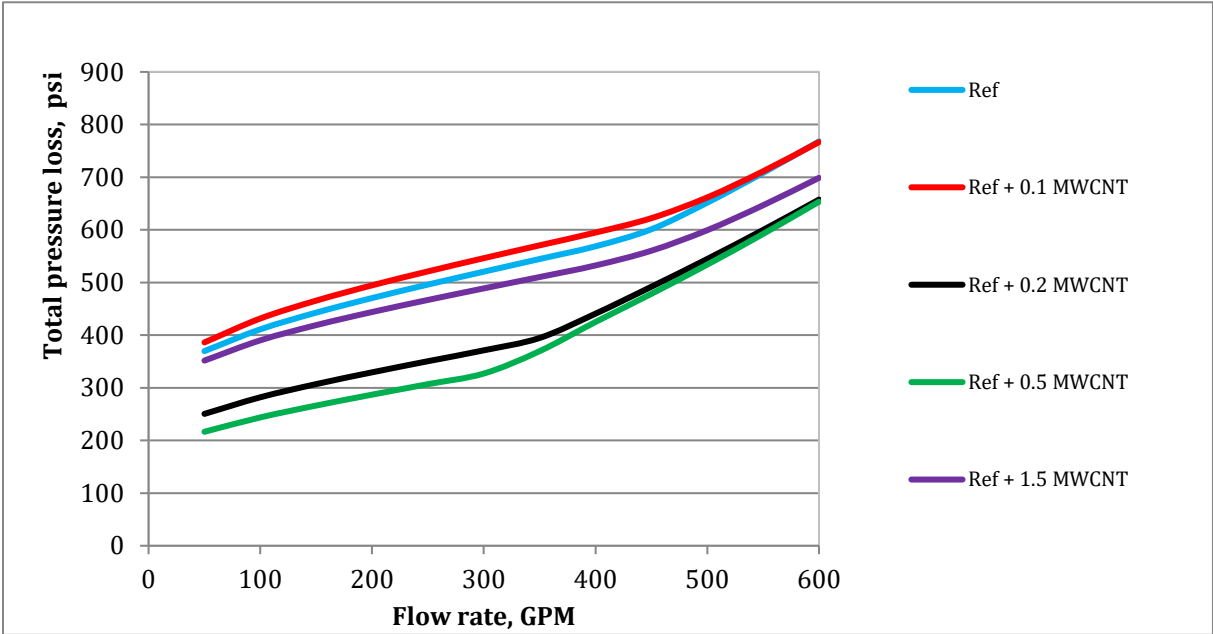


Figure 5.10: Pressure loss with increasing flow rate for the different drilling fluids.

5.3 Torque and drag

In 3.3 the theory part of torque and drag models are presented. Torque and drag problems are critical in inclined wells. An experimental study has shown that to increase the possible drilling length, a drilling fluid with better lubrication can be beneficial. Studies had shown that oil based muds is more lubricating then water based muds, but is expensive and less environmentally friendly. To achieve better lubricity in water based muds, the addition of nanoparticles may help. In the experimental study, it was shown that the addition of nanoparticles lowered the friction coefficient [20].

In this section, torque and drag simulation will be performed to see if it is possible to attain longer drilling lengths with the addition of nanoparticles in the drilling fluid.

5.3.1 Simulation Setup

Wellplan™ software from Landmark solutions was used to carry out torque and drag simulation [29]. Wellplan™ is developed by Halliburton for well design. To investigate how the fluid system listed in Table 5.7 effects the torque and drag, a deviated well set up was used. For the simulation a 5” OD drilling pipe with E-75 grade was used. For tripping in and tripping out, the speed was set to 60 ft/min, and the RPM to 100. The pump flow rate was set to 500 gpm.

The Fann 35 viscometer readings for the relevant drilling fluids are presented in Table 5.7, while the friction coefficient are presented in Table 5.8.

Table 5.7: Vicometer readings for the different fluids.

RPM	Ref [lbm/100 sq. Ft]	Ref + 0.1 MWCNT [lbm/100 sq. Ft]	Ref + 0.2 MWCNT [lbm/100 sq. Ft]	Ref + 0.5 MWCNT [lbm/100 sq. Ft]	Ref + 1.5 MWCNT [lbm/100 sq. Ft]
600	31.00	31.50	23.50	22.50	27.00
300	25.00	26.00	18.50	17.00	22.50
200	24.00	23.50	16.00	14.50	19.50
100	18.50	19.50	13.50	11.50	16.00
60	17.50	17.50	12.00	10.50	14.50
30	15.00	15.50	9.00	9.00	13.00
6	11.00	11.50	7.00	5.50	9.00
3	10.00	10.00	6.50	5.50	8.50

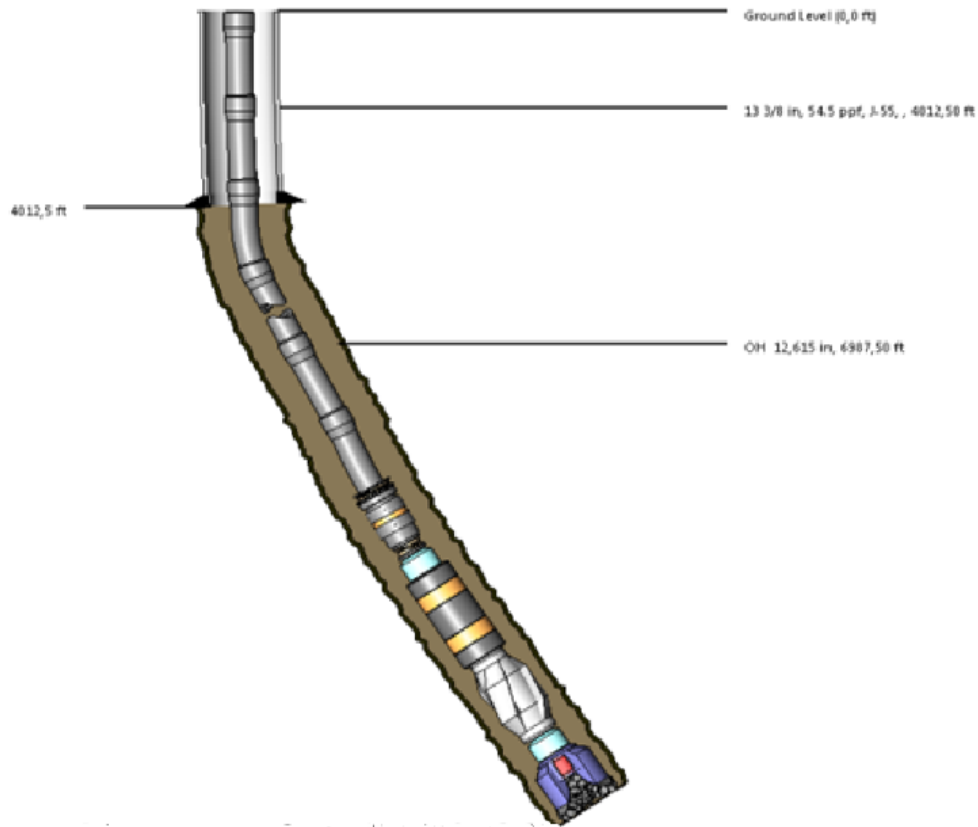


Figure 5.11: Schematic of well used for simulation.

The friction coefficients for the different fluids used for torque and drag simulation are listed in Table 5.8.

Table 5.8: Friction coefficient for the different fluid systems

Fluid system	Friction coefficient
Ref	0.241
Ref + 0.1 g MWCNT	0.221
Ref + 0.2 g MWCNT	0.204
Ref + 0.5 g MWCNT	0.176
Ref + 1.5 g MWCNT	0.160

5.3.2 Simulation Result

In Figure 5.12 the torque and drag graphs for the Ref and MWCNT system are presented.

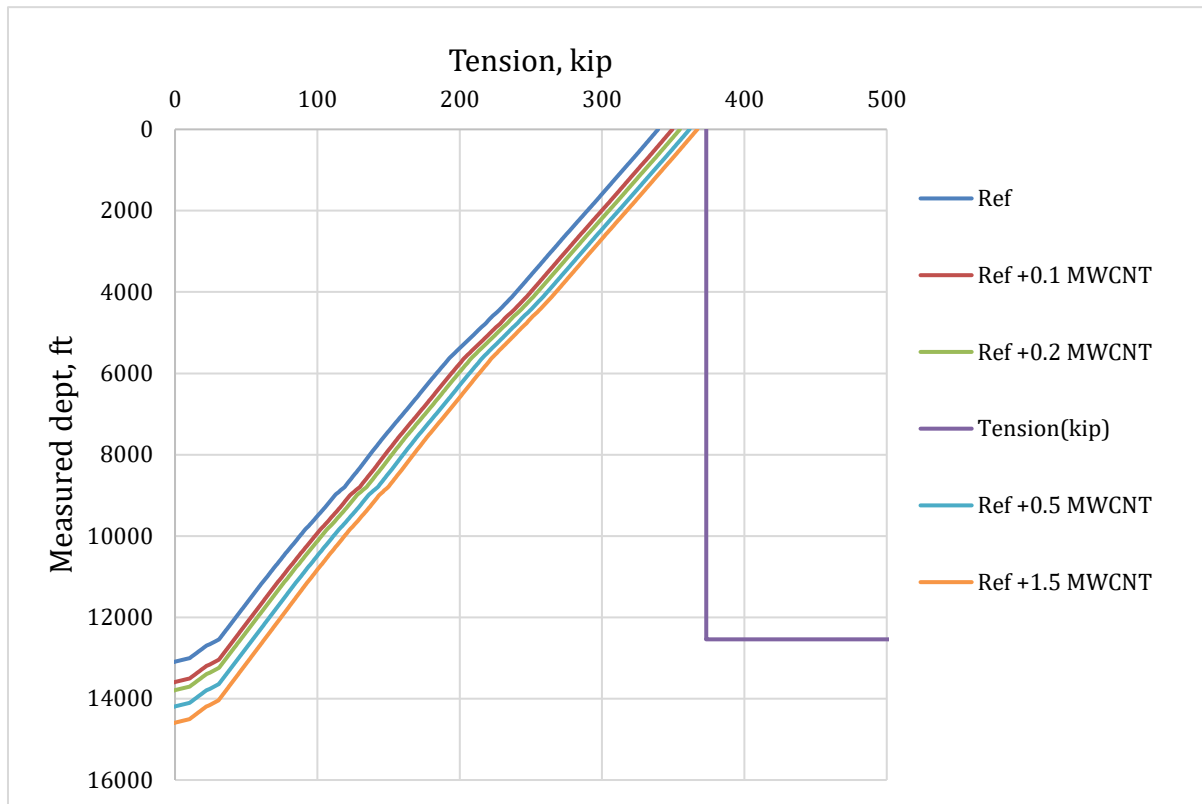


Figure 5.12: Drag chart for MWCNT fluids.

Figure 5.12 shows the drag chart for tripping out when simulating for the different fluids. It can be observed that none of the different systems exceeds the tensile limit, which indicates that the operations will be safe within the given parameter range. If the tensile limit is exceeded the drill pipe will start to yield. Figure 5.13 illustrated the different MD reaches for the formulated MWCNT drilling fluids. It can be observed that it is possible to drill the furthest with Ref + 1.5 g MWCNT, and the smallest distance with the Reference fluid. Tripping out operations are hardly safe for Ref + 0.5 g MWCNT and Ref + 1.5 g MWCNT, while the rest of the fluids shows a good margin to the tensile limit.

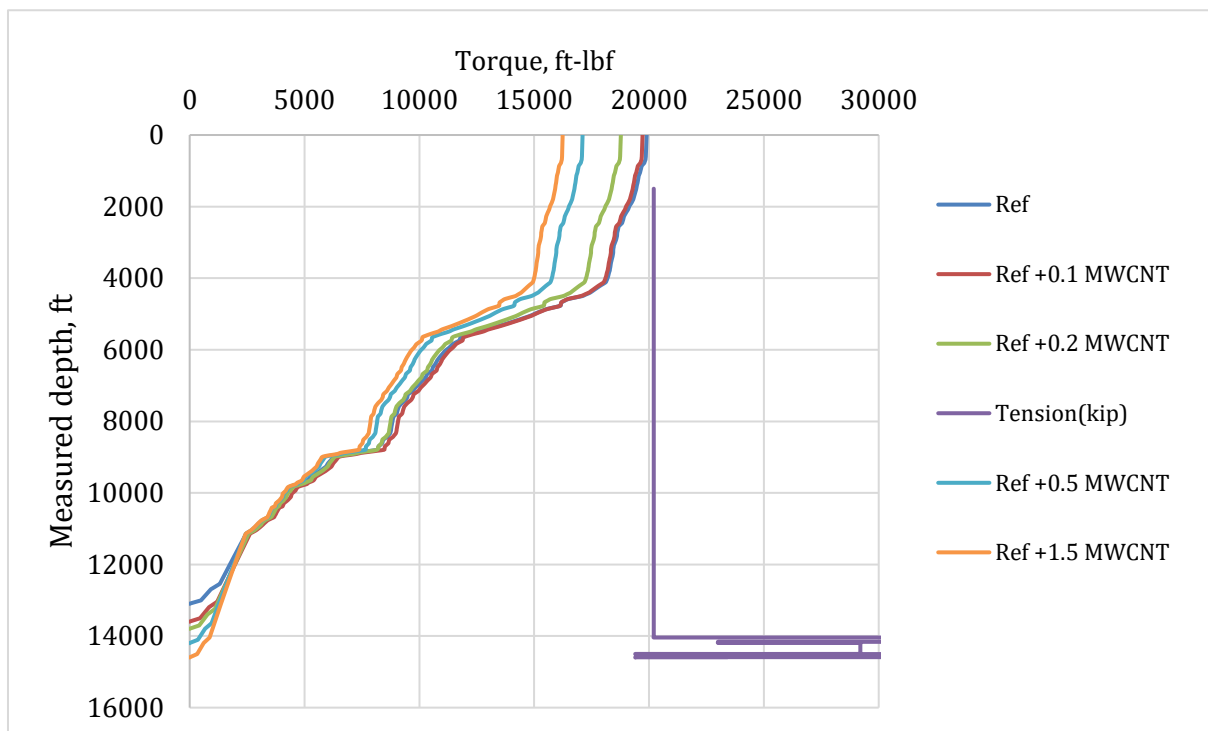


Figure 5.13: Torque chart for the different fluids.

For Ref + 0.1 g MWCNT and Ref + 0.2 g MWCNT tripping out operations are hardly safe at their given depths with the given parameters and it would not be possible to drill any further without drill pipe failure.

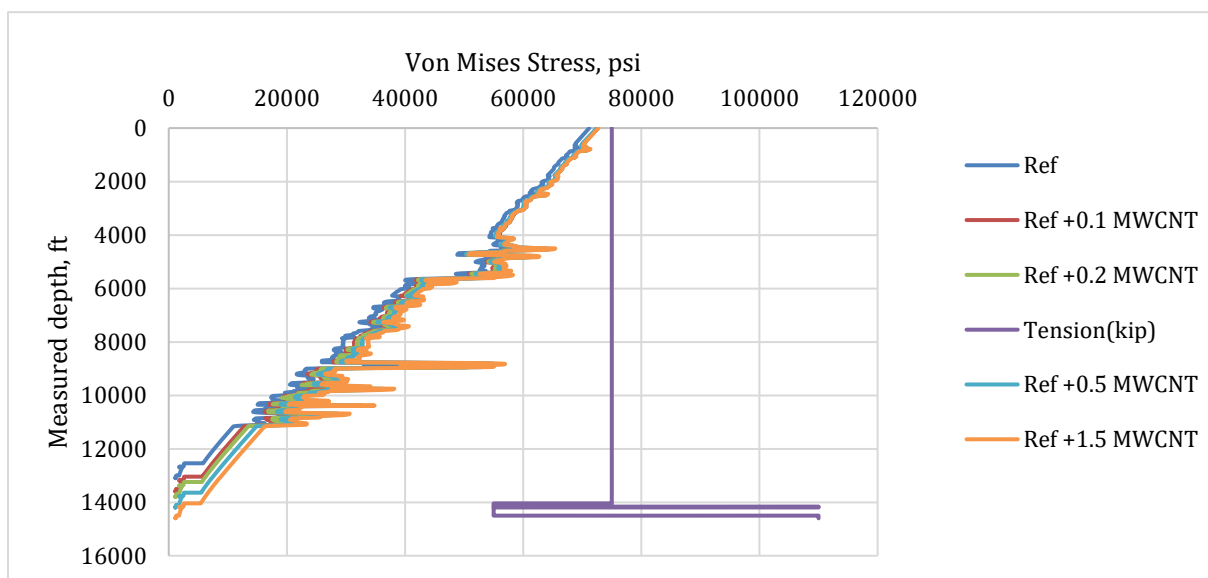


Figure 5.14: Von Mises stress for the different fluids.

The Von Mises stress does not exceed the stress limit for any of the drilling fluid, therefore it is safe to trip out for the relevant depths regarding to the stress limits.

It is possible to extend the drilling reach by adding MWCNT to the drilling fluid, which is shown in Table 5.9. Where the extended reach increased with increasing amount of nanoparticles in the mud. For the fluid containing 1.5 g MWCNT the coefficient of friction decreased by 33.6% and the drilling length increased with 11.45%, while 0.1 g MWCNT blended drilling fluid has shown an increase in drilling length by 3.82% and the 0.5 g MWCNT increased with 8.40%. When increasing the amount of MWCNT from 0.5 g to 1.5 g, one can observe that the additional 1 g MWCNT allowed to increase the drilling depth by 3.05%.

Table 5.9: Difference in CoF and reach with MWCNT as a additive

	Reference Fluid	Ref +0.1g MWCNT	Ref +0.2g MWCNT	Ref +0.5g MWCNT	Ref +1.5g MWCNT
CoF	0.241	0.221	0.204	0.176	0.16
% CoF reduction		-8.30	-15.35	-26.97	-33.6
Drilling MD (ft)	13100	13600	13800	14200	14600
% Drilling MD increase		3.82	5.34	8.4	11.45

5.4 Hole cleaning

Adequate hole cleaning is extremely important during drilling operations since poor hole cleaning will lead to a number of different drilling problems, such as stuck pipe, formation break down, low ROP, loss of circulation and high rotary torque. Since one of the main functions of a drilling fluid is the ability to suspend and transport drilled cuttings from down hole to the surface, it is necessary with hole cleaning simulations to check how the addition of MWCNT in a drilling fluid will affect hole cleaning. Hole cleaning efficiency is affected by parameters such as fluid viscosity, annular viscosity, inclination angle and size/shape of cuttings [30].

5.4.1 Simulation setup

The experimental well used for hole cleaning simulation is deviated and 14600 ft measured depth long. WellPlan-Software was used to perform the simulation.

Table 5.10: Drilling parameters

Parameter	Value
Cutting diameter	0,125
Cutting density	2.50 sg
ROP	60 ft/hr
RPM	90
Flow Rate	500 gpm
Bed porosity	36 %
Bit diameter	8.5 in
Annulus diameter	8.5 in
Joint Diameter	5,5 in
Minimum pump rate	100 gpm
Increment pump rate	200 gpm
Max pump rate	600 gpm

Drilling fluids

The data used for hole clean simulation are presented in Table 5.11, the table represents the readings from the Fann35 viscometer at different RPM values.

Table 5.11: Fann35 viscometer readings

RPM	BASE Fluid	BF+0,1MWCNT	BF+0.2MWCNT	BF+0,5MWCNT	BF+1,5MWCNT
600	31	31,5	23,5	22,5	27
300	25	26	18,5	17	22,5
200	24	23,5	16	14,5	19,5
100	18,5	19,5	13,5	11,5	16
6	11	11,5	6	5,5	9
3	10	10	3	5,5	8,5

5.4.2 Simulation results

5.4.2.1 Minimum flow rate

If the flow rate does not provide the sufficient fluid velocity required to lift cuttings from the wellbore, particles will start to settle in the annulus and form bed deposits. The most dominant drilling variable is fluid velocity, this due to the direct relation with the shear stress acting on the cuttings bed. Sufficient shear stress should be applied to remove the cuttings from a horizontal or deviated well and erode the developed well [31]. Minimum

flow rate simulation compare the five different fluids, and can tell which fluids that shows lowest needed flowrate without probability for cutting deposition. Simulation inputs are given in Figure 5.15

From the simulation results it could be concluded that Ref + 0.1 g MWCNT is the only one that displays better results than Ref. The fluids containing 0.2 g MWCNT and 0.5 g MWCNT shows poor results, and need a great increase in minimum flow rate to avoid bed deposits. The fluid which displays best results regarding friction requires a 10% increase in minimum flow rate.

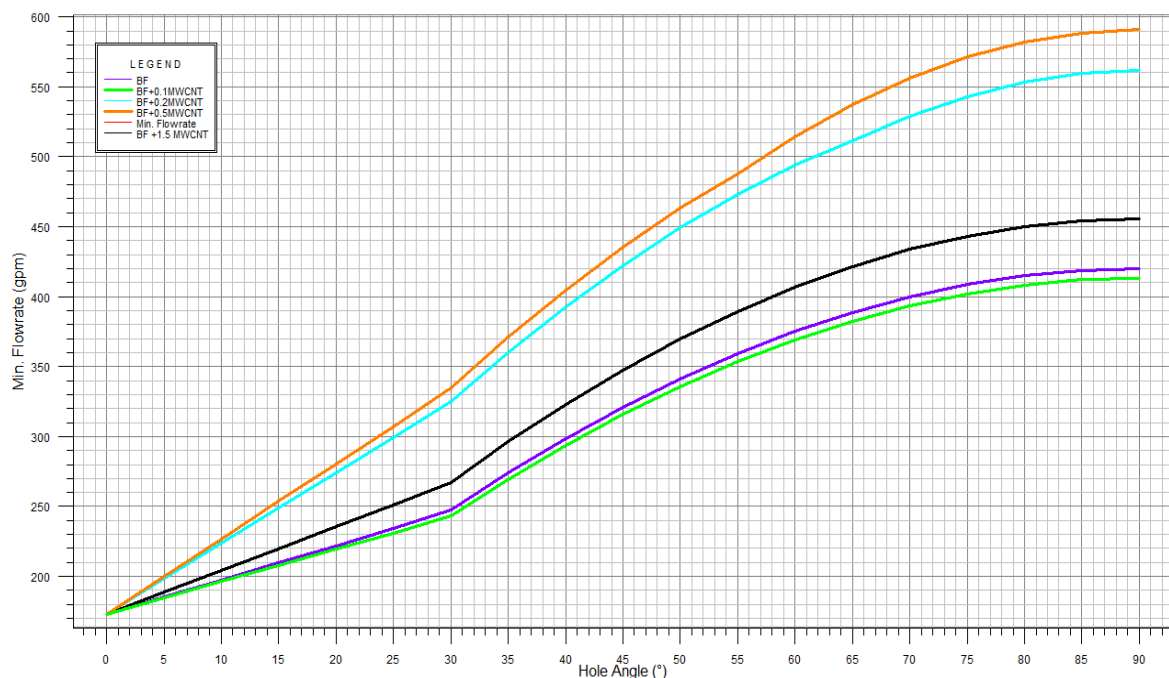


Figure 5.15: Minimum flow rate required to transport out the cuttings at different inclinations.

5.4.2.2 Bed height

When the hole-cleaning is inadequate the cuttings will be deposited on the bottom of the well, also known as cuttings bed. This will lead to problems such as increase in torque and drag, stuck pipes, loose control on density, difficult when running and cementing casings. To avoid these effects it is important with adequate hole-cleaning. Bed height simulation also gives a poor approximation of carrying capacity, and the major factors affecting this is fluid velocity, hole inclination, drilling fluid properties, penetration rate, pipe eccentricity, hole geometry, cuttings properties and drill pipe rotation speed [31].

The simulation was performed with a pump rate at 500 gpm. For other simulation inputs, see Table 5.12.

Table 5.12: Transport analyse data

ROP	60 ft/hr
Rotary speed	90 rom
Pump rate	500 gpm
Cuttings diameter	0.125 in
Cuttings density	2.5 sg
Bed porosity	36.0 %
MD calculation interval	100.0 ft

From Figure 5.16 it can be observed that Ref + 0.1 g MWCNT experience less problems with bed deposits than the rest of the fluids, while Ref + 0.2 g MWCNT and Ref + 0.5 g MWCNT experience the highest level of bed deposition.

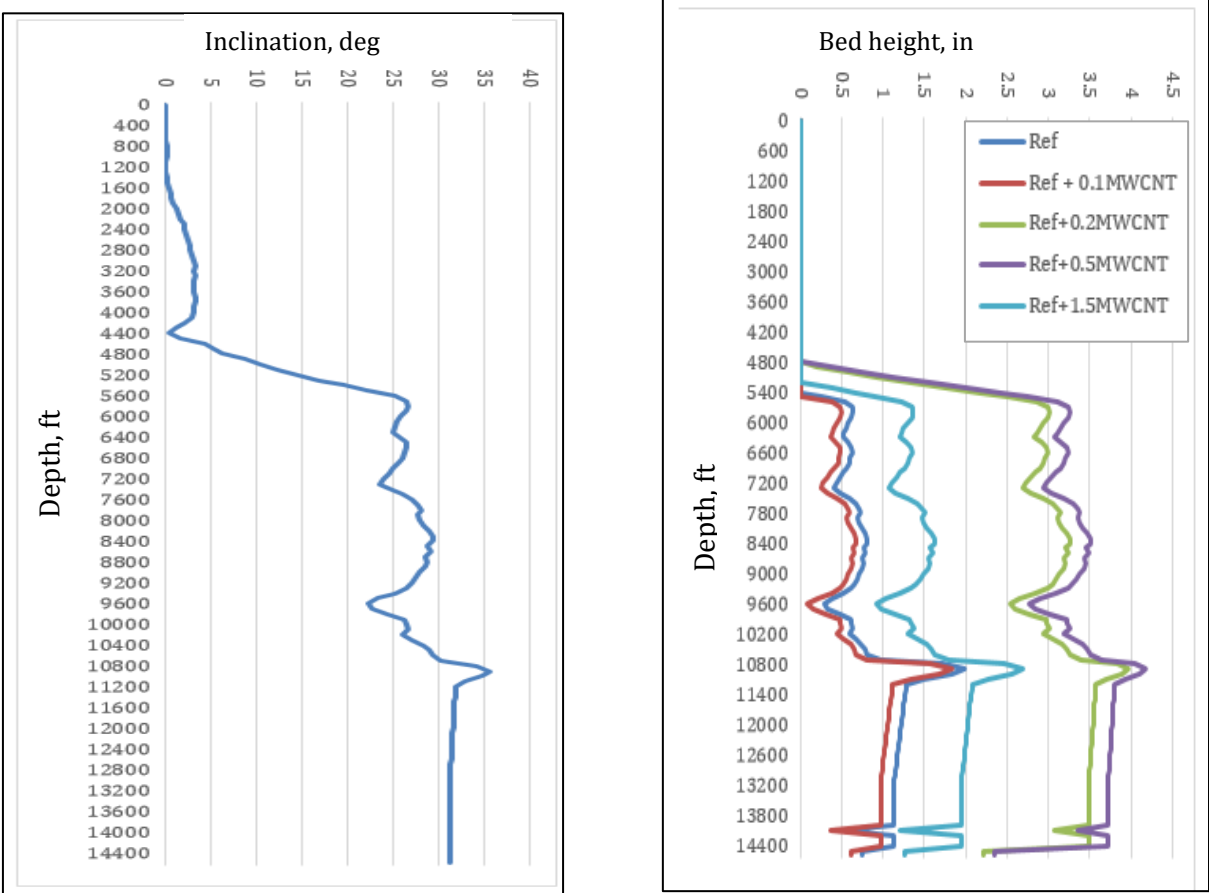


Figure 5.16: Well inclination and bed deposition.

6 Summary and discussion

In this section, the summary and discussion of the overall study will be presented. The purpose of the study was to experimentally investigate the impact of MWCNT on nanoparticle free laboratory drilling fluid (Ref). The investigation was under various mixing, pH and temperature conditions. The effect of mixing, pH and temperature was also investigated. Further, the best lubricity fluid systems performances have been evaluated through simulation studies, such as hole-cleaning, hydraulics and torque and drag.

5.1 Effect of MWCNT concentration on rheological properties

From the experimental work it is observed that MWCNT has impact on the rheological property of base fluid. However, the viscometer response varies nonlinearly as MWCNT concentration increases. Among the considered MWCNT concentration, the 0.2 g and 0.5 g additives have shown a higher viscometer response as compared with the base fluid (Ref). On the other hand, the drilling fluid with the highest concentration (1.5 g MWCNT) exhibit similar results regarding shear stress as Ref fluid.

In general it is observed that the effect of MWCNT in rheological properties of the based fluid is non-linearly. Depending on the concentration, the Bingham PV and Yield stress increased and also has shown to be decreased.

Except for 1.5 g MWCNT, all of the five fluids formulated showed pseudo plastic behavior, where the flow index increased. On the other hand the effect of nanoparticle has shown a decreasing effect, which is the opposite impact as observed for flow index.

With respect to filtrate loss, the MWCNT treated drilling fluid have shown an increase in fluids loss, except Ref + 0.5 g MWCNT, where the loss increased between 1.2% and 5.9 %, and Ref + 1.5 g MWCNT showed the largest loss. The cation concentration in the filtrate loss showed little difference and the SEM-pictures showed that the MWCNT accumulated in some areas, which may affect the filtrate loss. This shows that larger amounts of nanoparticles may lead to greater fluid loss, and that higher concentrations may not be the optimum for all of the parameters.

5.2 Effect of MWCNT on coefficient of friction

In this study the reference fluid were modified with four different amounts of MWCNT, to evaluate how the friction coefficient changed with increasing nanoparticle concentration. The addition of nanoparticles led to better lubricity for all of the drilling fluids. The reduction of friction coefficient (or increasing of lubricity) varies linearly as concentration of MWCNT increases. In terms of magnitude, result shows that the 0.1 g MWCNT and 1.5 g MWCNT additives increased the lubricity of the reference base fluid by 6.6% and 18.8% respectively.

5.3 Effect of temperature and pH on MWCNT systems

It is of highly importance to evaluate how the temperature affects the rheology of the drilling fluid, as the fluid can experience high temperatures while drilling. The temperature effects were evaluated for drilling fluids with both lower and higher pH. For the fluids with lower pH, it was observed that the shear stress slightly decreased with higher temperatures, and that YS decreased for all of the fluids when increasing the temperature from 72°F to 180°F. PV decreased for most of the fluids, but were quite stable for Ref + 1.5 g MWCNT. There was not observed any correlation for Power-Law parameters behavior and nanoparticle concentration. The fluids with higher pH showed rather similar behavior for the different parameters, but with some higher viscometer readings. With increasing temperature, the pH decreased for the tested fluids, perhaps due to the equilibrium condition of the auto ionization process which is affected by temperature. The viscometer readings for Ref fluid decreased with 16.3% when the temperature increased from 72°F to 180°F, while Ref + 1.5 g MWCNT decreased with 12.8%.

5.4 Effect of mixing on rheology and friction

Rheology test shows that different mixing methods effects the rheology of these fluids. The first drilling fluid was mechanical mixed, while the second drilling fluid was mixed mechanical and with sonication as described in 4.6. The second fluid experienced an increase in shear stress with 15%. For the second fluid, PV decreased with 9.1%, YS increased with 39.1% and LSYS increased with 27.3%. Both fluids displayed pseudo

plastic behavior. Friction test showed that mixing procedure causes little effect, and that the friction factor for the second fluid decreased with 2.9%. The second fluid might showed better readings due to better dispersion, where the different additives were mixed well.

5.5 Effect on viscoelasticity

In this study amplitude sweep measurement test were performed for the five different fluids to evaluate how the nanoparticles effect viscoelasticity. As described in 3.4, the viscoelastic properties are highly important, since these parameters characterize gel structure, gel strength, barite sag and hydraulic modeling.

The amplitude sweep measurement showed that the fluids containing MWCNT had both higher storage modulus and loss modulus compared with the reference fluid without nanoparticles, and that the storage modulus and loss modulus increased with increasing nanoparticle concentrations. Until the intersection points (where the fluid will turn into elastic behavior), all of the fluids had higher storage modulus than loss modulus. All of the five fluids had a LVER.

The flow point from the amplitude sweep measurement revealed that fluids with MWCNT increased their flow point, and that the flow point increased with increasing concentration of nanoparticles (except Ref + 0.5 g MWCNT).

This demonstrates that the nanoparticle fluids obtains a more stable gel structure with increasing concentration of MWCNT.

5.6 Effect on hydraulics

Hydraulic simulation is used to investigate the hydraulic properties, since these properties are important for ECD and cutting transport. For this simulation the Unified model was used, since this model gave very low error rate. The simulation showed that ECD increased for all of the fluids compared with the reference, except Ref + 0.5 g MWCNT that displayed some lower ECD. There were no correlation between nanoparticle concentration and ECD, since Ref + 0.5 g MWCNT displays higher ECD values than Ref +

1.5 g MWCNT. This indicates that the fluids with MWCNT additive contributes to negative effect for well stability.

5.7 Effect on torque and drag

Since the tribometer tests gave lower friction values for the nanofluids, torque and drag simulation were performed in Wellplan™5000.1 software program. For the simulation a fictional inclined well was used, as this is the most critical area regarding friction coefficient. Comparing with the base fluid (Ref), the addition of 1.5 g MWCNT (or 0.3wt%) reduced the friction coefficient and allowed to drill more about 11.45% in a considered well trajectory.

5.8 Effect on hole cleaning

The hole-cleaning efficiency with respect of cutting lifting and bed high deposition when in the selected drilling fluid have been simulated in a wellbore built in Landmark/WellPlan software. Simulation result showed that the MWCNT modified drilling fluids were less capable to carry cuttings out of the well (except Ref + 0.1 g MWCNT). It is also observed that there were no correlation between nanoparticle concentration and transport efficiency. Here also 0.1 g MWCNT (0.02wt%) have shown good hole cleaning performance.

7 Conclusion

The objective of this thesis was to study the effect of MWCNT on a conventional bases fluid under various pH, temperature and mixing condition. The bases fluid has been formulated by mixing water, bentonite, duovis, lignosulfonate, KCl. Nanoparticle based drilling fluid have been formulated by adding 0.02wt%, 0.04wt%, 0.1wt% and 0.3wt% MWCNT in the bases fluid (Ref). The performance of the drilling fluid have been evaluated through simulation study. From the experiments and simulations, the main observation on the effect of MWCNT on a conventional fluid can be summarized as follows:

- The effect of MWCNT on the bases fluid have shown impact on the rheological properties, but the effect was non-linearly as concentration increases
- Lowered the friction coefficient with increasing concentration of MWCNT. Addition of 0.3wt% MWCNT decrease the friction coefficient by 43.6%
- Shows the same behavior for the rheological parameters in fluid with higher and lower pH-values. However the drilling fluids with higher pH showed some higher viscometer reading
- Are affected by mixing procedure, where the drilling fluid mixed with sonication exhibits an increase in shear stress, YS and LSYS, while PV decreased. The friction coefficient decreased by 2.9 %
- In general the considered MWCNT concentrations have increased the filtrate loss of the base fluid
- Increase storage modulus and loss modulus as the concentration of MWCNT increases
- Allows for longer drilling length and where the drilling length increased with increasing concentration of MWCNT

- Except for the 1.5 g MWCNT system, temperature have reduced the PV of the drilling fluids

From the conclusion it was observed both negative and positive results when using MWCNT as an additive to improve the conventional WBM system. However, the impact and performance of MWCNT in the laboratory drilling fluid is valid in the Duovis polymer. Changing the polymer types, one may achieve different results.

References

1. A. Aftab, A. R. Ismail, Z. H. Ibupotp, H. Akeiber, M. G. K. Malghani, "Nanoparticles based drilling muds a solution to drill elevated temperature wells: A review" *Renewable and Sustainable Energy Reviews*, Volume 76, September 2017, Pages 1301-1313.
2. Guo B and Liu G. "Applied Drilling Circulation system" 1st Edition, United states, (ISBN 978-0-12-381957-4)
3. H. C. Lau, M. Yu, Q. P. Nguyen " Nanotechnology for oilfield applications: challenges and impact" *Journal of Petroleum Science and Engineering*, Volume 157, August 2017, Pages 1160-1169.
4. A. R. Ismail, T. C. Seong, N. A. Buang, W. R. W. Sulaiman, "improve performance of water- based drilling fluids using nanoparticles" Prepared for presentation at The 5th Sriwijaya International Seminar on Energy and Environmental Science & Technology Palembang, Indonesia, September 10-11, 2015 [online] Obtained from:https://www.researchgate.net/publication/316555100_Improve_Performance_of_Water-based_Drilling_Fluids_Using_Nanoparticles
5. M. Baghbanzadeha, A. Rashidi, A. H. Soleimanisalimc, D. Rashtchiana, "Investigating the rheological properties of water/hybrid nanostructure of spherical silica/mwcnt" *Thermochimica Acta*, Volume 578, February 2017, Pages 53-58.
6. R. Rafati, S. R. Smith, A. S. Haddad, R. Novara, H. Hamidi, "Effect of nanoparticles on the modifications of drilling fluids properties: a review of recent advances" *Journal of Petroleum Science and Engineering*, Volume 161, February 2018, Pages 61-76.
7. A. Aftaba, A. R. Ismaila, Z. H. Ibupotod, H. Akeiberf, M. G. K. Malghanig, "Nanoparticles based drilling muds a solution to drill elevated temperature wells: A review" *Renewable and Sustainable Energy Reviews*, Volume 76, September 2017, Pages 1301-1313.
8. Skjeggstad O. (1989) "Boreslamsteknologi: Teori og praksis" Alma Mater Forlag. (ISBN: 82-419-0010-4)
9. Stand S. (2014) "Øvinger i Bore og Brønnvæsker" Compendium in the BIP 200 class, Univeristy of Stavanger, Stavanger, Rogaland (January 2014)
10. Fink J. (2011) "Petroleum Engineer's Guide to Oil Field Chemicals and Fluids" Gulf Professional Publishing. (ISBN:978-0-12-383844-5)
11. Kumine Industries Co ., LTD, (accessed 1. June 2018) <https://www.kunimine.co.jp/english/bent/basic.html>
12. R. Bleier, "Selecting a drilling fluid" SPE-20986-PA, *Journal of Petroleum Technology*, Volume 42, Issue 7, July 1990.
13. MISwaco Manual. (1998) Polymer chemistry and applications. In *Drilling Fluids Engineering Manual*. Chap 6. 6.7 6.5
14. R. Jain, T. K. Mahto, V. Mahto, "Rheological investigations of water based drilling fluid system developed using synthesized nanocomposite" *Korea-Australia Rheology Journal*, Volume 28, Issue, Pages 55-65, February 2016.
15. J. H. Lehman, M. Terrones, E. Mansfield, K. E. Hurst, V. Meunier, "Evaluating the characteristics of multiwall carbon nanotubes" *Carbon*, Volume 49, Issue 8, Pages 2581-2602, July 2011

16. Lan Ma-Hock et al. Toxicological Sciences, Volume 112, Issue 2, Pages 468-481, December 2009
17. Ochoa M. V. (2006) "Analysis of Drilling Fluid Rheology and Tool Joint Effect to Reduce Errors in Hydraulics Calculations." PhD Dissertation, Texas A&M University, College Station, Texas (August 2006)
18. A. P. Deshpande, J. M. Krishnan, P.B. S. Kumar, "*Rheology of Complex Fluids*" 1st Edition, New York, USA, Springer, 2010, DOI 10.1007/978-1-4419-6494-6
19. Belayneh (2017) "Advanced drilling lecture note" UiS
20. M. S. Aston, P. J. Hearn, G. McGhee, "Techniques for solving torque and drag problems in today's drilling environment" SPE-48939-MS, Prepared for presentation at SPE Annual Technical Conference and Exhibition, 27-30 september, 1998, New Orleans, Louisiana.
21. Mezger T.G (2011)"The Rheology Handbook" 3rd Revised Edition. Hanover. (ISBN: 3-86630-864-7)
22. B. Werner, V. Myrseth, A. Saasen, " Viscoelastic properties of drilling fluids and their influence on cuttings transport", Journal of Petroleum Science and Engineering, Volume 156, Pages 845-851, July 2017
23. Bui B., Saasen A., Maxey J., Ozbayoglu M. E., Miska S. Z., Yu M. and Takach N.E. (2012)" Viscoelastic Properties of Oil-Based Drilling Fluids" Annular Transactions of the Nordic Rheology Society Vol.20, 2012.
24. J. J. Azar, G. Robello, "*Drilling Engineering*" Oklahoma USA, PennyWell Corporation, 2007 ISBN: 9781593700720
25. J. Sadigov (2013) "Comparisons of Rheology and Hydraulics Prediction of Mud Systems in Concentric and Eccentric Well Geometry" MSc Thesis, University of Stavanger, Stavanger, Rogaland (June 2013)
26. Labcompare (accessed 12. May)
<https://www.labcompare.com/Spectroscopy/26-Inductively-Coupled-Plasma-Spectrometer-ICP-AES-ICP-OES/>
27. Carl Zeiss AG (accessed 5. June)
<http://www.fis.unipr.it/dokuwiki/lib/exe/fetch.php?media=lmn:brochure.pdf>
28. Huang et al. "Surface Chemistry and Rheological Properties of API bentonite drilling fluid: pH effect, yield stress, zeta potential and ageing behaviour" Journal of Petroleum Science and Engineering. 146. 10.1016/j.petrol.2016.07.016.
29. H. Wellplan (Landmark)TM Software, WellPlan (Landmark) TM Software, Halliburton, 2016
30. H. H. Al-Kayiem, N. M. Zaki, M. Z. Asyraf, M. E. Elfeel, "Simulation of the Cuttings Cleaning During the Drilling Operation", American Journal of Applied Sciences 7, 2010, ISSN 1546-9239
31. M. E. Ozbayoglu , A. Saasen , M. Sorgun & K. Svanes (2010) Critical Fluid Velocities for Removing Cuttings Bed Inside Horizontal and Deviated Wells, Petroleum Science and Technology, 28:6, 594-602, DOI: 10.1080/10916460903070181

Appendix

Appendix A

Table A.1: Base fluid 1 formulation

Base fluid 1	
Ingredients	Concentration
Water, [g]	500
Bentonite [g]	25
Duovis [g]	1
KCl [g]	2.5
Lignosulfonate	x

Table A.2: Base fluid 1 parameters

Base Fluid 1			
Rheology Parameters	Temperature		
	72°F	130°F	180°F
PV [cP]	6.5	8.0	8.0
YS [lbf/100ft ²]	43	38	35
LSYS [lbf/100ft ²]	22.5	20.5	19.5
n	0.178	0.231	0.246
K [lbf*sec ⁿ /1000ft ²]	16	11	9
Filtration [ml]			
pH	8.36		
CoF	0.3655		
Base Fluid 1 + 0.05 g MWCNT			
Rheology Parameters	Temperature		
	72°F	130°F	180°F
PV [cP]	8.5	8.0	9.0
YS [lbf/100ft ²]	41.0	39.5	36.0
LSYS [lbf/100ft ²]	22.5	21.0	20.0
n	0.228	0.224	0.263
K [lbf*sec ⁿ /1000ft ²]	12	12	9
Filtration [ml]			
pH	8.22		
CoF	0.355		
Base Fluid 1 + 0.1 g MWCNT			
Rheology Parameters	Temperature		
	72°F	130°F	180°F

PV [cP]	8.0	9.0	8.0
YS [lbf/100ft ²]	41.0	38.0	37.0
LSYS [lbf/100ft ²]	22.5	22.0	20.5
n	0.218	0.253	0.236
K [lbf*sec ⁿ /1000ft ²]	13	10	10
Filtration [ml]			
pH	8.61		
CoF	0.192		
Base Fluid 1 + 2.0 g MWCNT			
Rheology Parameters	Temperature		
	72°F	130°F	180°F
PV [cP]	8.5	10.0	6.0
YS [lbf/100ft ²]	48.0	43.5	44.0
LSYS [lbf/100ft ²]	30.5	27.5	22.5
n	0.202	0.247	0.163
K [lbf*sec ⁿ /1000ft ²]	16	11	18
Filtration [ml]			
pH	8.31		
CoF	0.281		
Base Fluid 1.1 (500 g H₂O, 25 g Bentonite, 7.5 g KCl, 1 g Douvis)			
Rheology Parameters	Temperature		
	72°F	130°F	180°F
PV [cP]	11.5	13.0	10.5
YS [lbf/100ft ²]	86.0	75.0	67.0
LSYS [lbf/100ft ²]	25.0	22.5	24.0
n	0.16	0.20	0.18
K [lbf*sec ⁿ /1000ft ²]	35.78	25.49	24.72
Filtration [ml]			
pH			
CoF			

Table A.3: Base fluid 2 formulation

Base fluid 2	
Ingredients	Concentration
Water, [g]	500
Bentonite [g]	25
Duovis [g]	1.0
KCl [g]	2.5
Lignosulfonate	2.0

Table A.4: Base fluid 2 parameters

Base Fluid 2			
Rheology Parameters	Temperature		
	72°F	130°F	180°F
PV [cP]	6.0	5.5	4.0
YS [lbf/100ft ²]	8.5	8.5	10.0
LSYS [lbf/100ft ²]	3.5	4.5	3.5
n	0.50	0.48	0.36
K [lbf*sec ⁿ /1000ft ²]	0.64	0.71	1.46
Filtration [ml]			
pH	7.68		
CoF	0.2345		
Base Fluid 2 + 2.0 g MWCNT			
Rheology Parameters	Temperature		
	72°F	130°F	180°F
PV [cP]	6.5	6.5	4.5
YS [lbf/100ft ²]	8.0	7.5	9.5
LSYS [lbf/100ft ²]	3.5	3.5	4
n	0.53	0.55	0.40
K [lbf*sec ⁿ /1000ft ²]	0.52	0.45	1.14
Filtration [ml]			
pH	7.68		
CoF	0.215		
Base Fluid 2.1 (500 g H ₂ O, 25 g Bentonite, 2.5 g KCl, 1.0 g Douvis, 0.5 Lignosulfonate) + 2 g MWCNT			
Rheology Parameters	Temperature		
	72°F	130°F	180°F
PV [cP]	8.0	8.0	6.5
YS [lbf/100ft ²]	30.5	30.0	30.0
LSYS [lbf/100ft ²]	22.5	21.5	22.0

n	0.27	0.28	0.24
K [lbf*sec ⁿ /1000ft ²]	7.05	6.82	8.36
Filtration [ml]			
pH			
CoF			

Table A.5: Base fluid 3 formulation

Base fluid 3	
Ingredients	Concentration
Water, [g]	500
Bentonite [g]	25
Duovis [g]	0.5
KCl [g]	5.0
Lignosulfonate	

Table A.6: Base fluid 3 parameters

Base Fluid 3			
Rheology Parameters	Temperature		
	72°F	130°F	180°F
PV [cP]	8.5	6	5.5
YS [lbf/100ft ²]	15	17.5	12
LSYS [lbf/100ft ²]	7	7.5	5
n	0.45	0.33	0.39
K [lbf*sec ⁿ /1000ft ²]	1.46	3.04	1.50
Filtration [ml]			
pH	8.21		
CoF	0.234		
Base Fluid 3 + 0.05 g MWCNT			
Rheology Parameters	Temperature		
	72°F	130°F	180°F
PV [cP]	5	4.5	5
YS [lbf/100ft ²]	18.5	17	12.5
LSYS [lbf/100ft ²]	6.5	6.5	4
n	0.28	0.27	0.36
K [lbf*sec ⁿ /1000ft ²]	4.15	3.89	1.83
Filtration [ml]			
pH	8.29		
CoF	0.243		
Base Fluid 3 + 0.10 g MWCNT			
Rheology Parameters	Temperature		

	72°F	130°F	180°F
PV [cP]	5	6.5	5
YS [lbf/100ft ²]	14.5	11.5	7.5
LSYS [lbf/100ft ²]	5.5	5	3.5
n	0.33	0.45	0.49
K [lbf*sec ⁿ /1000ft ²]	2.50	1.13	0.61
Filtration [ml]			
pH	8.32		
CoF	0.277		
Base Fluid 3 + 0.15 g MWCNT			
Rheology Parameters	Temperature		
	72°F	130°F	180°F
PV [cP]	5.0	5.5	4.5
YS [lbf/100ft ²]	13.5	11.5	11.0
LSYS [lbf/100ft ²]	7	5	5
n	0.35	0.40	0.37
K [lbf*sec ⁿ /1000ft ²]	2.15	1.37	1.57
Filtration [ml]			
pH	8.35		
CoF	0.235		
Base Fluid 3 + 0.5 g MWCNT EX-SITU			
Rheology Parameters	Temperature		
	72°F	130°F	180°F
PV [cP]	5	5.5	4.5
YS [lbf/100ft ²]	25	21	19
LSYS [lbf/100ft ²]	8.4	8	9
n	0.22	0.27	0.25
K [lbf*sec ⁿ /1000ft ²]	7.50	4.86	4.86
Filtration [ml]			
pH	8.06		
CoF	0.241		
Base Fluid 3 + 1.0 g MWCNT EX-SITU			
Rheology Parameters	Temperature		
	72°F	130°F	180°F
PV [cP]	4	6.5	5.5
YS [lbf/100ft ²]	24.5	19.5	18.5
LSYS [lbf/100ft ²]	7	7.5	8.5
n	0.19	0.32	0.30
K [lbf*sec ⁿ /1000ft ²]	8.75	3.50	3.75
Filtration [ml]			
pH	8.02		
CoF	0.195		
Base Fluid 3 + 1.5 g MWCNT EX-SITU			
Rheology Parameters	Temperature		

	72°F	130°F	180°F
PV [cP]	5.0	5.5	5.5
YS [lbf/100ft ²]	22.5	20.5	17.0
LSYS [lbf/100ft ²]	7.0	8.0	9.0
n	0.24	0.28	0.32
K [lbf ⁿ *sec ⁿ /1000ft ²]	6.12	4.63	3.15
Filtration [ml]			
pH	8.06		
CoF	0.161		
Base Fluid 3 + 2.0 g MWCNT EX-SITU			
Rheology Parameters	Temperature		
	72°F	130°F	180°F
PV [cP]	6.5	6.0	6.0
YS [lbf/100ft ²]	30.0	27.5	21.5
LSYS [lbf/100ft ²]	8.5	9.5	9.5
n	0.24	0.24	0.29
K [lbf ⁿ *sec ⁿ /1000ft ²]	8.36	7.61	4.66
Filtration [ml]			
pH	7.98		
CoF	0.176		

Table A.7: Base fluid 4 formulation

Base fluid 4	
Ingredients	Concentration
Water, [g]	500
Bentonite [g]	25
Duovis [g]	0.5
KCl [g]	5.0
Lignosulfonate	0.2

Table A.8: Base fluid 4/Reference fluid parameters

Base 4/Reference fluid			
Rheology Parameters	Temperature		
	72°F	130°F	180°F
PV [cP]	5.0	5.0	4.5
YS [lbf/100ft ²]	13	12	11
LSYS [lbf/100ft ²]	6.5	6.0	6.5
n	0.353	0.372	0.368
K [lbf*sec ⁿ /1000ft ²]	1.99	1.67	1.57
Filtration [ml]			
pH	8.12		
CoF	0.279		
Ref + 0.1 g MWCNT			
Rheology Parameters	Temperature		
	72°F	130°F	180°F
PV [cP]	5.5	5.0	4.5
YS [lbf/100ft ²]	12.0	11.5	11.0
LSYS [lbf/100ft ²]	6.0	6.0	5.5
n	0.39	0.38	0.37
K [lbf*sec ⁿ /1000ft ²]	1.50	1.53	1.57
Filtration [ml]			
pH	8.11		
CoF	0.261		
Ref + 0.15 g MWCNT			
Rheology Parameters	Temperature		
	72°F	130°F	180°F
PV [cP]	5.0	4.5	4.5
YS [lbf/100ft ²]	13.0	12.5	10.5
LSYS [lbf/100ft ²]	6.5	6.0	5.0
n	0.353	0.339	0.378

K [lbf*sec ⁿ /1000ft ²]	1.99	2.06	1.42
Filtration [ml]			
pH	8.1		
CoF	0.252		
Ref + 0.20 g MWCNT			
Rheology Parameters	Temperature		
	72°F	130°F	180°F
PV [cP]	5.0	4.5	3.5
YS [lbf/100ft ²]	11.0	10.5	10.0
LSYS [lbf/100ft ²]	5.5	3.5	3.1
n	0.39	0.38	0.33
K [lbf*sec ⁿ /1000ft ²]	1.39	1.42	1.70
Filtration [ml]			
pH	8.0		
CoF	0.2533		
Ref + 0.5 g MWCNT			
Rheology Parameters	Temperature		
	72°F	130°F	180°F
PV [cP]	5.0	4.0	4.5
YS [lbf/100ft ²]	8.5	10.0	7.5
LSYS [lbf/100ft ²]	3.0	3.5	1.5
n	0.45	0.36	0.46
K [lbf*sec ⁿ /1000ft ²]	0.79	1.46	0.69
Filtration [ml]			
pH	8.16		
CoF	0.2275		
Ref + 1.0 g MWCNT			
Rheology Parameters	Temperature		
	72°F	130°F	180°F
PV [cP]	5.0	6.0	4.5
YS [lbf/100ft ²]	12.0	9.5	10.0
LSYS [lbf/100ft ²]	5.5	4.5	3.5
n	0.37	0.47	0.39
K [lbf*sec ⁿ /1000ft ²]	1.67	0.82	1.28
Filtration [ml]			
pH	8.09		
CoF	0.208		
Ref + 1.5 g MWCNT			
Rheology Parameters	Temperature		
	72°F	130°F	180°F
PV [cP]	4.5	6.0	4.5
YS [lbf/100ft ²]	14.0	10.5	11.5
LSYS [lbf/100ft ²]	6.0	5.5	3.5
n	0.31	0.45	0.36

K [lbf*sec ⁿ /1000ft ²]	2.61	1.01	1.72
Filtration [ml]			
pH	8.18		
CoF	0.158		
Ref + 3.0 g MWCNT			
Rheology Parameters	Temperature		
	72°F	130°F	180°F
PV [cP]	5.0	5.0	5.5
YS [lbf/100ft ²]	13.0	12.5	9.5
LSYS [lbf/100ft ²]	5.0	5.0	5.5
n	0.35	0.36	0.45
K [lbf*sec ⁿ /1000ft ²]	1.99	1.83	0.90
Filtration [ml]			
pH	8.17		
CoF	0.163		
Ref + NaOH			
Rheology Parameters	Temperature		
	72°F	130°F	180°F
PV [cP]	6.0	6.0	4.0
YS [lbf/100ft ²]	19.0	18.0	18.0
LSYS [lbf/100ft ²]	9.0	7.0	9.0
n	0.31	0.32	0.24
K [lbf*sec ⁿ /1000ft ²]	3.61	3.23	4.90
Filtration [ml]	17		
pH	9.05	8.74	8.37
CoF	0.241		
Ref + 0.1 g MWCNT (NaOH)			
Rheology Parameters	Temperature		
	72°F	130°F	180°F
PV [cP]	5.5	9.06	8.61
YS [lbf/100ft ²]	20.5	20.5	17.0
LSYS [lbf/100ft ²]	8.5	8.0	8.0
n	0.28	0.24	0.27
K [lbf*sec ⁿ /1000ft ²]	4.63	5.64	3.89
Filtration [ml]	17.2		
pH	9.43	9.06	8.61
CoF	0.221		
Ref + 0.2 g MWCNT (NaOH)			
Rheology Parameters	Temperature		
	72°F	130°F	180°F
PV [cP]	5.0	4.5	4.0
YS [lbf/100ft ²]	13.5	13.5	12.0
LSYS [lbf/100ft ²]	6.0	4.5	5.5
n	0.35	0.32	0.32
K [lbf*sec ⁿ /1000ft ²]	2.15	2.42	2.15
Filtration [ml]	17.5		
pH	9.09	8.77	8.58
CoF	0.204		
Ref + 0.5 g MWCNT (NaOH)			

Rheology Parameters	Temperature		
	72°F	130°F	180°F
PV [cP]	5.5	6.0	3.5
YS [lbf/100ft ²]	11.5	9.5	11.5
LSYS [lbf/100ft ²]	5.5	3.5	3.5
n	0.40	0.47	0.30
K [lbf*sec ⁿ /1000ft ²]	1.37	0.82	0.30
Filtration [ml]	17.0		
pH	9.12	8,78	8.54
CoF	0.176		
Ref + 1.5 g MWCNT (NaOH)			
Rheology Parameters	Temperature		
	72°F	130°F	180°F
PV [cP]	4.5	5.5	3.5
YS [lbf/100ft ²]	18.0	15.5	16.5
LSYS [lbf/100ft ²]	8.0	8.0	7.0
n	0.26	0.34	0.23
K [lbf*sec ⁿ /1000ft ²]	4.37	2.59	4.69
Filtration [ml]	18.0		
pH	9.91	9.46	9.17
CoF	0.160		
Ref (NaOH) mixed mechanical			
Rheology Parameters	Temperature		
	72°F	130°F	180°F
PV [cP]	5.5	5.0	4.5
YS [lbf/100ft ²]	11.5	11.0	10.0
LSYS [lbf/100ft ²]	5.5	4.5	3.5
n	0.40	0.39	0.39
K [lbf*sec ⁿ /1000ft ²]	1.37	1.39	1.28
Filtration [ml]			
pH	9.50		
CoF	0.287		
Ref (NaOH) mixed mechanical + sonication			
Rheology Parameters	Temperature		
	72°F	130°F	180°F
PV [cP]	5.0	5.0	5.0
YS [lbf/100ft ²]	16.0	15.0	12.5
LSYS [lbf/100ft ²]	7.0	7.0	6.5
n	0.31	0.32	0.36
K [lbf*sec ⁿ /1000ft ²]	3.08	2.69	1.83
Filtration [ml]			
pH	9.52		
CoF	0.278		

Appendix B: Viscoelasticity of drilling fluids

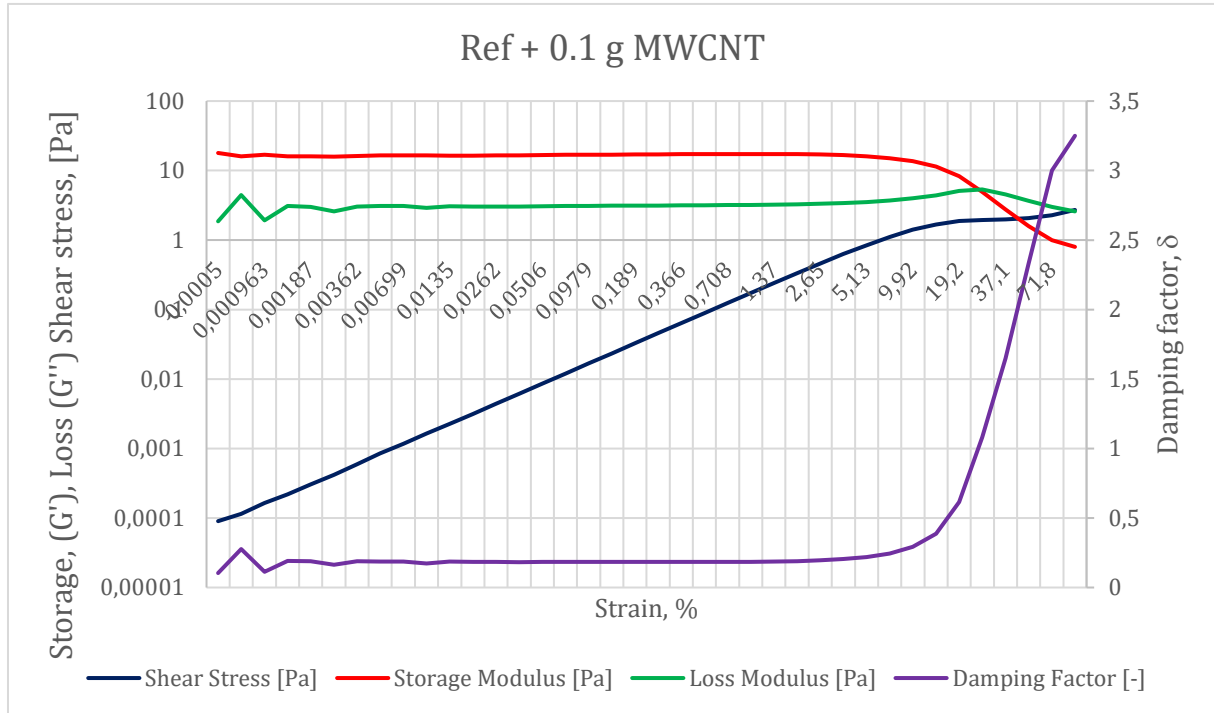


Figure B.1: Amplitude sweep measurements for Ref + 0.1 g MWCNT

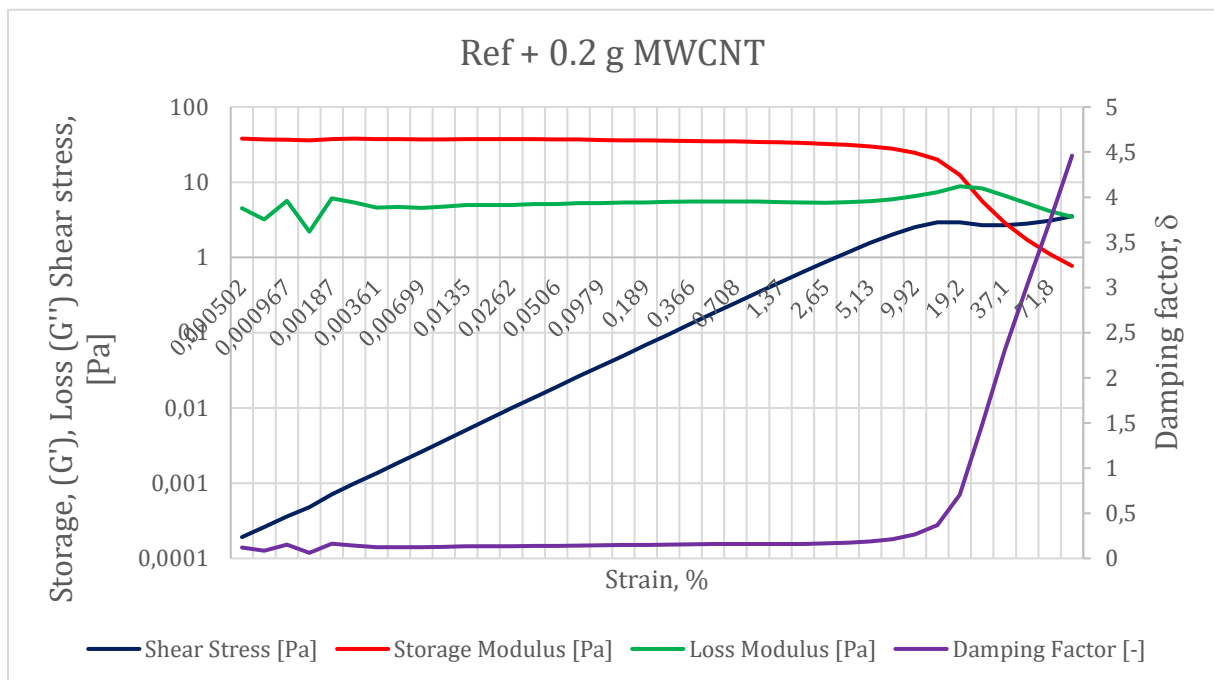


Figure B.2: Amplitude Sweep measurements for Ref + 0.2 g MWCNT

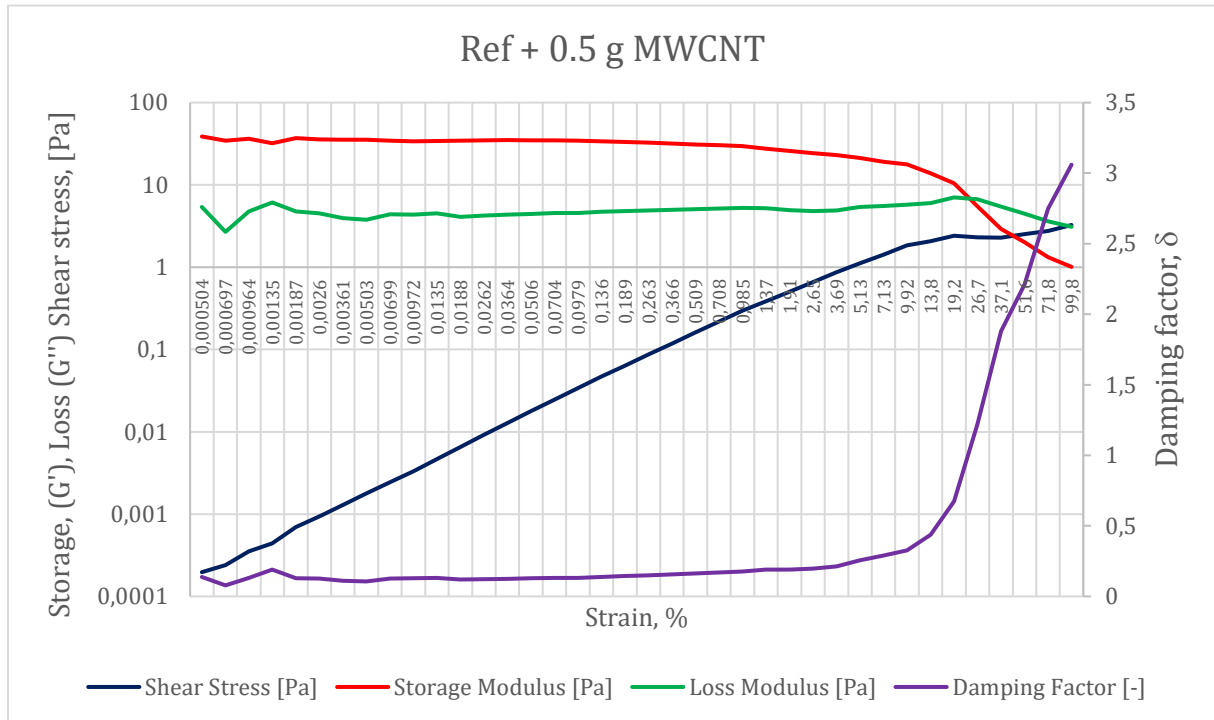


Figure B.3: Amplitude sweep measurements for Ref + 0.5 g MWCNT

Appendix C: Summary of test matrix results

Fluids	Filtrate	Friction	Torque and drag	Hole cleaning
Ref + 0.1 g MWCNT	Increased	Decreased	Drilling length increased	Improved
Ref + 0.2 g MWCNT	Increased	Decreased	Drilling length increased	Worsened
Ref + 0.5 g MWCNT	No change	Decreased	Drilling length increased	Worsened
Ref + 1.5 g MWCNT	Increased	Decreased	Drilling length increased	Worsened

List of Abbreviations

MWCNT – Multi Walled Carbon Nanotubes
WBM – Water Based Mud
OBM – Oil Bases Mud
HPHT – High Pressure High Temperature
ROP – Rate of Penetration
PV – Plastic Viscosity
YP – Yield Point
RPM – Rotation per Minute
LVE – Linear Viscoelastic Range
ECD – Equivalent circulation density
TVD – True vertical depth
API – American Petroleum Institute
ICP-OES - Inductively Coupled Plasma-Optical Emission spectrometry
SEM – Scan Electron Microscope
LSYS – Lower shear Yield stress
Ref – Reference Fluid
CoF – Coefficient of Friction
GPM – Gallon per minute
MD – Measured depth
nm - Nanometer

Nomenclature

τ	Shear Stress
μ	Viscosity
γ	Shear rate
θ_{600}	600 RPM
θ_{300}	300 RPM
μ_p	Plastic Viscosity
τ_y	Yield point
K	Consistency index

n	Flow behavior index
τ_0	Yield stress
γ^*	Geometric mean of shear rate
φ	Azimuth
θ	Inclination
“+”	Running out of the hole
“-“	Running into the hole
T_i	Torque at bit.
μ_t	Tangential coefficient of friction given as[19]:
V_a	Axial velocity
n	number of rotation.
G'	Storage Modulus
G''	Loss modulus
δ	Phase angle.
p_p	Pump Pressure
Δp_s	Pressure loss in surface equipment
Δp_{dp}	Pressure loss indside drill pipe
Δp_{dc}	Pressure loss inside the drill collars
Δp_{mt}	Pressure loss inside the mud motor
Δp_b	Pressure drop at the bit
Δp_{dca}	Pressure loss in the drill collar annulus
Δp_{dpa}	Pressure loss in the drill pipe annulus
ρ_{st}	Static mud density
ΔP	Pressure loss in annulus

List of figures

Figure 1.1: Mud circulating system [2]	6
Figure 1.2: Investigation methodology	7
Figure 2.1: SEM picture of Bentonite from a filter cake (Christian Erevik Riise, 2018) ...	10
Figure 2.2: Structure of octahedral structure and octahedral sheet, modified after Riise [9]	11
Figure 2.3: Structure of silica tetrahedral and layer structure of tetrahedral structurel , modified after Riise[9].....	11
Figure 2.4: Montmorillonite structure [11].....	12
Figure 2.5: Arrangement of clay particles in drilling fluid [9]	13
Figure 2.6: Structure of Lignosulfonate [9]	14
Figure 2.7: Scanning electron microscopy (SEM) image of entangled MWCNT particles. (Christian Riise, 2018).....	15
Figure 4.1: Picture of Fann 35 viscometer	30
Figure 4.2: Picture of filter press.....	31
Figure 4.3: Picture of pH-meter	31
Figure 4.4: Picture of tribometer.....	32
Figure 4.5: Rheometer with cooling apparatus	33
Figure 4.6: Picture of Inductively Coupled Plasma-Optical Emission spectrometry	33
Figure 4.7: Picture of Supra 40VP	34
Figure 4.8: Viscometer data for MWCNT fluids.....	36
Figure 4.9: Bingham parameters for MWCNT fluids.	37
Figure 4.10: Power-Law parameters for MWCNT drilling fluids.....	38
Figure 4.11: Coefficient of friction for the different drilling fluids.....	39
Figure 4.12: Percent change for coefficient of friction.....	39
Figure 4.13: Viscometer data for comparison of NaOH effect.....	41
Figure 4.14: Bingham parameters for comparison of NaOH-effect.	42
Figure 4.15: Power-Law parameters for comparison of NaOH-effect.....	43
Figure 4.16: comparison of friction coefficient.....	44
Figure 4.17: Viscometer response for the different drilling fluids with increasing temperature.....	45
Figure 4.18: Bingham parameters for the different drilling fluids with increasing temperature.....	46
Figure 4.19: Power Law parameters for the different drilling fluids with increasing temperature.....	46
Figure 4.20: Viscometer response for the different drilling fluids with increasing temperature.....	48
Figure 4.21: Bingham parameters for the different drilling fluids with increasing temperature.....	48
Figure 4.22: Power Law parameters for the different drilling fluids with increasing temperature.....	49

Figure 4.23: Fluid A and B after mixing and addition of MWCNT. Figure 4.24: Fluid A and B after 24 hours.....	50
Figure 5.1: Viscometer readings and the different rheology models. Table 5.1: Overview of the different rheology models for Ref fluid.....	60
Figure 5.2: Viscometer readings and the different rheology models for Ref + 0.1 g MWCNT	61
Figure 5.3: Viscometer readings and the different rheology models for Ref + 0.2 g MWCNT	62
Figure 5.4: Viscometer readings and the different rheology models for Ref + 0.5 g MWCNT	63
Figure 5.5: Viscometer readings and the different rheology models for Ref + 1.5 g MWCNT	64
Figure 5.6: Comparison between the different fluids and rheology models.....	65
Figure 5.7: Illustration of well for hydraulic simulations.....	69
Figure 5.8: Percent deviation in ECD for the different drilling fluids with MWCNT compared to Ref.....	70
Figure 5.9: ECD deviation for the drilling fluids.....	70
Figure 5.10: Pressure loss with increasing flow rate for the different drilling fluids.....	71
Figure 5.11: Schematic of well used for simulation.....	73
Figure 5.12: Drag chart for MWCNT fluids.....	74
Figure 5.13: Torque chart for the different fluids.....	75
Figure 5.14: Von Mises stress for the different fluids.....	75
Figure 5.15: Minimum flow rate required to transport out the cuttings at different inclinations.....	78
Figure 5.16: Well inclination and bed deposition.....	79
Figure B.1: Amplitude sweep measurements for Ref + 0.1 g MWCNT	98
Figure B.2: Amplitude Sweep measurements for Ref + 0.2 g MWCNT	98
Figure B.3: Amplitude sweep measurements for Ref + 0.5 g MWCNT	99

List of Tables

Table 3.1: Viscometer readings for Reference fluid.....	19
Table 3.2: Field unit transformed data.....	19
Table 4.1: Additives in Reference fluid.....	34
Table 4.2: Formulation of the different drilling fluids.....	35
Table 4.3: pH of drilling fluids with and without NaOH.....	40
Figure 5.1: Viscometer readings and the different rheology models. Table 5.1: Overview of the different rheology models for Ref fluid.....	60
Table 5.2: Overview of the different rheology models for Ref + 0.1 g MWCNT.....	61
Table 5.3: Overview of the different rheology models for Ref + 0.2 g MWCNT.....	62
Table 5.4: Overview of the different rheology models for Ref + 0.5 g MWCNT.....	63
Table 5.5: Overview of the different rheology models for Ref + 1.5 g MWCNT.....	64
Table 5.6: Rheology parameters for the different models.....	66
Table 5.7: Viscometer readings for the different fluids.....	72
Table 5.8: Friction coefficient for the different fluid systems.....	73
Table 5.9: Difference in CoF and reach with MWCNT as a additive.....	76
Table 5.10: Drilling parameters.....	77
Table 5.11: Fann35 viscometer readings.....	77
Table 5.12: Transport analyse data.....	79
Table A.1: Base fluid 1 formulation.....	88
Table A.2: Base fluid 1 parameters.....	88
Table A.3: Base fluid 2 formulation.....	90
Table A.4: Base fluid 2 parameters.....	90
Table A.5: Base fluid 3 formulation.....	91
Table A.6: Base fluid 3 parameters.....	91
Table A.7: Base fluid 4 formulation.....	94
Table A.8: Base fluid 4/Reference fluid parameters.....	94